ISM dynamics and star formation

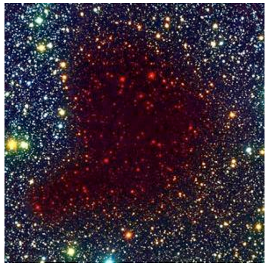

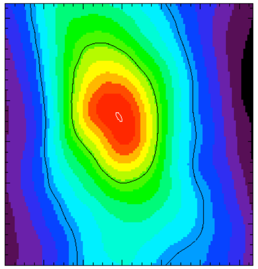

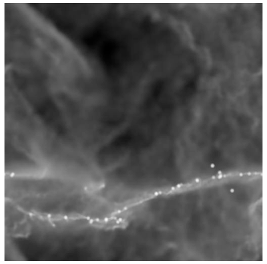

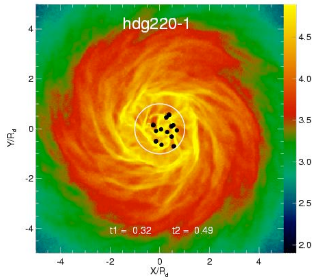

Ralf Klessen

Zentrum für Astronomie der Universität Heidelberg
Institut für Theoretische Astrophysik

ISM dynamics: theoretical considerations

- star formation on large scales
- structure of galactic disk
- phases of the ISM
- molecular clouds

phenomenology

- derivation of the hydrodynamic equations
- virial theorem
- Jeans criterion (critical mass for gravitational collapse)

theory

literature

Literature

- Star Formation:
  - Stahler, S., & Palla, F., 2004, "The Formation of Stars" (Weinheim: Wiley-VCH)
  - Osterbrock, D., & Farland, G., 2006, Astrophysics of Gaseous Nebulae & Active Galactic Nuclei, 2nd ed. (Sausalito: Univ. Science Books)
  - Lada, C. F., & Kylafis, N. D. 1999, "The Origin of Stars and Planetary Systems", NATO ASI Series 540 (Kluwer Academic Publisher)
  - Mannings, V., Boss, A. P., & Russell, S. S. 2000, "Protostars and Planets IV" (University of Arizona Press, Tucson)
- General:
  - Binney, J., & Tremaine, S. 1987, "Galactic Dynamics" (Princeton University Press)
  - Shu, F. 1991, "The Physics of Astrophysics I: Radiation" (University Science Books, Mill Valley)
  - Shu, F. 1991, "The Physics of Astrophysics II: Gas Dynamics" (University Science Books, Mill Valley)
  - Landau, L. D., & Lifschitz, E. M. 1986, "Hydrodynamik" (Akademie Verlag, Berlin)
- Review articles:
  - Mac Low, M.-M., Klessen, R.S., 2004, "The control of star formation by supersonic turbulence", Rev. Mod. Phys., 76, 125 - 194
  - Bromm, V., Larson, R.B., 2004, "The first stars", ARAA, 42, 79 - 118
  - Larson, R.B., 2003, "The physics of star formation", Rep. Prog. Phys, 66, 1651 - 1697
  - Shu, F.H, Adams, F.C., Lizano, S., 1987, "Star formation in molecular clouds: Observations and theory", ARAA, 25, 23 - 81

phenomenology

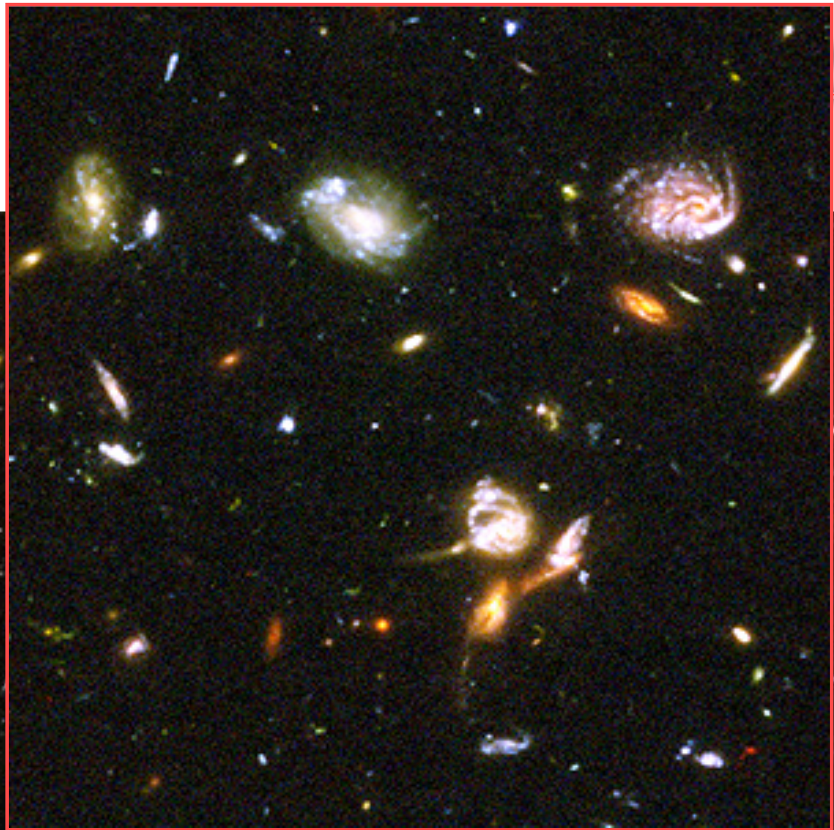

tion

rly

(less than 1Gyr
after big bangl)

Stars form in
galaxies and
protogalaxies

(Hubble Ultra-Deep Field, from HST Web site)

Star formation in interacting galaxies:

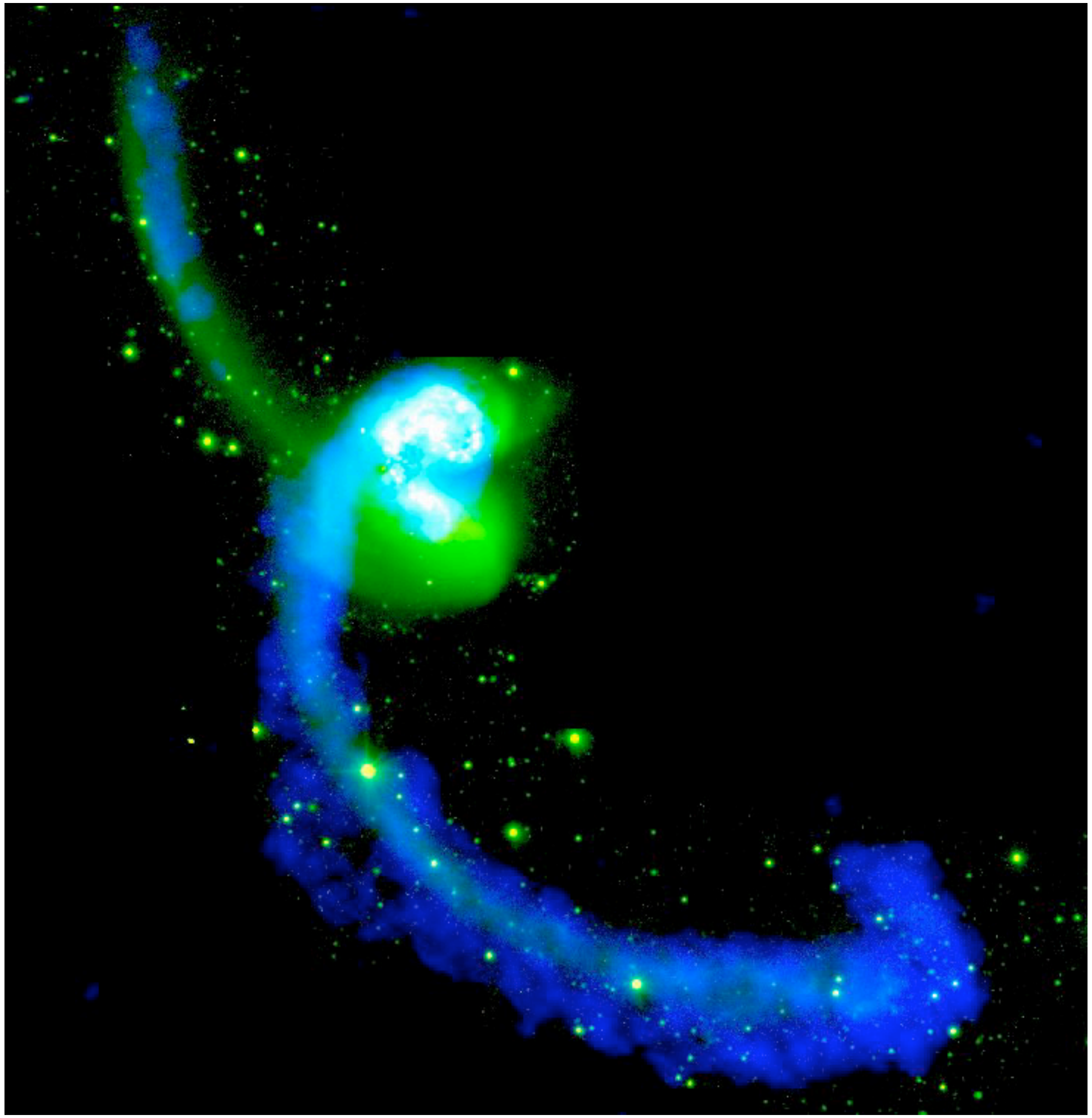

(from the Chandra Webpage)

Antennae galaxy

- *NGC4038/39*
- *distance: 19.2Mpc*
- *vis. Magn: 11.2*
- *optical: white, green*
- *radio: blue*

Star formation in interacting galaxies:

(HST: Whitmore & Schweizer 1997)

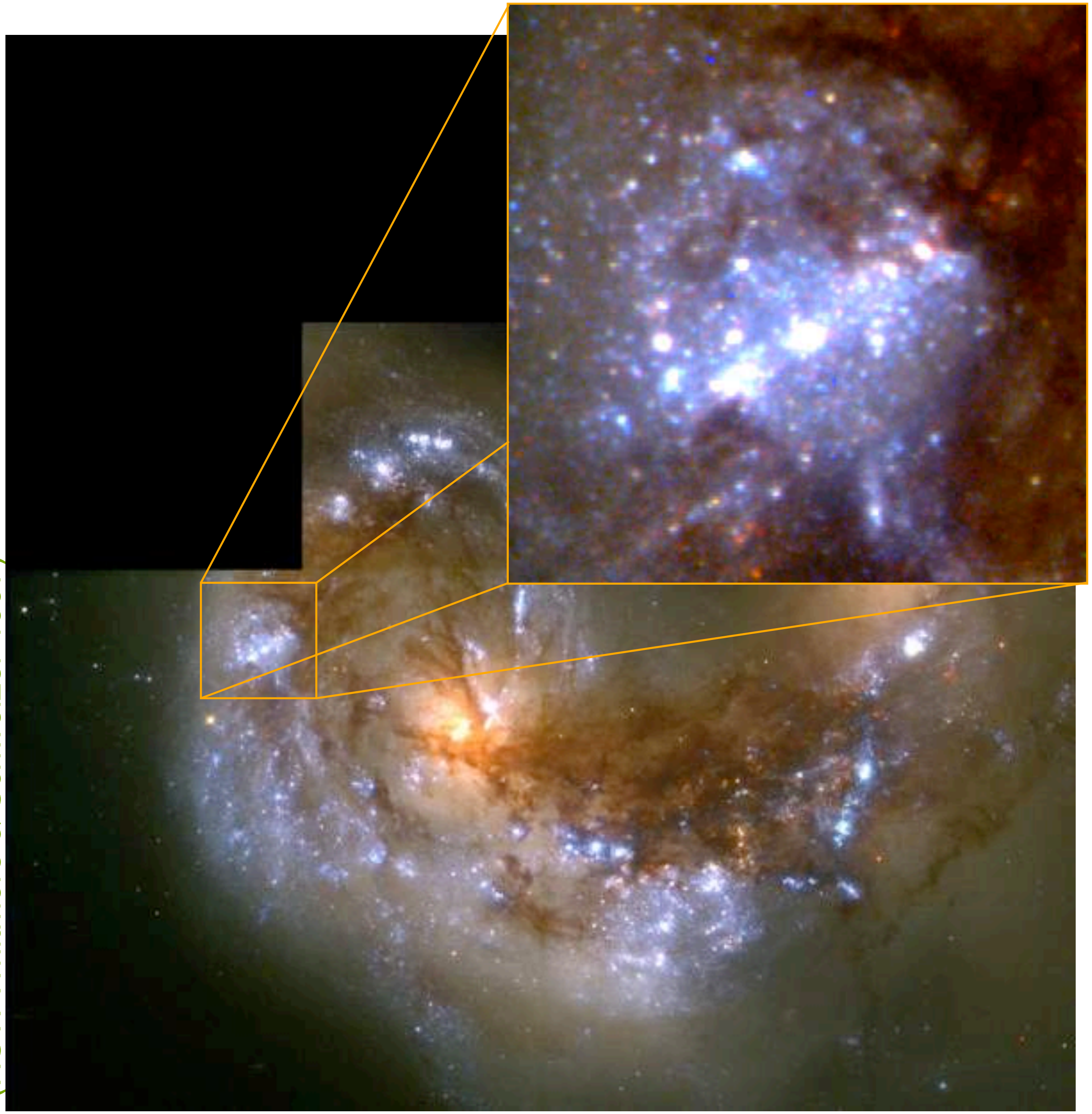

Antennae galaxy

- Star formation burst in interacting (merging) galaxies
- Strong perturbation SF in tidal “tales”
- Large-scale gravitational motion determines SF
- Stars form in “knobs” (i.e. superclusters)

Star formation in "typical" spiral:

(from the Hubble Heritage Team)

NGC4622

- Star formation *always* is associated with *clouds of gas and dust*.
- Star formation is essentially a ***local phenomenon*** (on ~pc scale)
- HOW is star formation is *influenced* by ***global*** properties of the galaxy?

Star forming clouds in the Milky Way

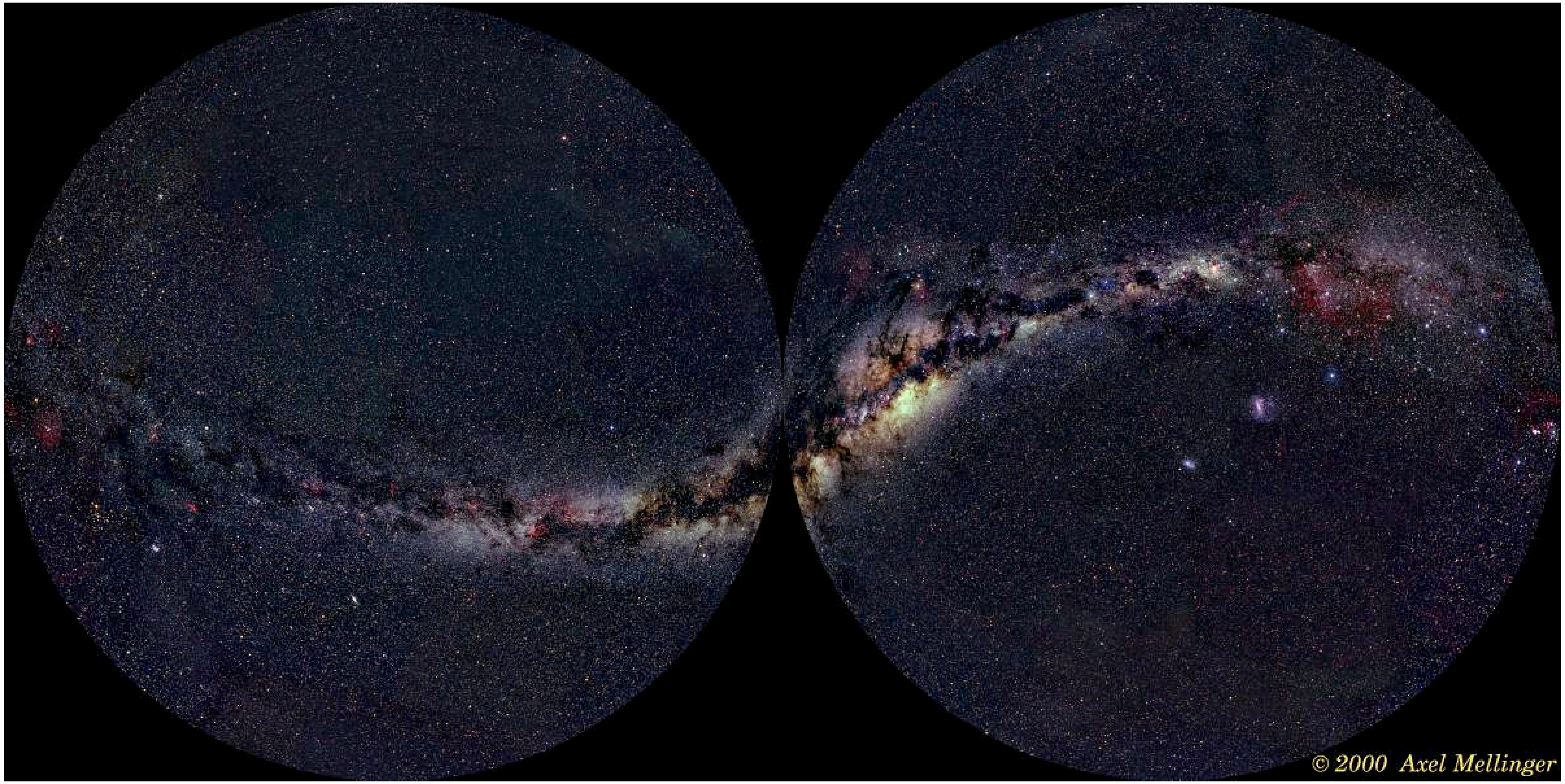

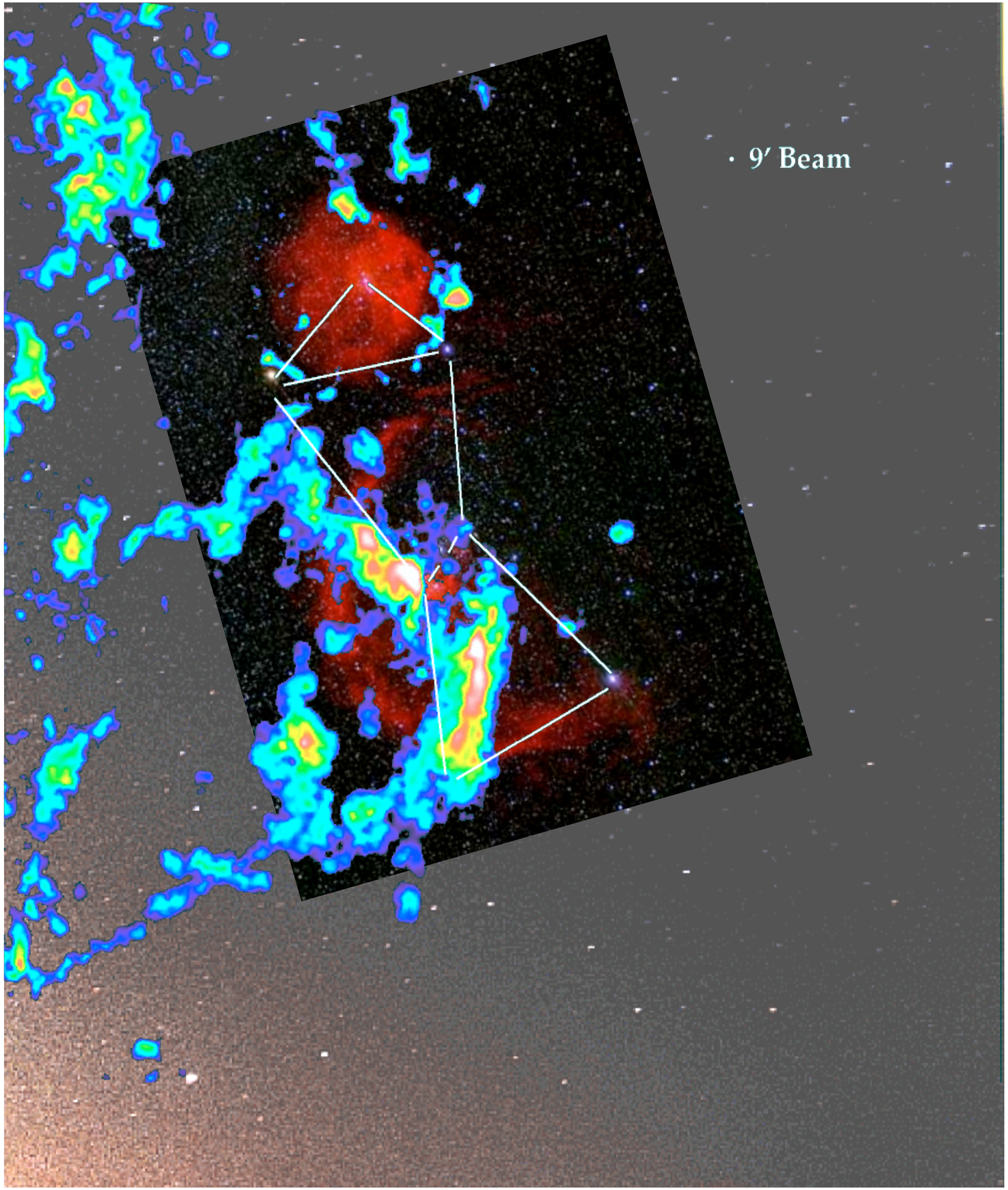

Star formation in Orion

We see

- *stars* (in optical light)
- *atomic hydrogen* (in Hα -- red)
- *molecular hydrogen H_2* (radio -- color coded)

Local star forming region: The Trapezium Cluster in Orion

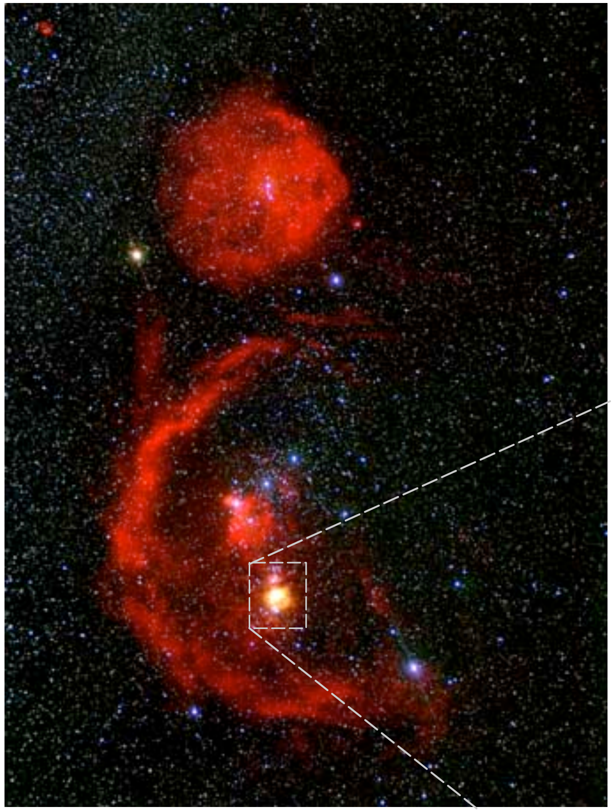

Orion molecular cloud

The Orion molecular cloud is the birth- place of several young embedded star clusters.

The Trapezium cluster is only visible in the IR and contains about 2000 newly born stars.

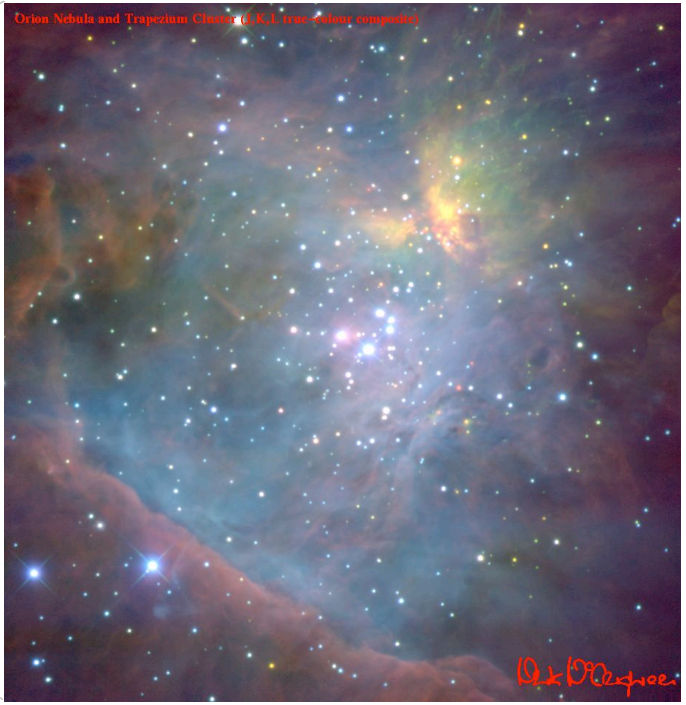

Trapezium cluster

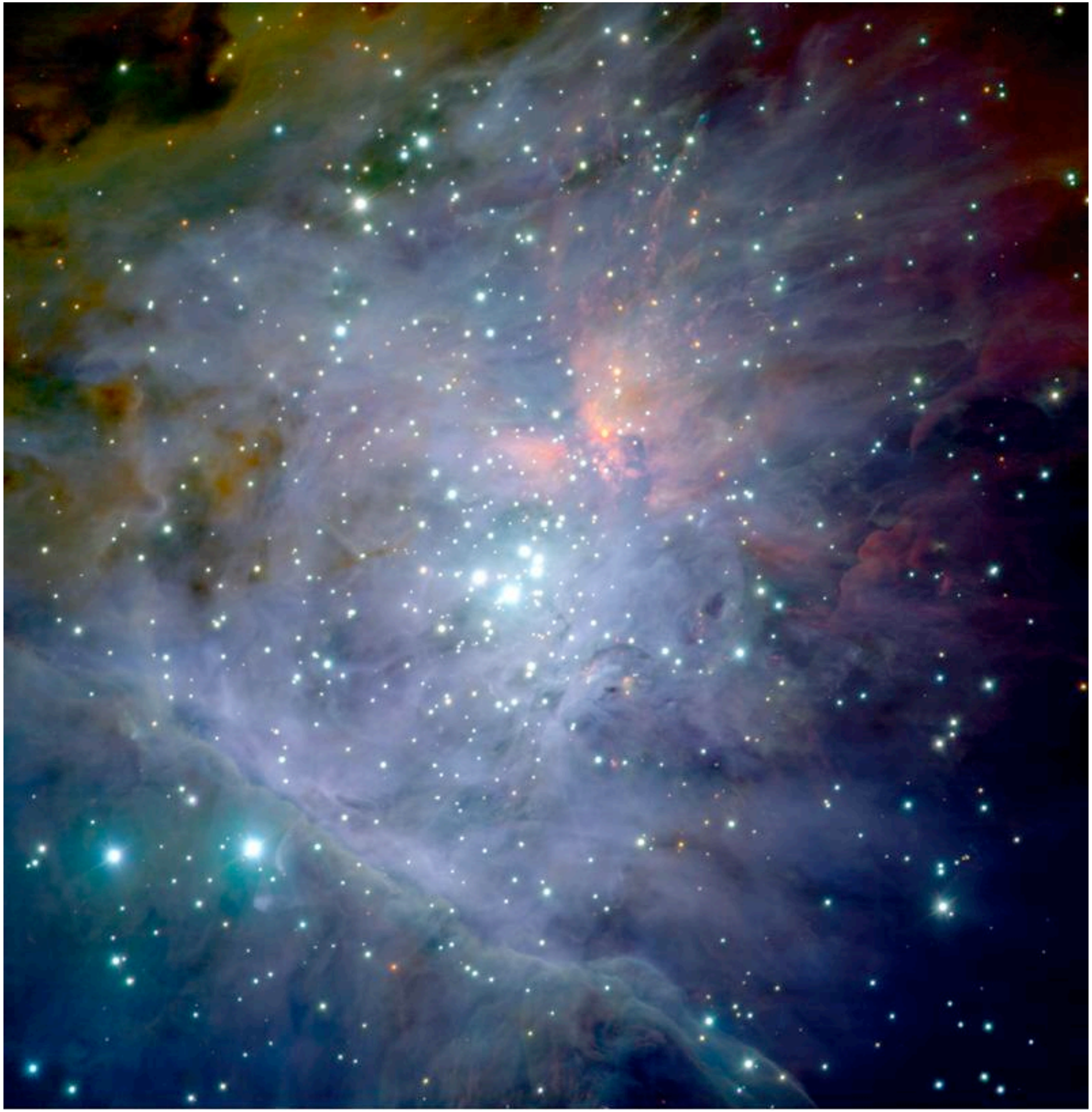

Trapezium Cluster

(detail)

- stars form in clusters
- stars form in molecular clouds
- (proto)stellar feedback is important

(color composite J,H,K by M. McCaughrean, VLT, Paranal, Chile)

Trapezium Cluster: Central Region

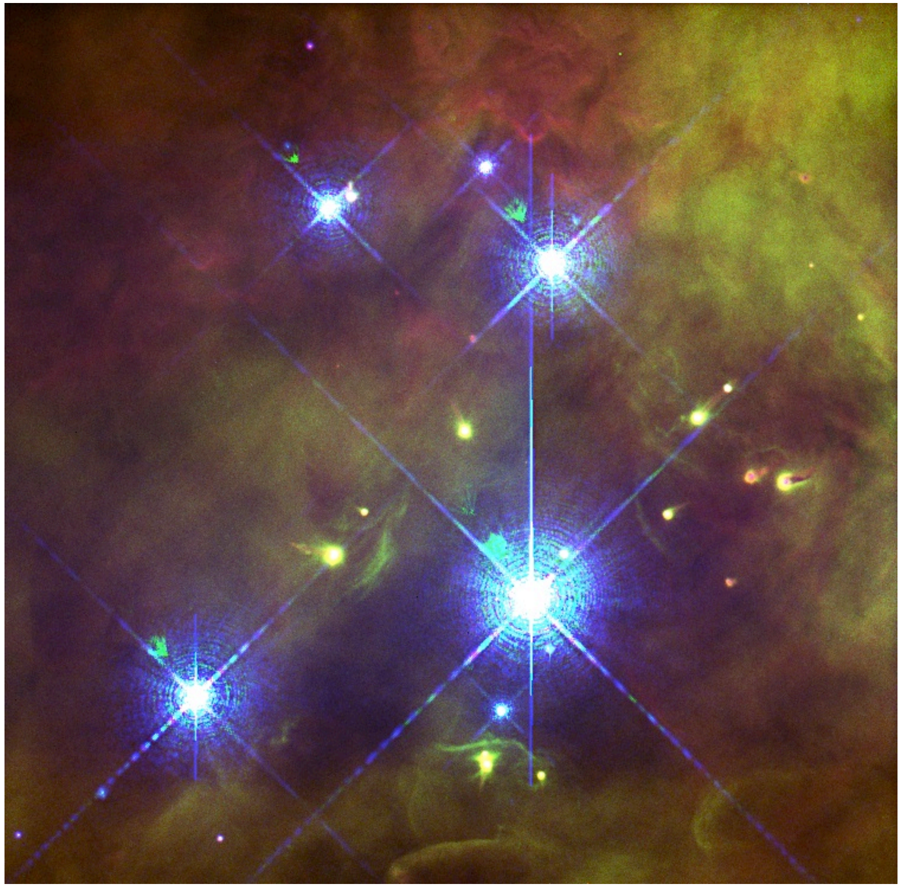

Ionizing radiation from central star
Θ1C Orionis

Proplyds: Evaporating ``protoplanetary´´ disks around young low-mass protostars

(images: Doug Johnstone et al.)

Futher Details: Siluette Disks in Orion

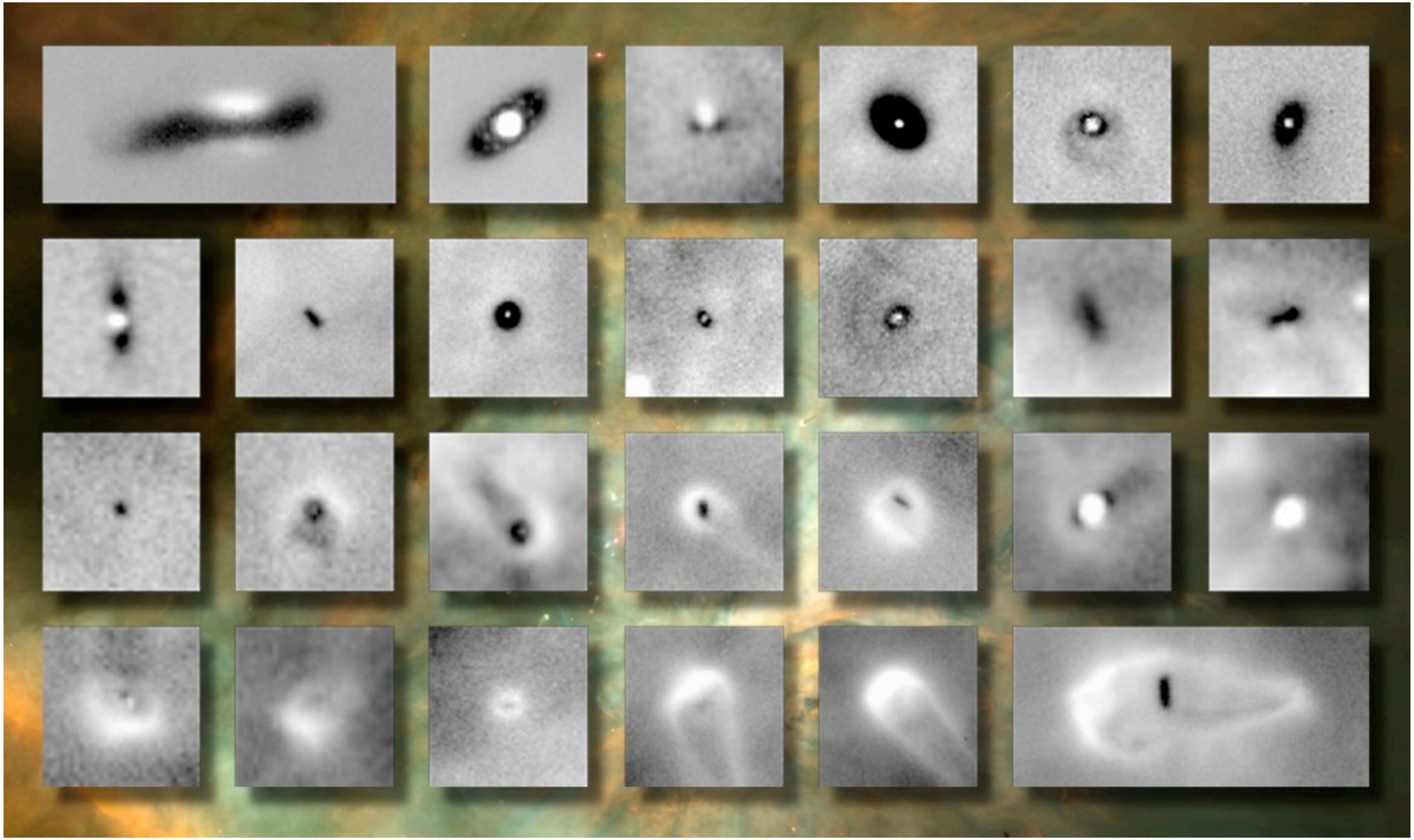

protostellar disks: dark shades in front of the photodissociation region in the background. Each image is 750 AU x 750 AU.

(data: Mark McCaughrean)

Star clusters in powers of 10:

30 Dor:
~100 O-stars

NGC3603:
~10 O-stars

Trapezium:
~1 O-star

all images are scaled to same distance (LMC)

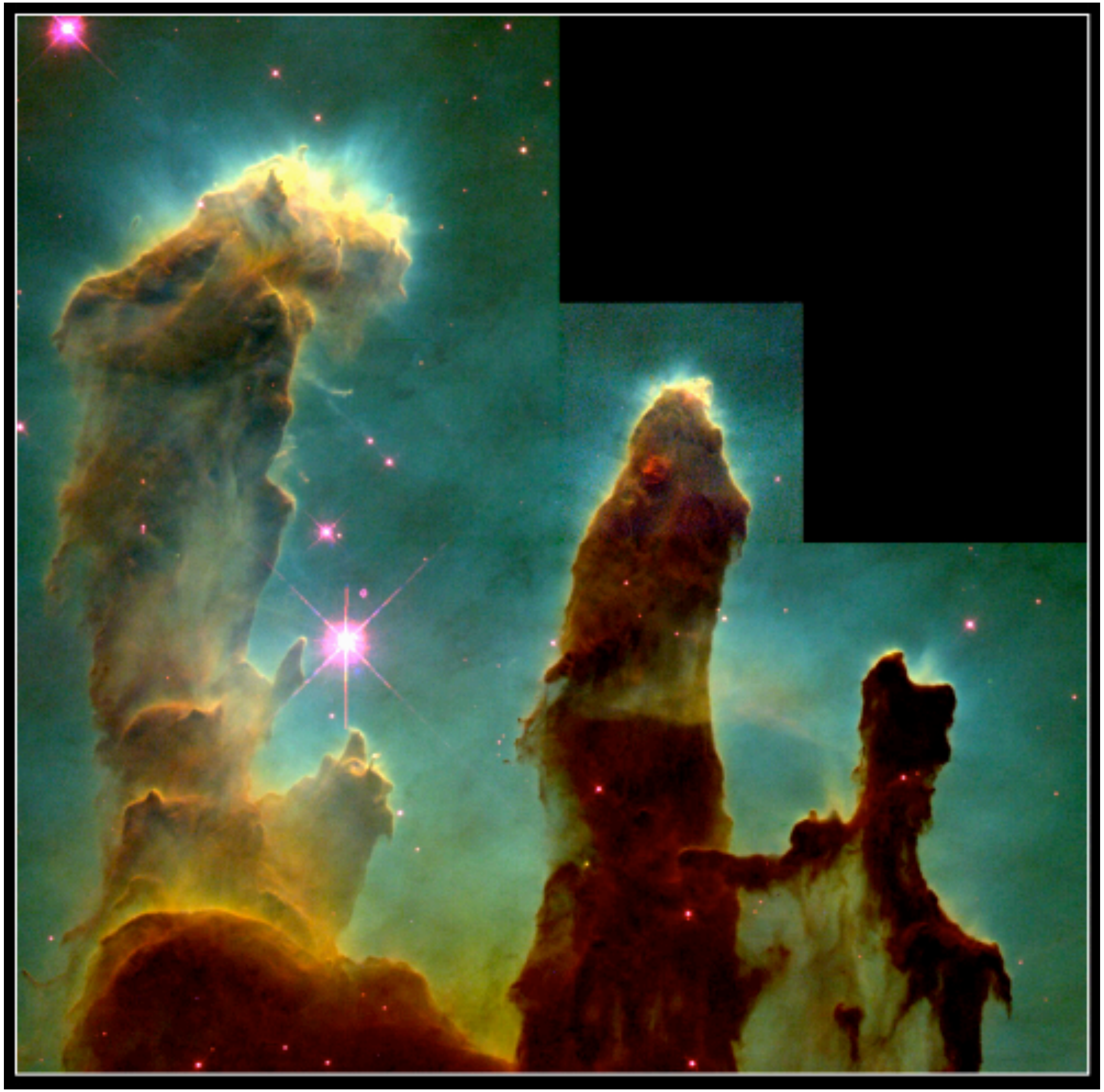

HST Aufnahme

Pillars of God (in Eagle Nebula): Formation of small groups of young stars in the tips of the columns of gas and dust ….

Infrared observation

IR observation with ESO-VLT

Pillars of God (in Eagle Nebula): Formation of small groups of young stars in the tips of the columns of gas and dust ….

IR observation with ESO-VLT

Pillars of God (in Eagle Nebula): Formation of small groups of young stars in the tips of the columns of gas and dust ….

multi-wavelength obseravations

How do we observe star forming clouds?

Different wavelength give different information.

→astronomer use the full electromagnetic spectrum

• Radio:	interstellar gas (line emission -> velocity information)
• sub-mm range:	dust (thermal emission)
• infrared & optical:	stars
• x-rays:	stars (coronae), supernovae remnants (very hot gas)
• γ-rays:	supernovae remnants (radioactive decay, e.g. ^{26}Al), compact objects, merging of neutron stars (γ-ray burst)

Multi-wavelength Andromeda

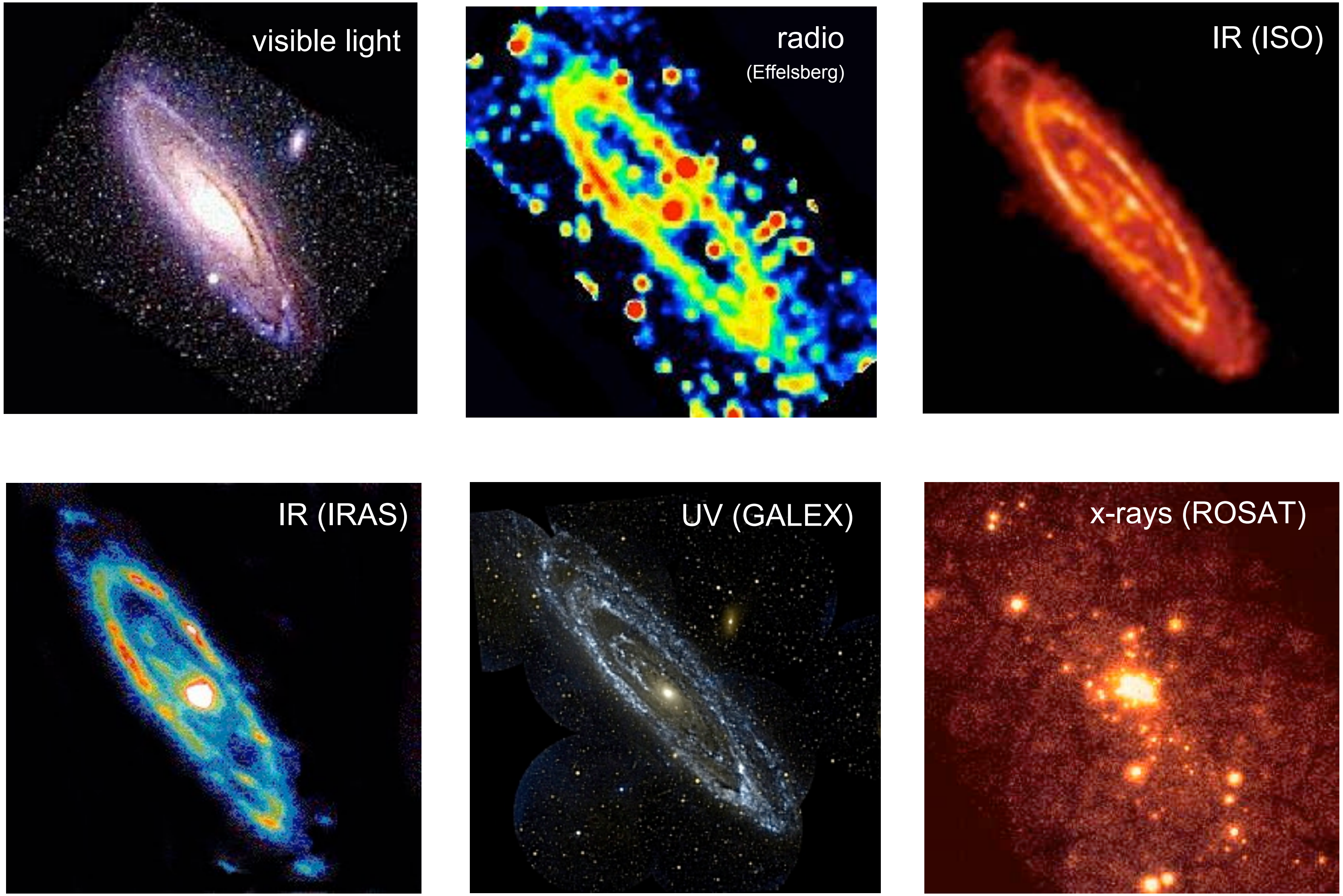

M31 seen in different wavelengths, from radio to x-rays.

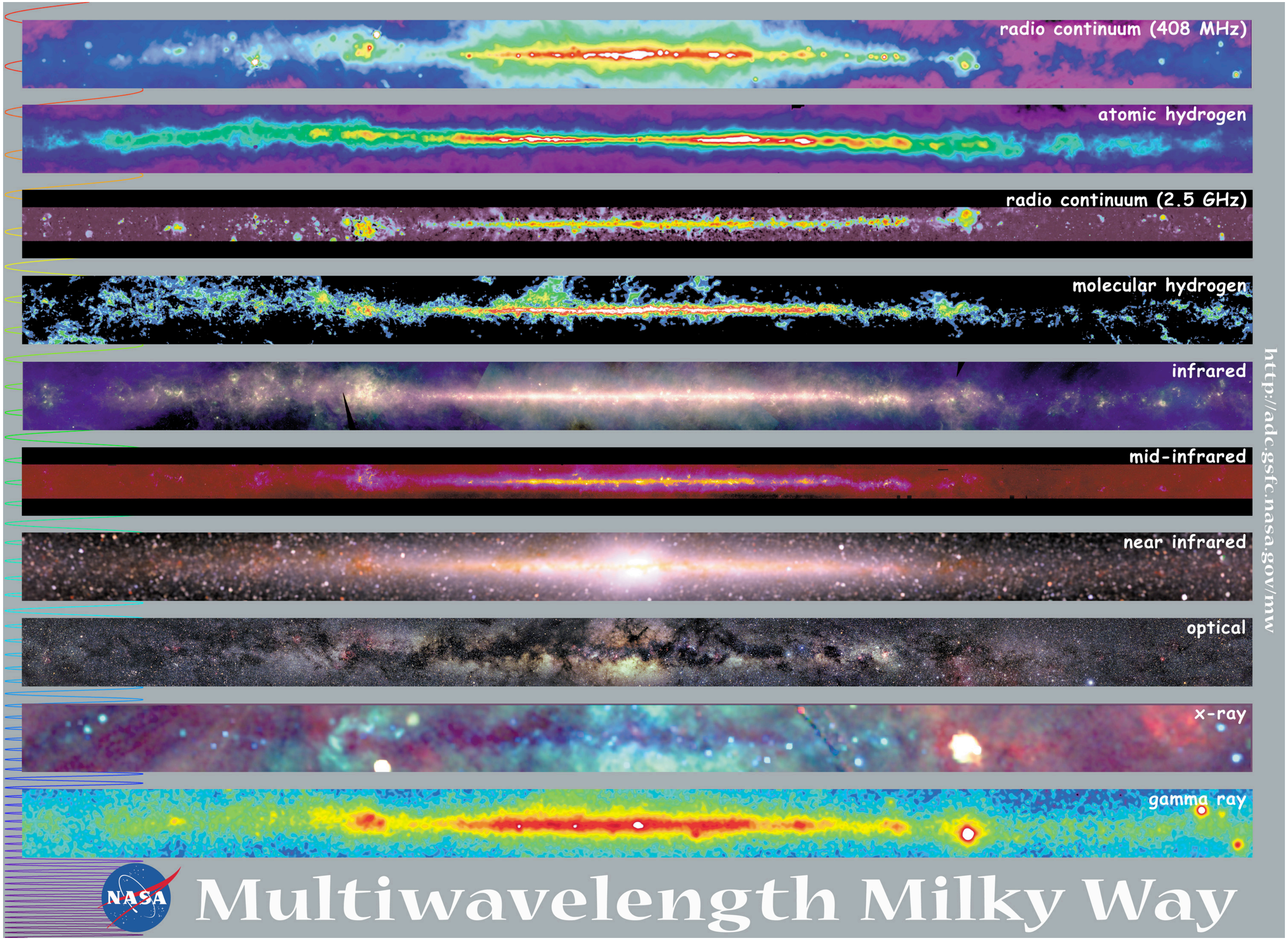
radio continuum (408 MHz)
atomic hydrogen
radio continuum (2.5 GHz)
molecular hydrogen
infrared
mid-infrared
near infrared
optical
x-ray
gamma ray
http://adc.gsfc.nasa.gov/mw
NASA
Multiwavelength Milky Way

phases of ISM

Interstellar Matter: ISM

Abundances, scaled to 1.000.000 H atoms

element		atomic number	abundance
Wasserstoff	H	1	1.000.000
Deuterium	${}_1H^2$	1	16
Helium	He	2	68.000
Kohlenstoff	C	6	420
Stickstoff	N	7	90
Sauerstoff	O	8	700
Neon	Ne	10	100
Natrium	Na	11	2
Magnesium	Mg	12	40
Aluminium	Al	13	3
Silicium	Si	14	38
Schwefel	S	16	20
Calcium	Ca	20	2
Eisen	Fe	26	34
Nickel	Ni	28	2

Hydrogen is by far the most abundant element (more than 90% in number).

Phases of the ISM

Because hydrogen is the dominating element, the classification scheme is based on its chemical state:

ionized atomic hydrogeN	*HII* (H^+)	Ionisation
neutraler atomic hydrogen	*HI (H)*	Phasenübergang
molecular hydrogen	H_2	

different regions consist of almost 100% of the appropriate phase, the transition regions between HII, H and H_2 are very thin.

star formation always takes place in dense and cold molecular clouds.

The multi-phase ISM

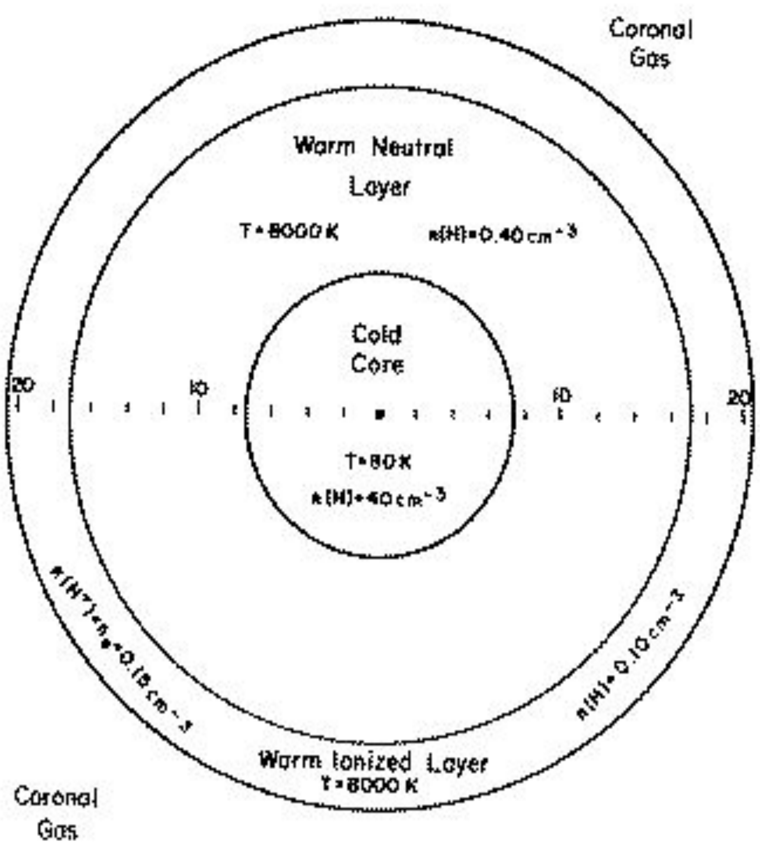

Fig. 8. Structure of a composite cloud. Values of $n(H)$, the neutral hydrogen density, and temperature T are indicated for the cold central core and the two warm envelopes; the electron density n_e is also specified for the outer envelope. The horizontal scale shows radii in light years.

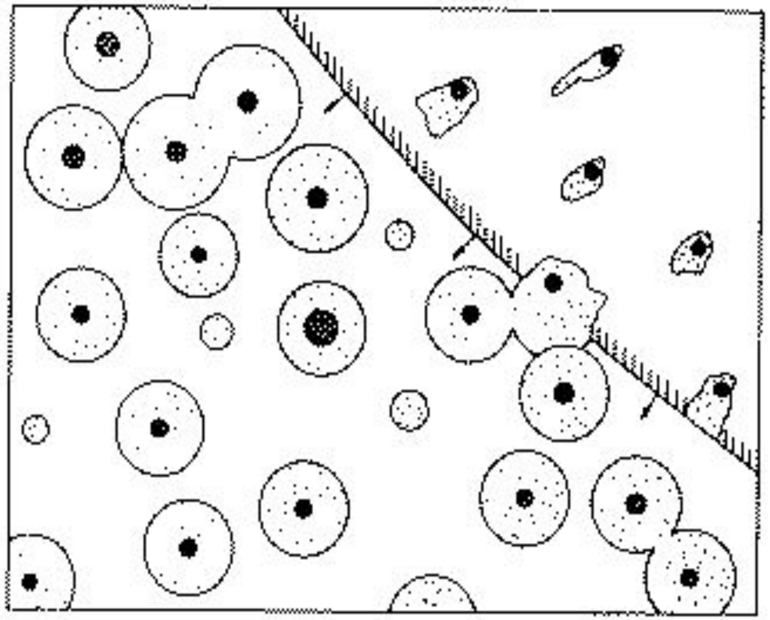

Fig. 9. Clouds in the galactic disc. Each cloud intersecting the galactic plane is represented by its cross-section through the cloud center. The dark central cores represent cold diffuse clouds, while the surrounding dotted circles represent envelopes of warm gas. The hot coronal gas fills the space between the clouds. An expanding supernova remnant advances in the upper right [50].

Life-cycle of ISM

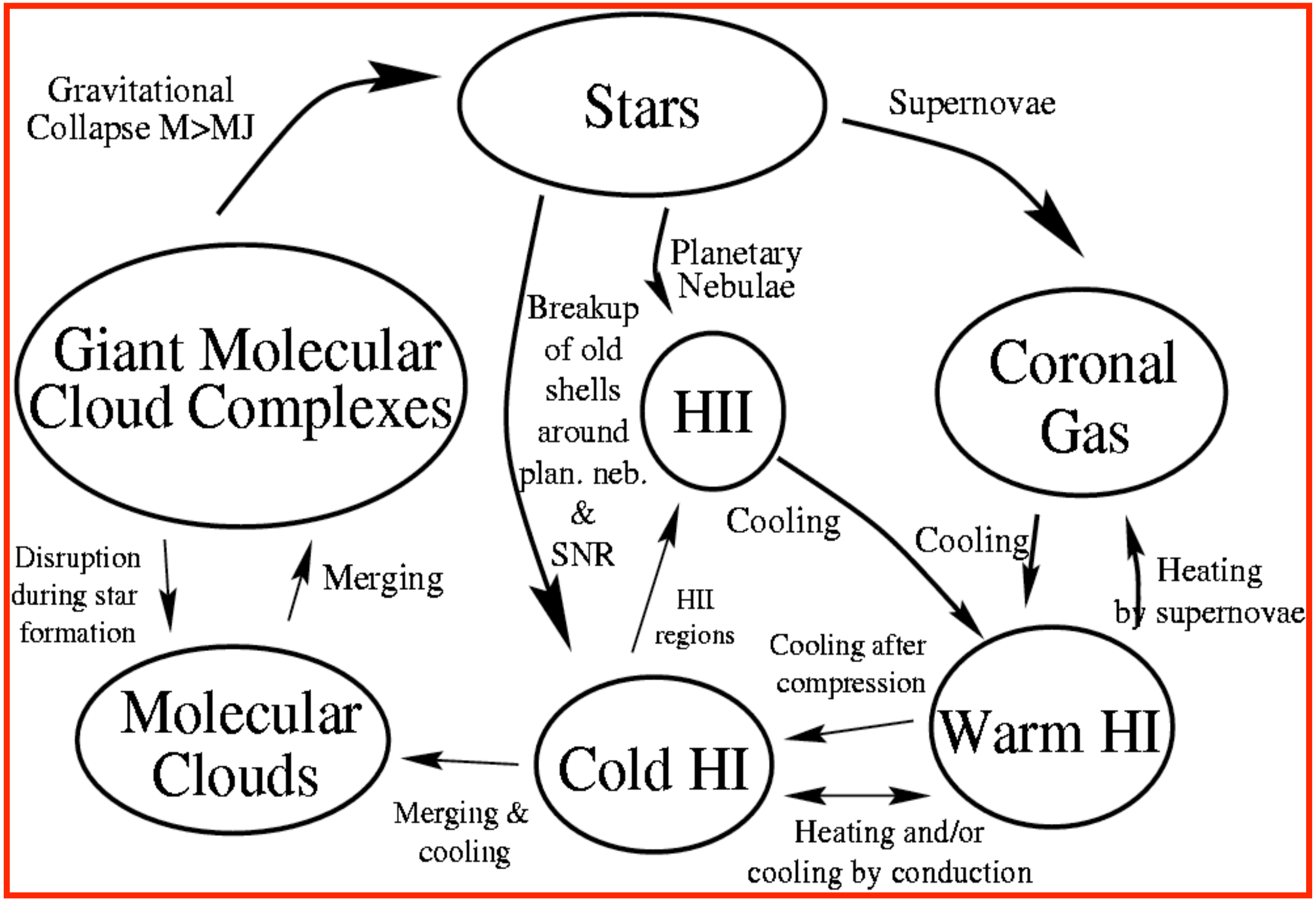

Correlation between H_2 and HI

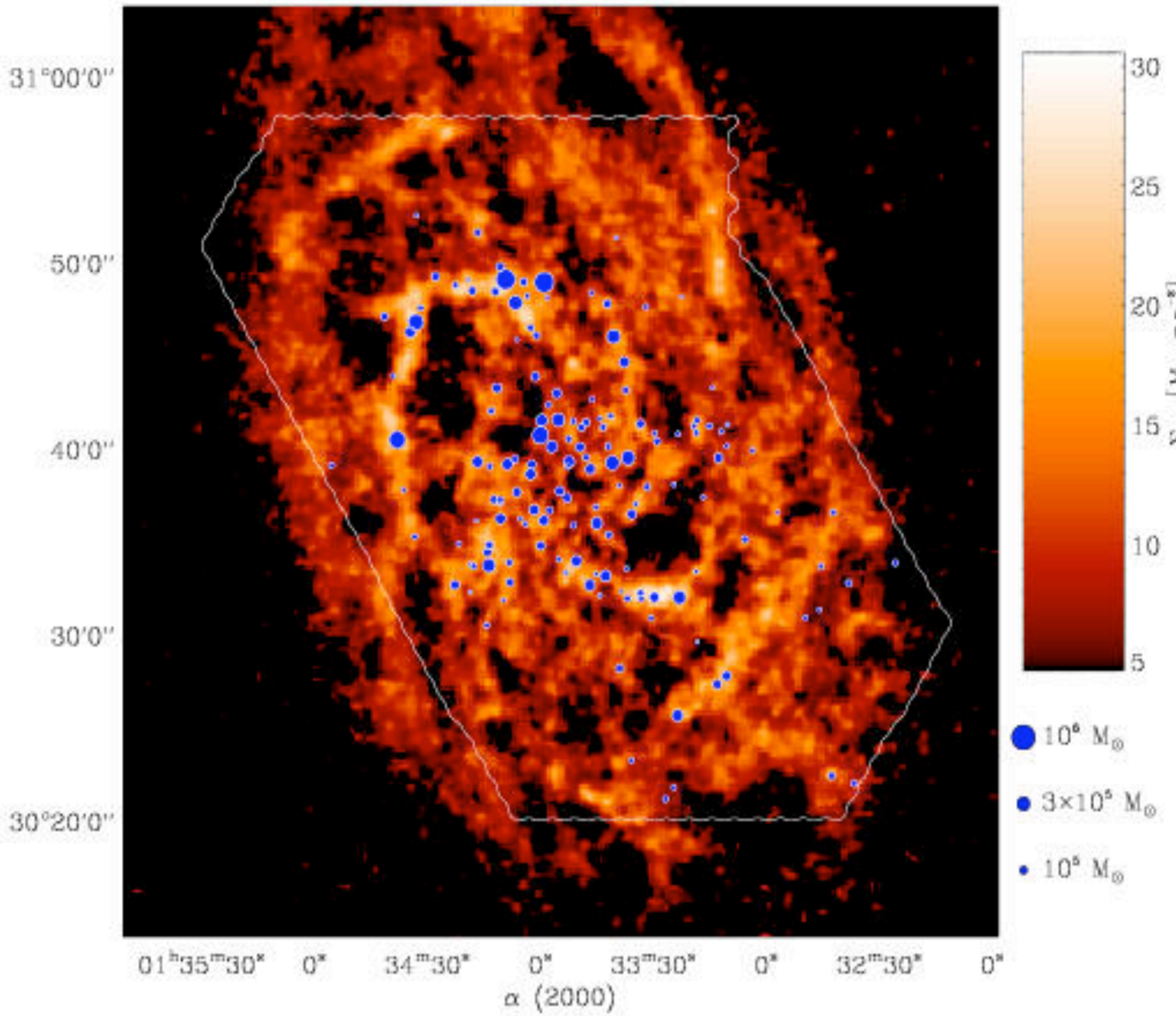

Compare H_2 - HI in M33:

- H_2: BIMA-SONG Survey, see Blitz et al.
- HI: Observations with Westerbork Radio T.

H_2 clouds are seen in regions of high HI density
(in spiral arms and filaments)

(Deul & van der Hulst 1987, Blitz et al. 2004)

Star formation in present day galaxies:

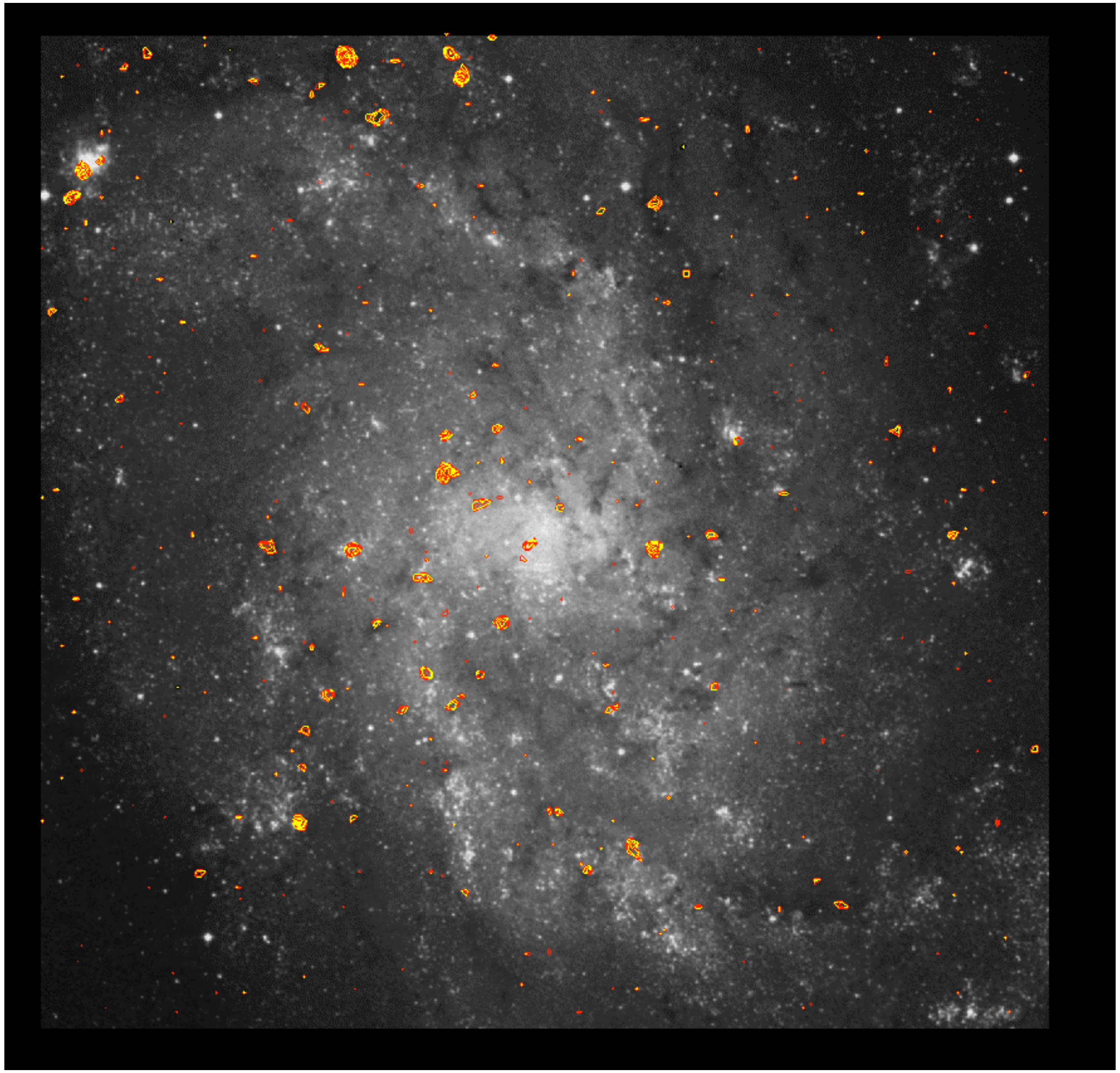

(BIMA: Blitz, Rosolowsky, Engargiola, & Plambeck, in prep.)

M33

- Star formation is *influenced* by *global* properties of the galaxy, BUT:
- Star formation is essentially a ***local phenomenon!!!***

Some further information

- About comparable amounts of H_2 and HI gas in the Galaxy
- $M(H_2) \sim 10^9\ M_\odot$
- But: Very different radial distribution
  - H_2 is centrally concentrated, and in a molecular ring at 4-8kpc (seen in our Galaxy, and in external ones)
  - HI depleted in the center and more radially extended
- H_2 is clumped in clouds and superclouds
- Both H_2 and HI have about the same velocity dispersion σ_g=5-10km/s (and this holds more or less for all spiral galaxies)

HI & CO in M31

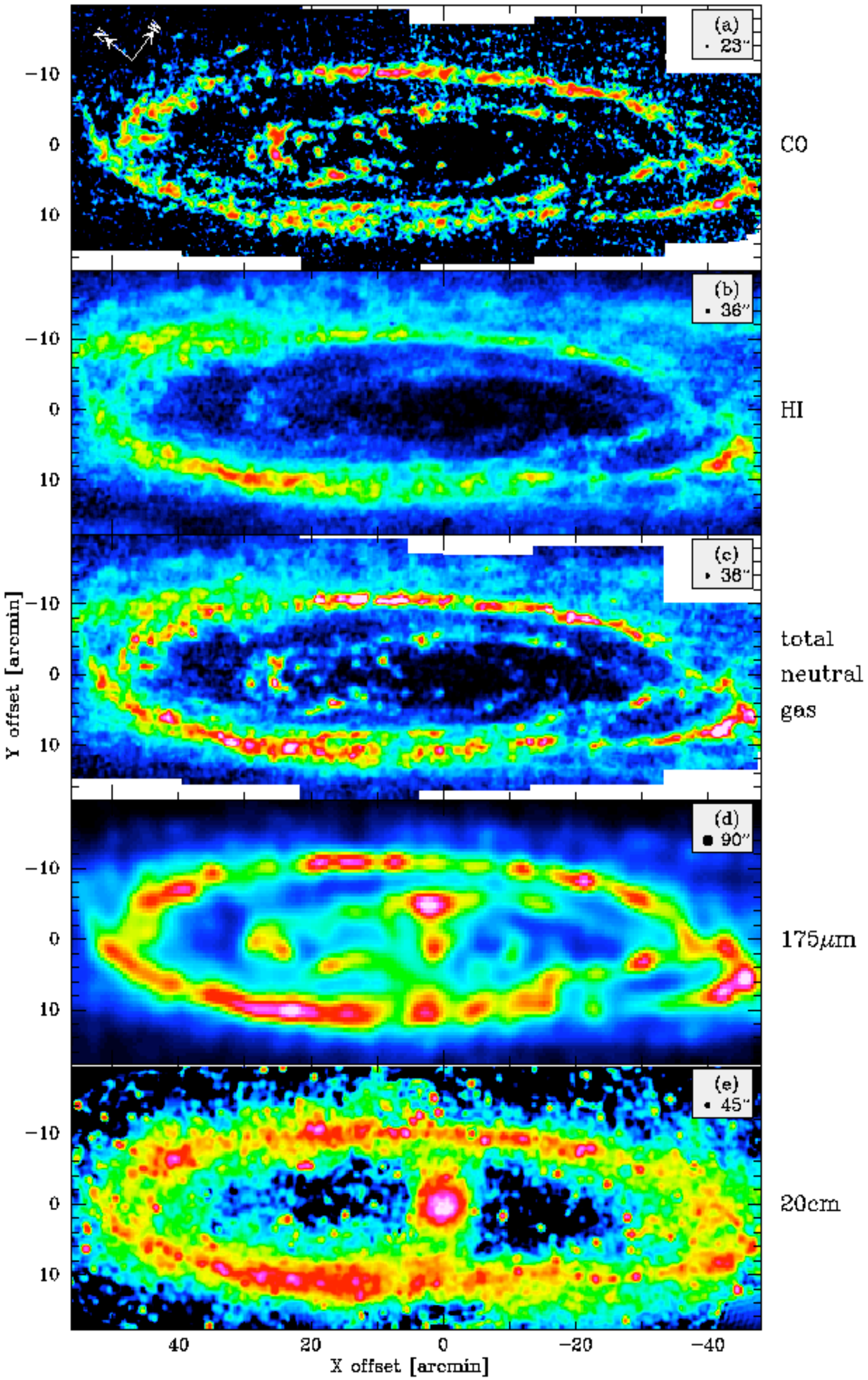

(a) 23″
CO
(b) 36″
HI
(c) 38″
total neutral gas
(d) 90″
175μm
(e) 45″
20cm
Y offset [arcmin]
X offset [arcmin]

Radial Distribution in Spirals

- HI versus H_2:
  - H_2 is restricted to the optical disk
  - while the HI extends 2-4 x optical radius
- HI hole or depression in the centers, sometimes compensated by H_2
- often H_2 is exponential like stars, HI does *not* follow in most cases

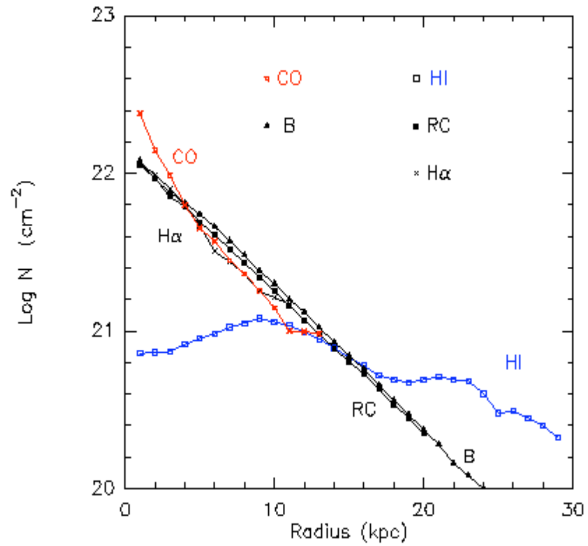

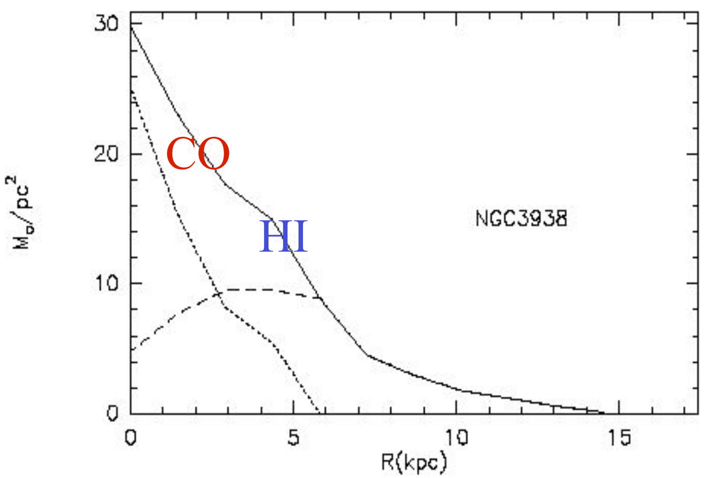

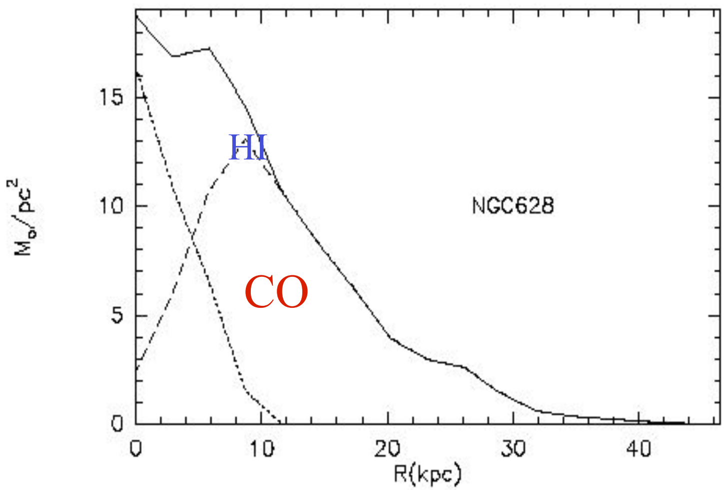

Radial profiles

Comparison of radial CO and HI profiles in 7 CO-bright galaxies confirms the tendency for H_2 to be more centrally concentrated than HI.

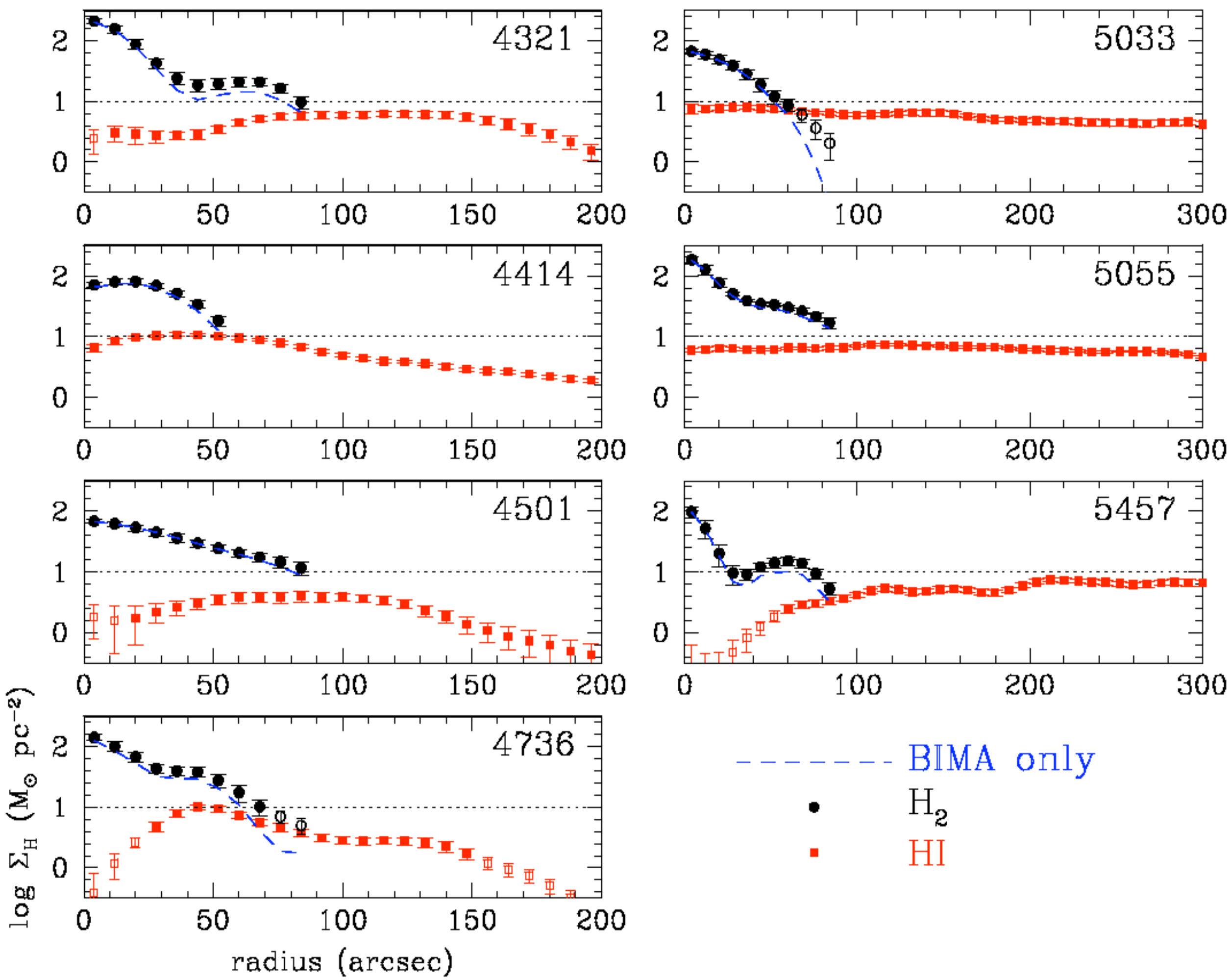

Wong & Blitz 2002

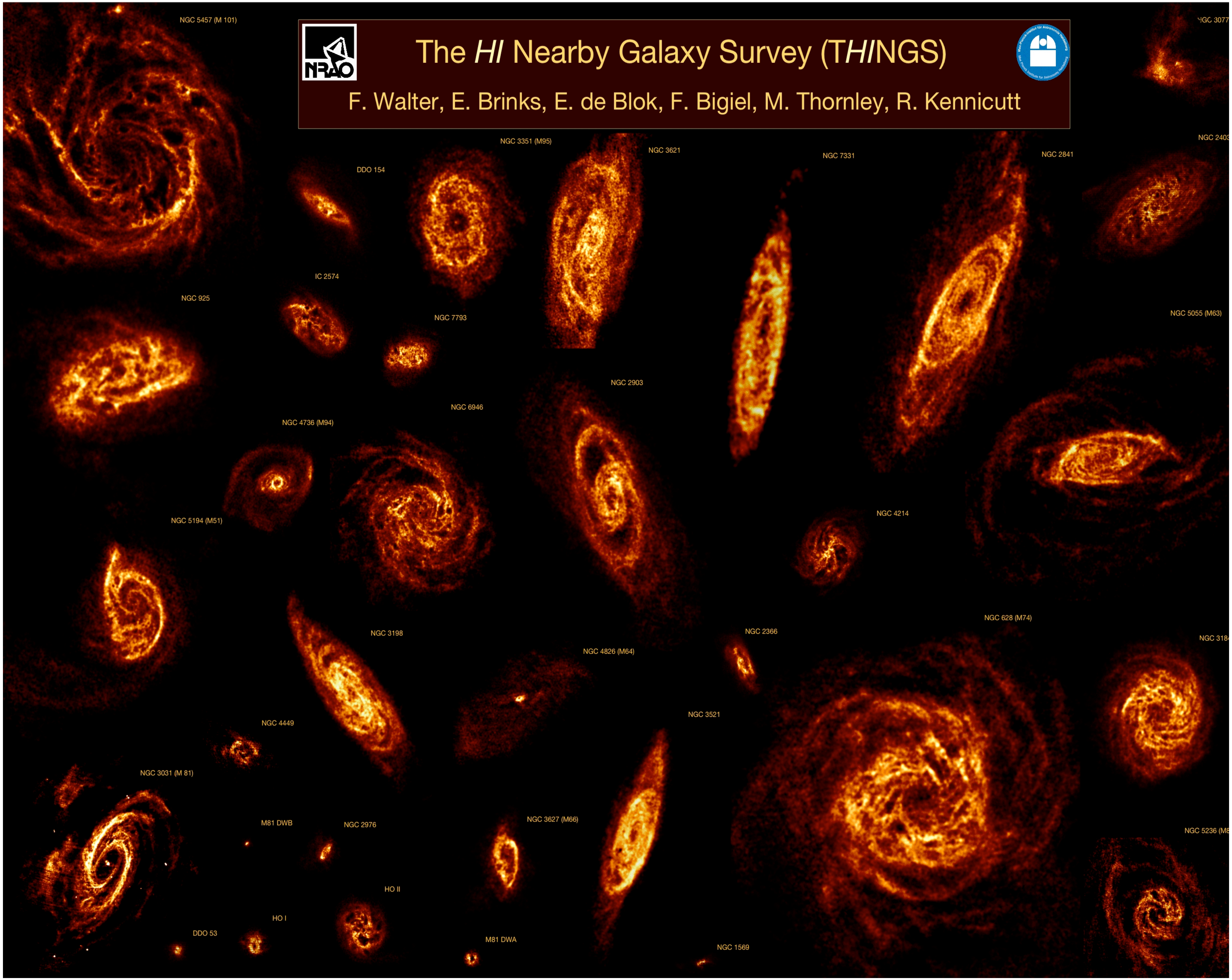
The HI Nearby Galaxy Survey (THINGS)
F. Walter, E. Brinks, E. de Blok, F. Bigiel, M. Thornley, R. Kennicutt
NRAO
NGC 5457 (M 101)
NGC 3351 (M95)
NGC 3621
NGC 7331
NGC 2841
DDO 154
IC 2574
NGC 925
NGC 7793
NGC 5055 (M63)
NGC 2903
NGC 6946
NGC 4736 (M94)
NGC 4214
NGC 5194 (M51)
NGC 628 (M74)
NGC 3198
NGC 2366
NGC 4826 (M64)
NGC 3521
NGC 4449
NGC 3031 (M 81)
M81 DWB
NGC 2976
NGC 3627 (M66)
HO II
HO I
DDO 53
M81 DWA
NGC 1569

ISM properties

- most important for star formation: **molecular hydrogen**
- most important wavelength: **IR and Radio emission**
  (dust continuum and molecular lines: CO, NH_3, CS, etc.)
  (more than 170 different molecules identified)
- Problem: only projection along the line of sight (real 3d structure of molecular clouds illusive)
- column density from intensity of line emission
- LOS velocity by Doppler shift of observed lines

atomic gas

Phases of interstellar matter

HI regions

Detection with 21cm line (1420 MHz, $6x10^{-6}$ eV))

Parallel spin (higher energy level)   antiparallel spins (lower energy level)

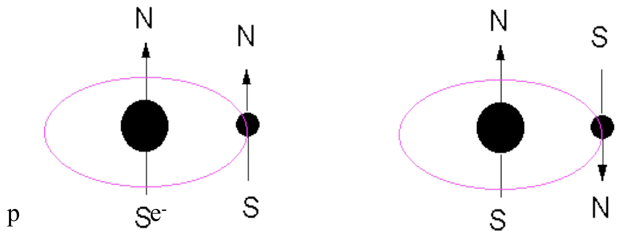

- Excitation by collisions (t_c ~ 500 yr)
- Deexcitation by radiation (t_r ~ $1x10^7$ yr)
- (hyperfine structure transition)

Properties of HI gas	Galactic plane	mean density n ~ 1 cm^{-3} (~$1,7x10^{-18}$ g/cm^3)
	envelope of MC's cold clouds in disk	n ~ 10 ... 100 cm^{-3} T_k > 100 K
	dilute matter between clouds	n ~ 0,05 ... 0,2 cm^{-3} T_k > 1000 K

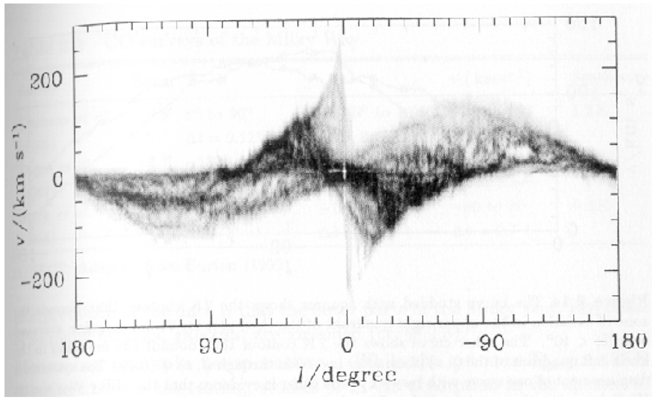

Radial velocity of 21cm radiation as function of galactic longitute (Leiden/Dwingeloo Survey)

- forbidden transition
- n~1cm^{-3}, l~1pc~$3x10^{18}$cm, ¾ of atoms are excited
  → 10^{18} atoms cm^{-2} → t=10^{14}s → 10^4 transitions $s^{-1}cm^{-2}pc^{-1}$
- optically thin: $I_\nu = B_\nu \tau$~const. $\kappa_\nu \sim 5.5x10^{-14}\, N_\nu/T$ & B~T
- T dependence cancels → directly get cm^{-2} column Nl

molecular clouds

ISM: transition HI to H_2

consistent models of ISM dynamics require to go beyond the simple models!

- magnetohydrodynamics (account for large-scale dynamics + turbulence)
- time-dependent chemistry (reduced network, focus on few dominant species, e.g. H_2)
- radiation (currently simple assumptions)

H2 forms rapidly in shocks / transient density fluctuations / H2 gets destroyed slowly in low density regions / result: turbulence greatly enhances H2-formation rate

(Glover & Mac Low 2006ab:)

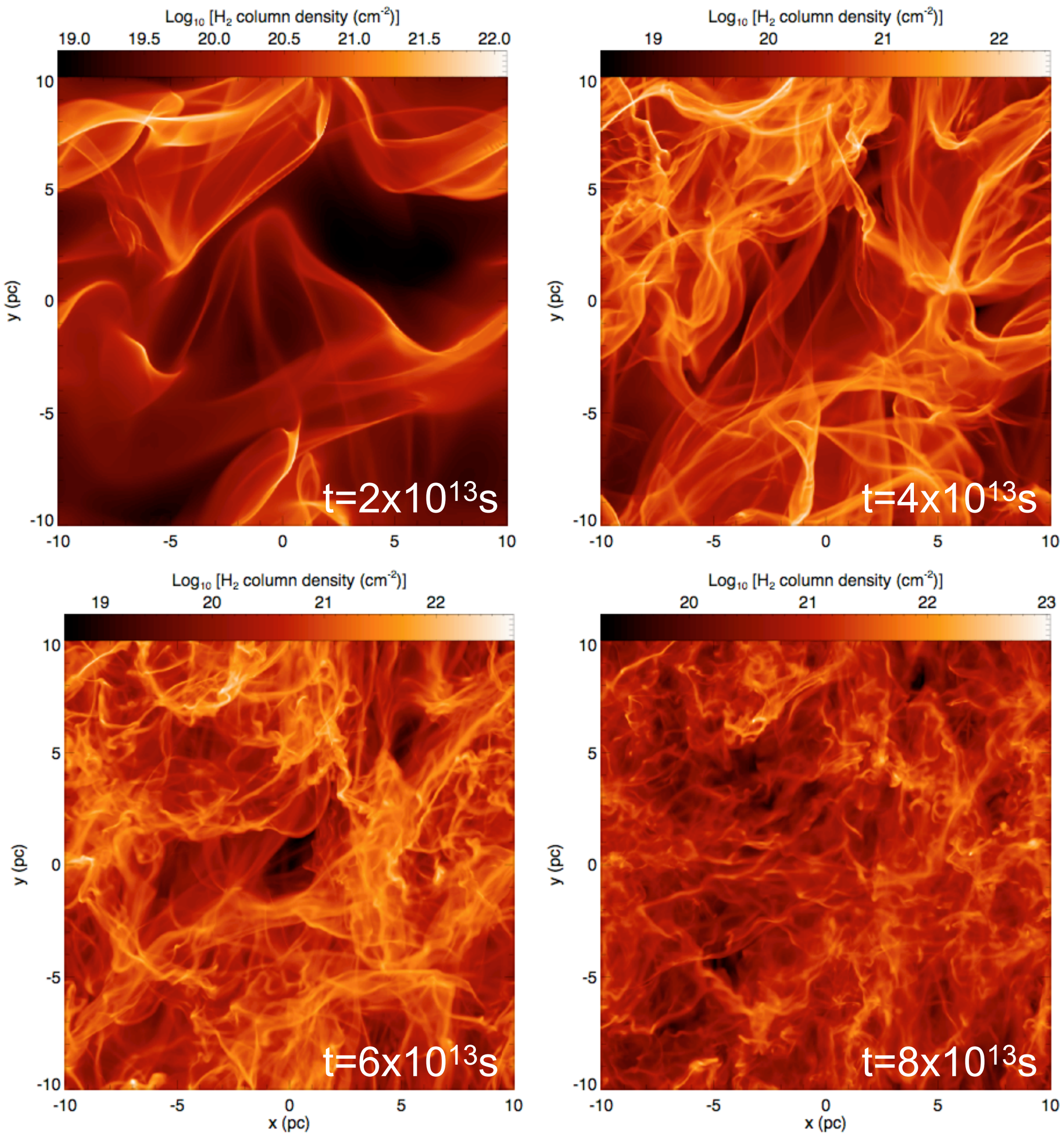

Reduced chemical network

Table 1. The set of chemical reactions that make up our model of non-equilibrium hydrogen chemistry.

Reaction	Reference
1. $H + H + \text{grain} \rightarrow H_2 + \text{grain}$	Hollenbach & McKee (1979)
2. $H_2 + H \rightarrow 3H$	Mac Low & Shull (1986) (low density), Lepp & Shull (1983) (high density)
3. $H_2 + H_2 \rightarrow 2H + H_2$	Martin, Keogh & Mandy (1998) (low densit Shapiro & Kang (1987) (high density)
4. $H_2 + \gamma \rightarrow 2H$	See § 2.2.1
5. $H + \text{c.r.} \rightarrow H^+ + e$	Liszt (2003)
6. $H + e \rightarrow H^+ + 2e$	Abel *et al.* (1997)
7. $H^+ + e \rightarrow H + \gamma$	Ferland *et al.* (1992)
8. $H^+ + e + \text{grain} \rightarrow H + \text{grain}$	Weingartner & Draine (2001)

here: e^-, H^+, H, H_2

in primordial gas we do:

e^-, H^+, H, H^-, H_2^+, H_2, C, C^+, O, O^+

Table 2. Processes included in our thermal model.

Process	References
Cooling:	
C II fine structure lines	Atomic data – Silva & Viegas (2002)
	Collisional rates (H_2) – Flower & Launay (1977)
	Collisional rates (H, $T < 2000$ K) – Hollenbach & McKee (1989)
	Collisional rates (H, $T > 2000$ K) – Keenan *et al.* (1986)
	Collisional rates (e^-) – Wilson & Bell (2002)
O I fine structure lines	Atomic data – Silva & Viegas (2002)
	Collisional rates (H, H_2) – Flower, priv. comm.
	Collisional rates (e^-) – Bell, Berrington & Thomas (1998)
	Collisional rates (H^+) – Pequignot (1990, 1996)
Si II fine structure lines	Atomic data – Silva & Viegas (2002)
	Collisional rates (H) – Roueff (1990)
	Collisional rates (e^-) – Dufton & Kingston (1991)
H_2 rovibrational lines	Le Bourlot, Pineau des Forêts & Flower (1999)
Gas-grain energy transfer[1]	Hollenbach & McKee (1989)
Recombination on grains	Wolfire *et al.* (2003)
Atomic resonance lines	Sutherland & Dopita (1993)
H collisional ionization	Abel *et al.* (1997)
H_2 collisional dissociation	See Table 1
Heating:	
Photoelectric effect	Bakes & Tielens (1994); Wolfire *et al.* (2003)
H_2 photodissociation	Black & Dalgarno (1977)
UV pumping of H_2	Burton, Hollenbach & Tielens (1990)
H_2 formation on dust grains	Hollenbach & McKee (1989)
Cosmic ray ionization	Goldsmith & Langer (1978)

(Glover & Mac Low 2006ab)

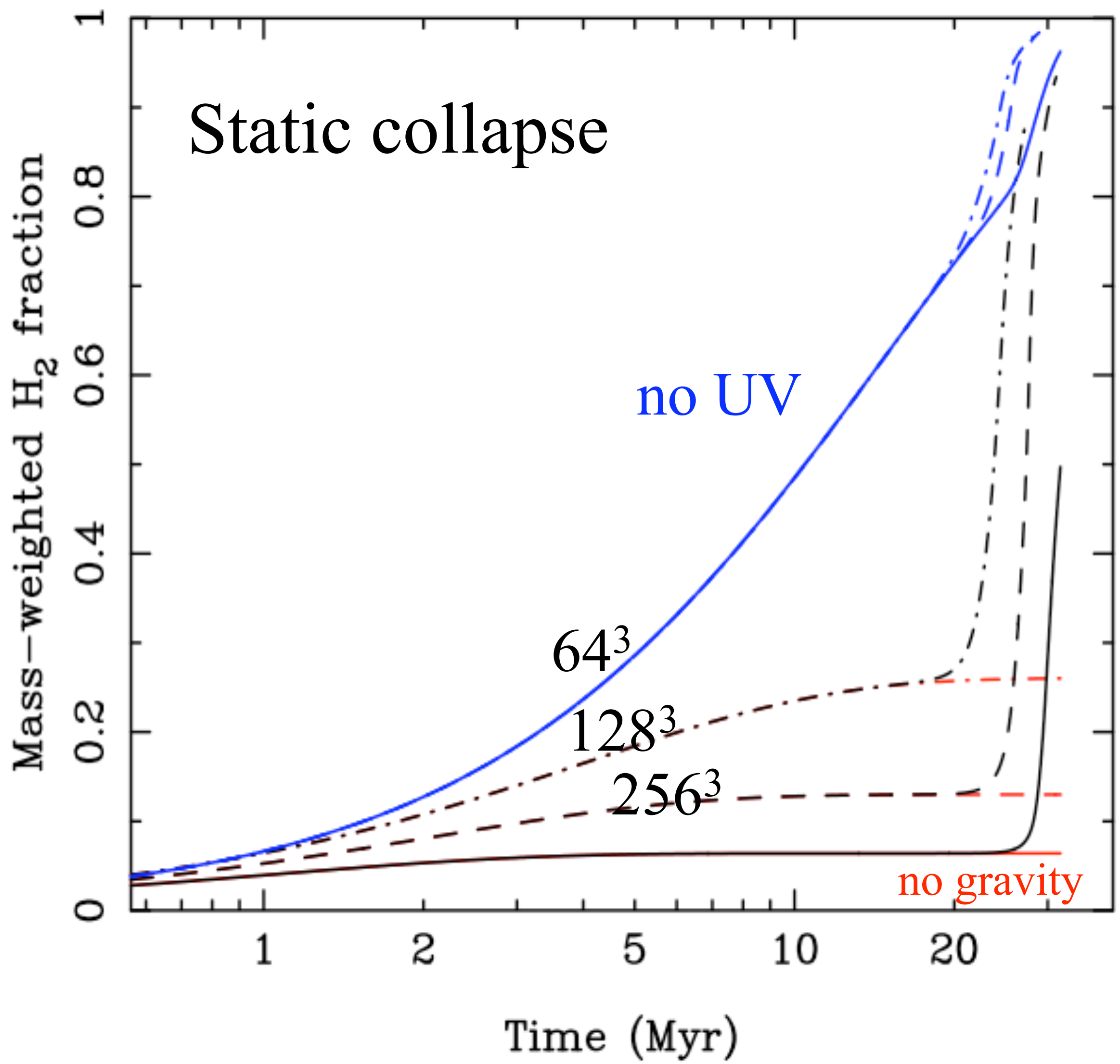

L = 40 pc, n_0 = 100 cm-3, B_0 = 5.85 mG, v_{rms} = 0.0

(Glover & Mac Low 2006a)

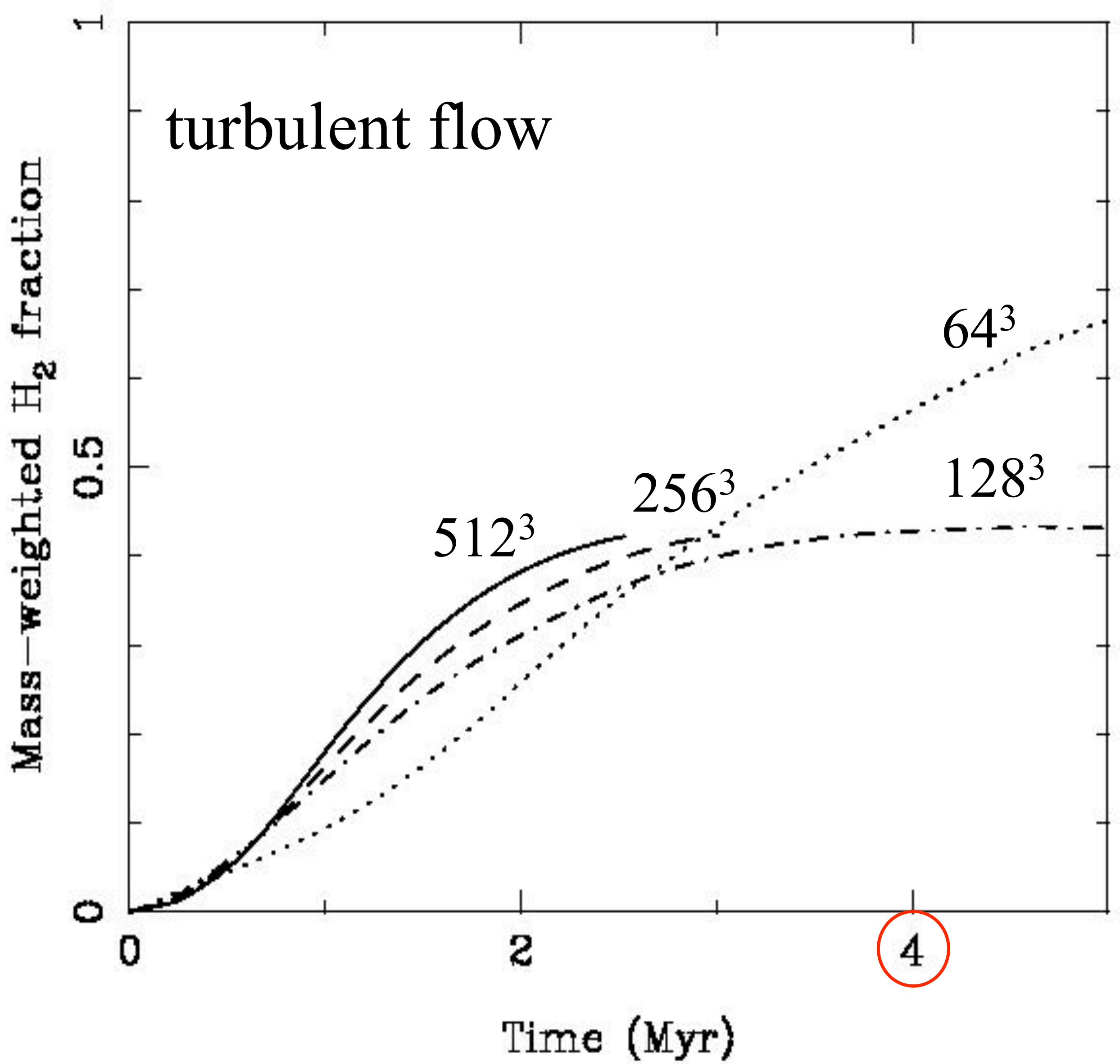

L = 20 pc, B_0 = 5.85 mG, v_{rms} = 10 km/s

(Glover & Mac Low 2006a)

Phases of interstellar matter

Das molekulare Gas

H_2, CO, ...

Transitions of two-atomic molecules

a) Rotational transitions (needs dipole moment)
b) Ro-vibrational transitions
c) Electronic Ro-vibrational transitions

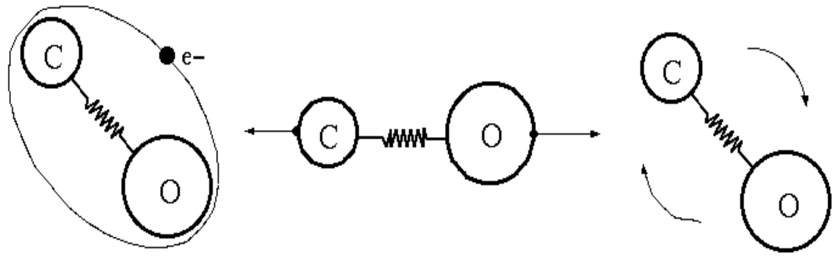

c) b) a)

Abbildung 7.2: *Energie von (a) H_2^+ (b) H_2 als Funktion des Abstands r der Kerne relativ zum Bohrschen Radius a_o.*

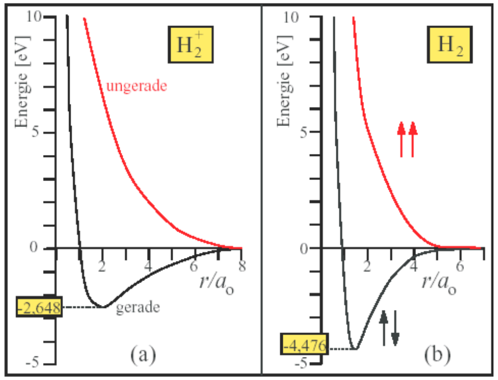

Abbildung 7.3: *Rotations- und Vibrationsniveaus eines zweiatomigen Moleküls mit den nach den Auswahlregeln möglichen Übergängen.*

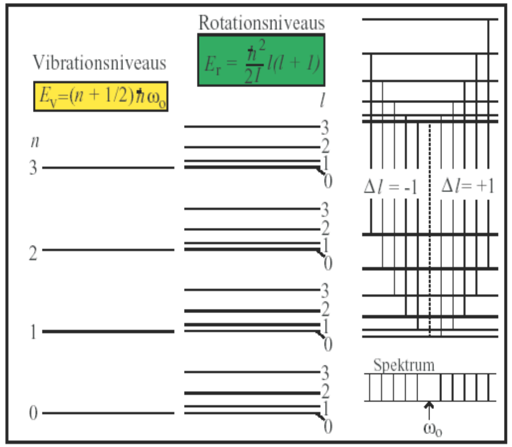

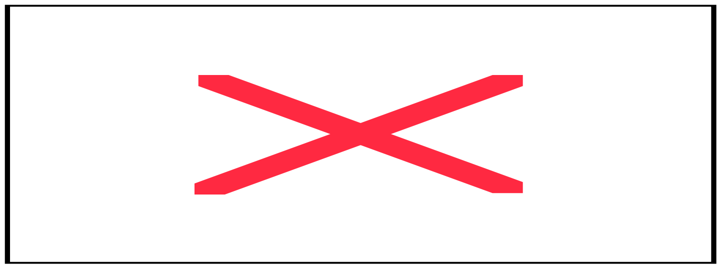

Niedrigste Rotations- und Schwingungsübergänge

	J = 1 – 0			n = 1 - 0		
	Frequenz	Wellenlänge	T	Frequenz	Wellenlänge	T
H_2	3,87 THz	77 µm	185 K	131 THz	2,28 µm	6300 K
^{12}CO	115 GHz	2,6 mm	5,5 K	64 THz	4,63 µm	3100 K

Phases of interstellar matter

Molecular Gas

Global properties of molecular clouds

	Temperature	Density	Radius	Mass	velocity gradient	E_{rot}/E_{pot}
diffuse molecular clouds (10 ... 50% of total H_2 mass)	T = 40 ... 80 K	n = 100 cm^{-3}				
Dark clouds/globules	T = 20 ... 40 K	n = 10^3 ... 10^4 cm^{-3}	R = 0,1 ... 5 pc	1 ... 10 $M_\odot$	0,5 ... 4 km/s/pc	10^{-3}... 0.3
Giant molecular clouds	T = 10 ... 50 K	n = 10^4 ... 10^6 cm^{-3}	R = 10 ... 100 pc	10^3 ... 10^6 $M_\odot$	0,1 ... 0,2 km/s/pc	10^{-4}... 0.1
Hot cores in MCs	T = 100 ... 300 K	n > 10^7 cm^{-3}	R < 0,1 pc	10 ... 100 $M_\odot$		

Giant molecular clouds are strongly concentrated in the galactic plane and towards the center of the Galaxy (similar holds for external galaxies)

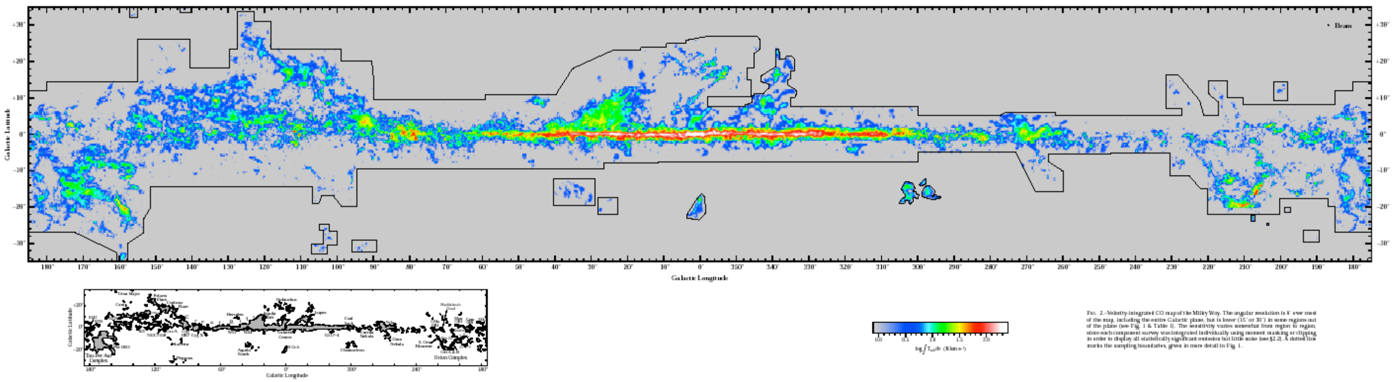

CO Survey of Milky Way
(Dame et al. 2001)

Wall posters available from authors : Thomas Dame : tdame@cfa.harvard.edu

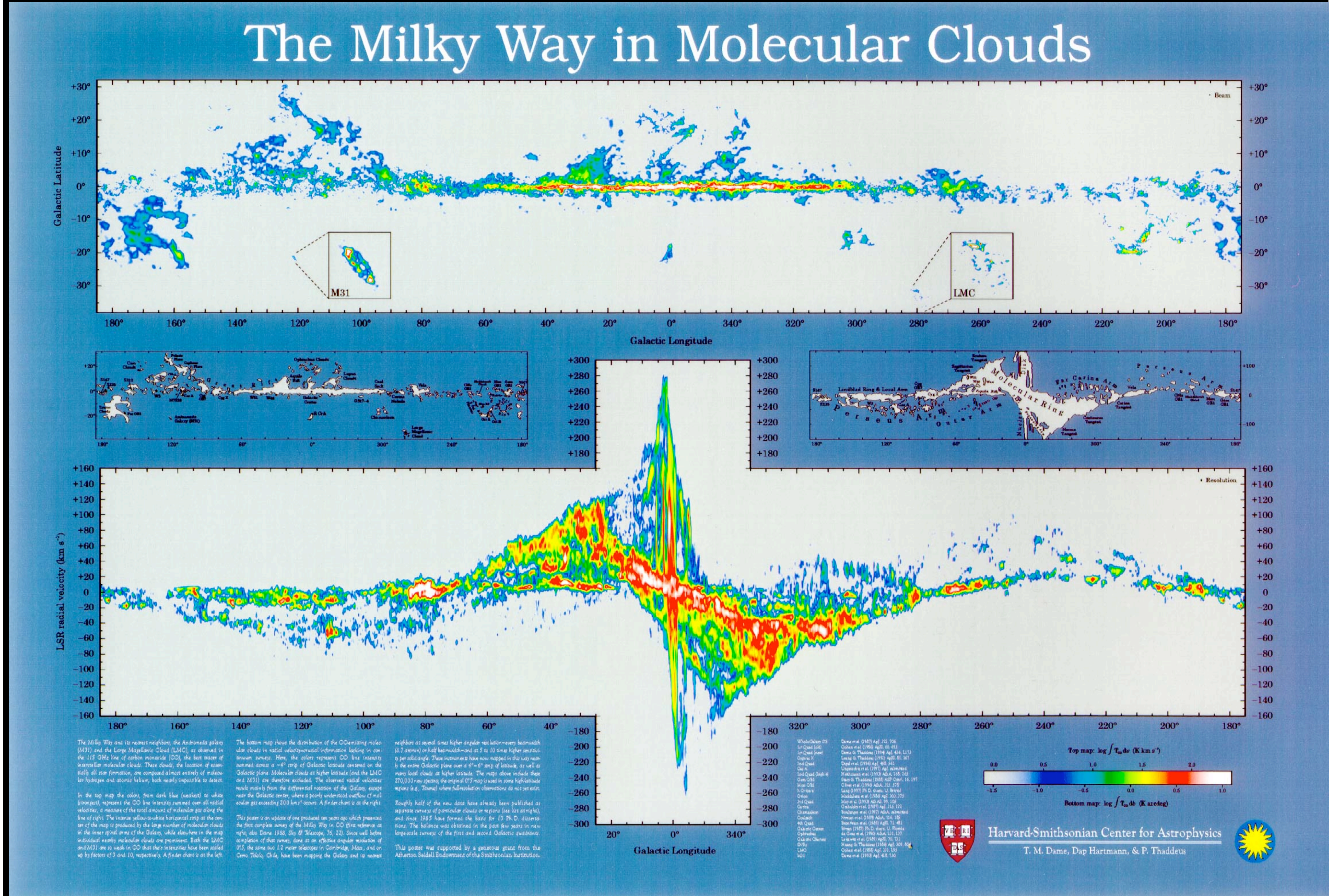

Data from Thomas Dame, CfA Harvard

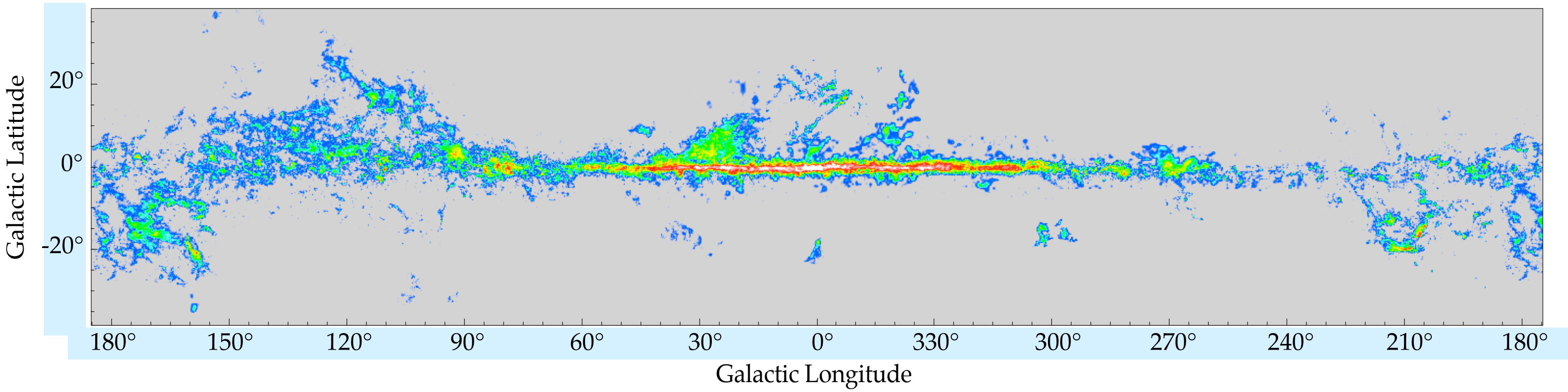

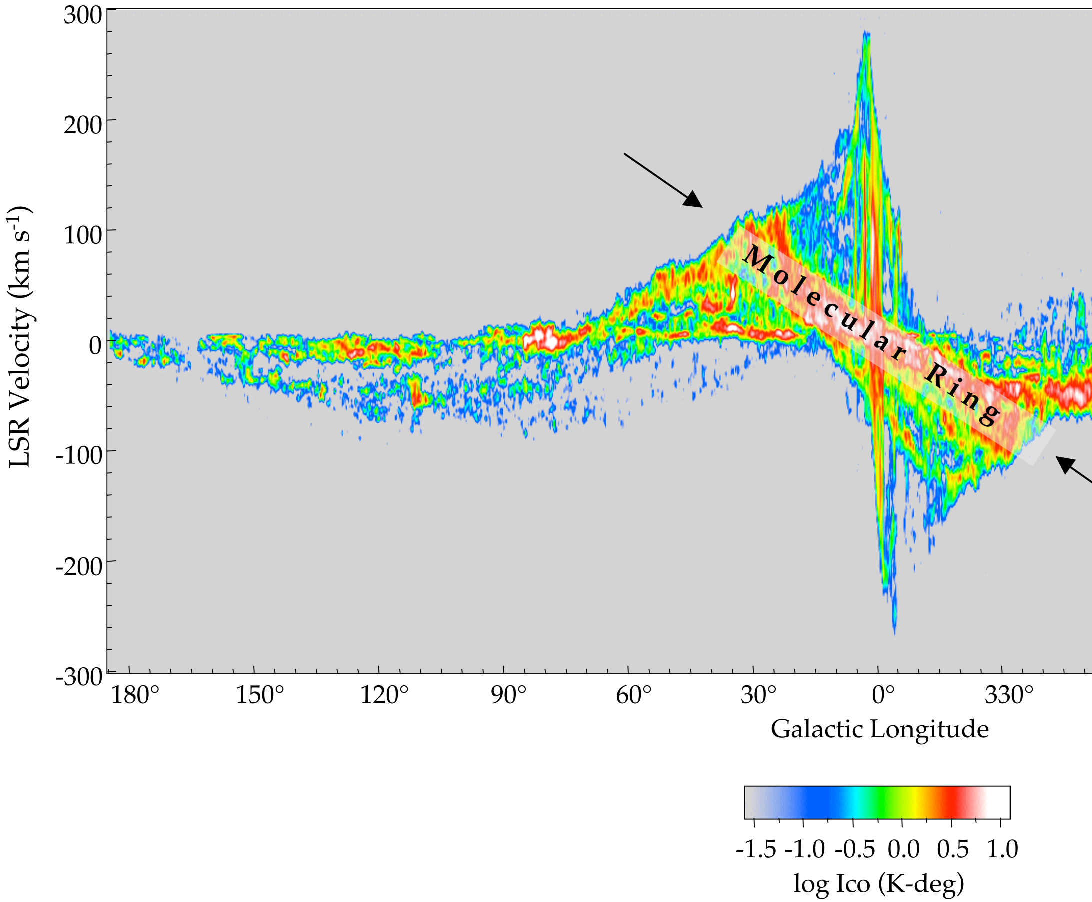

M_{tot} (H_2) ~ 1.3 x 10^9 M_o

M_{tot} (H I) ~ 7 x 10^9 M_o

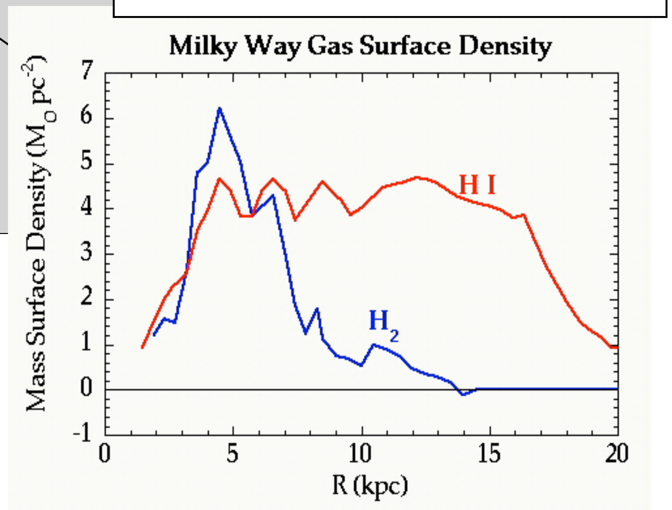

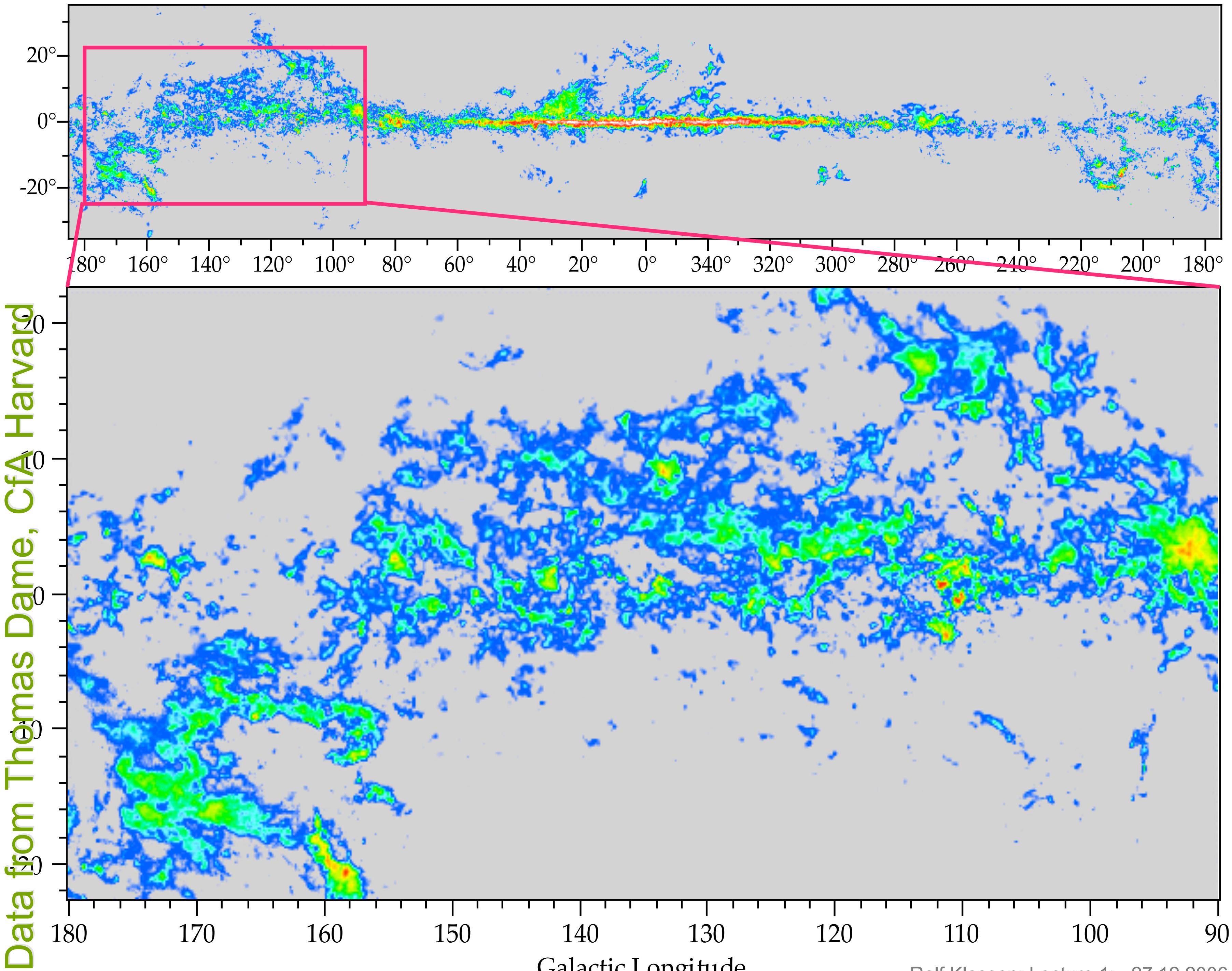
20°
0°
-20°
180° 160° 140° 120° 100° 80° 60° 40° 20° 0° 340° 320° 300° 280° 260° 240° 220° 200° 180°
180 170 160 150 140 130 120 110 100 90
Galactic Longitude
Data from Thomas Dame, CfA Harvard

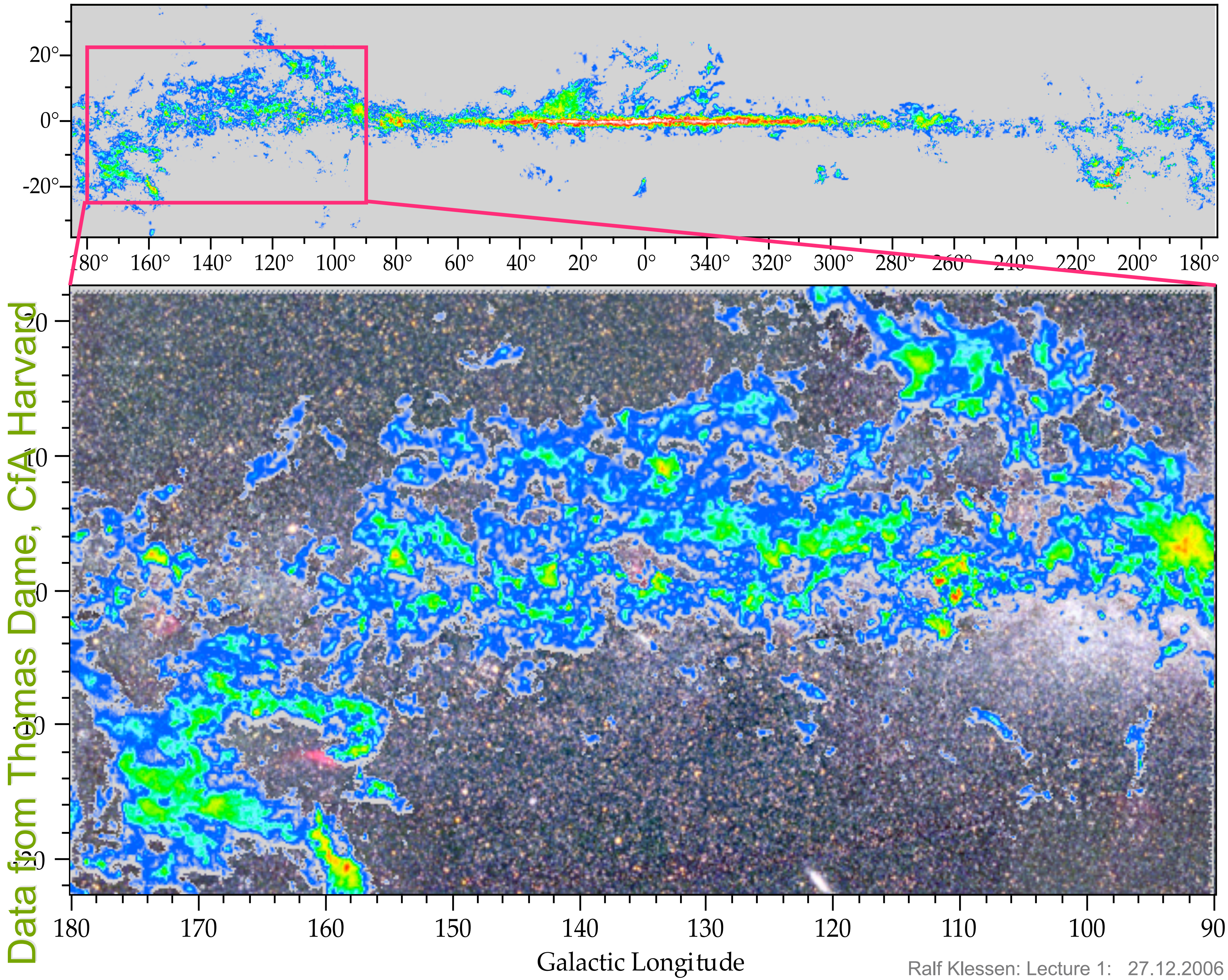
20°
0°
-20°
180°
160°
140°
120°
100°
80°
60°
40°
20°
0°
340°
320°
300°
280°
260°
240°
220°
200°
180°
180
170
160
150
140
130
120
110
100
90
Galactic Longitude
Data from Thomas Dame, CfA Harvard

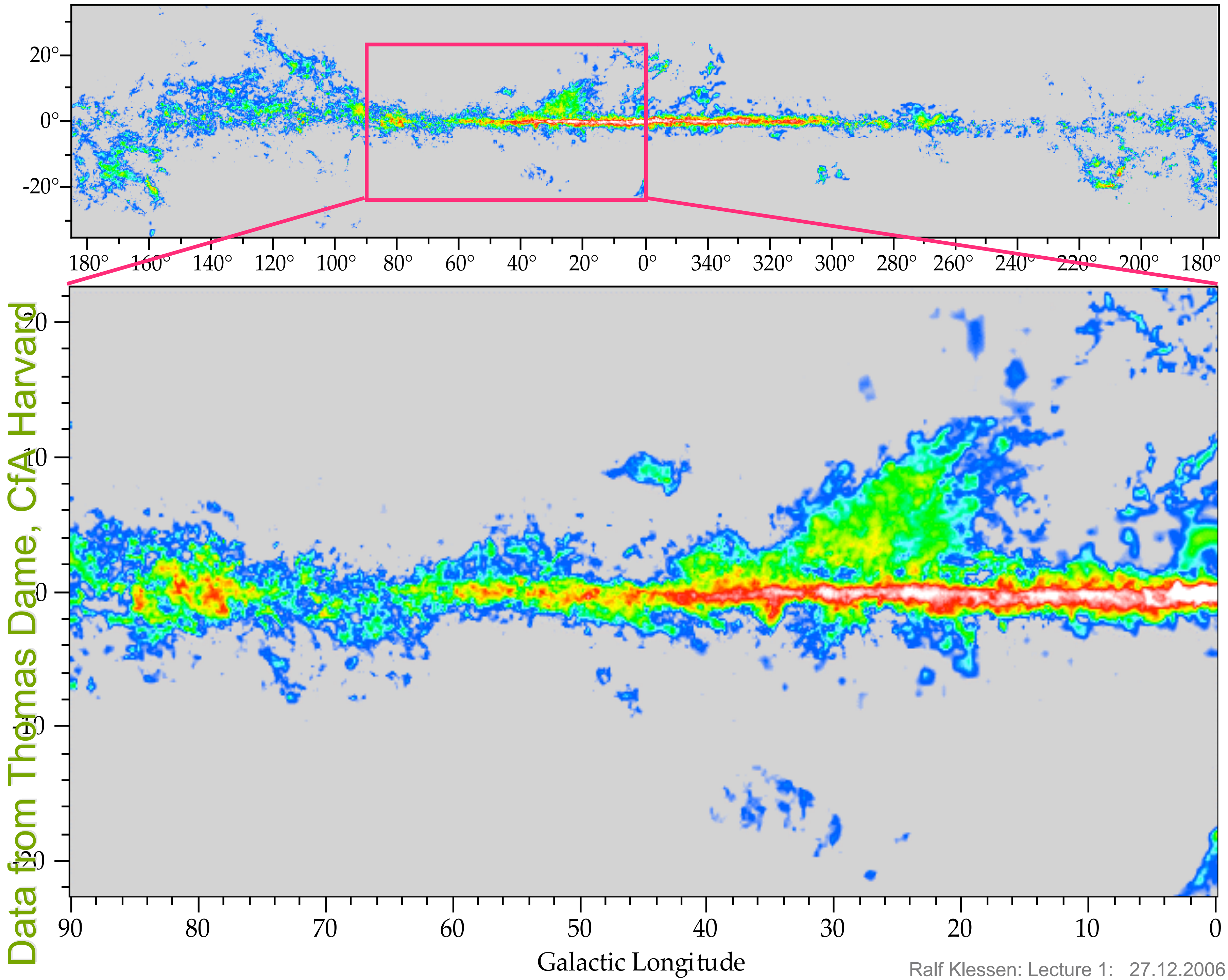

20°
0°
-20°
180°
160°
140°
120°
100°
80°
60°
40°
20°
0°
340°
320°
300°
280°
260°
240°
220°
200°
180°
20
10
0
-10
-20
90
80
70
60
50
40
30
20
10
0
Galactic Longitude
Data from Thomas Dame, CfA Harvard

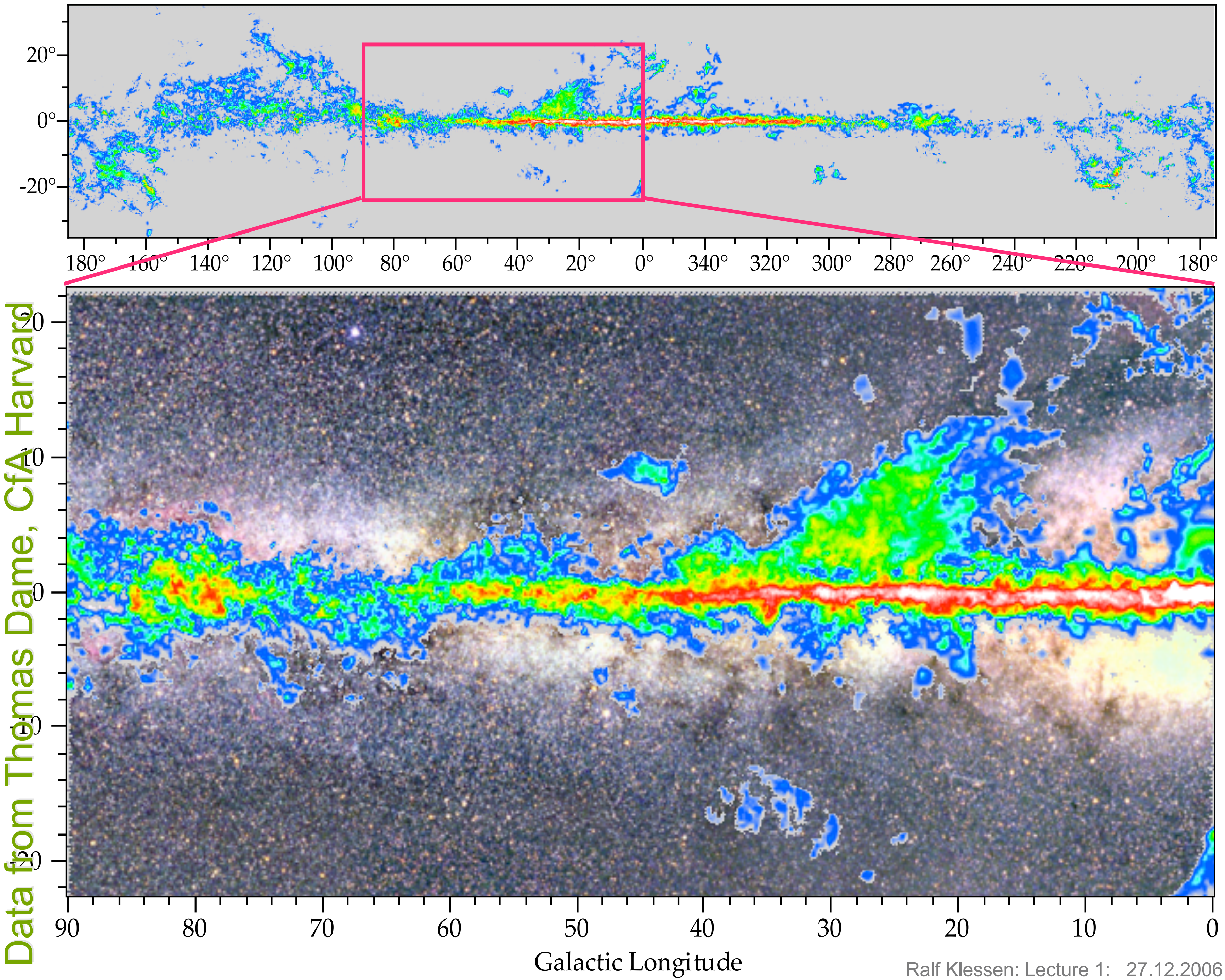
20°
0°
-20°
180° 160° 140° 120° 100° 80° 60° 40° 20° 0° 340° 320° 300° 280° 260° 240° 220° 200° 180°
Data from Thomas Dame, CfA Harvard
90 80 70 60 50 40 30 20 10 0
Galactic Longitude

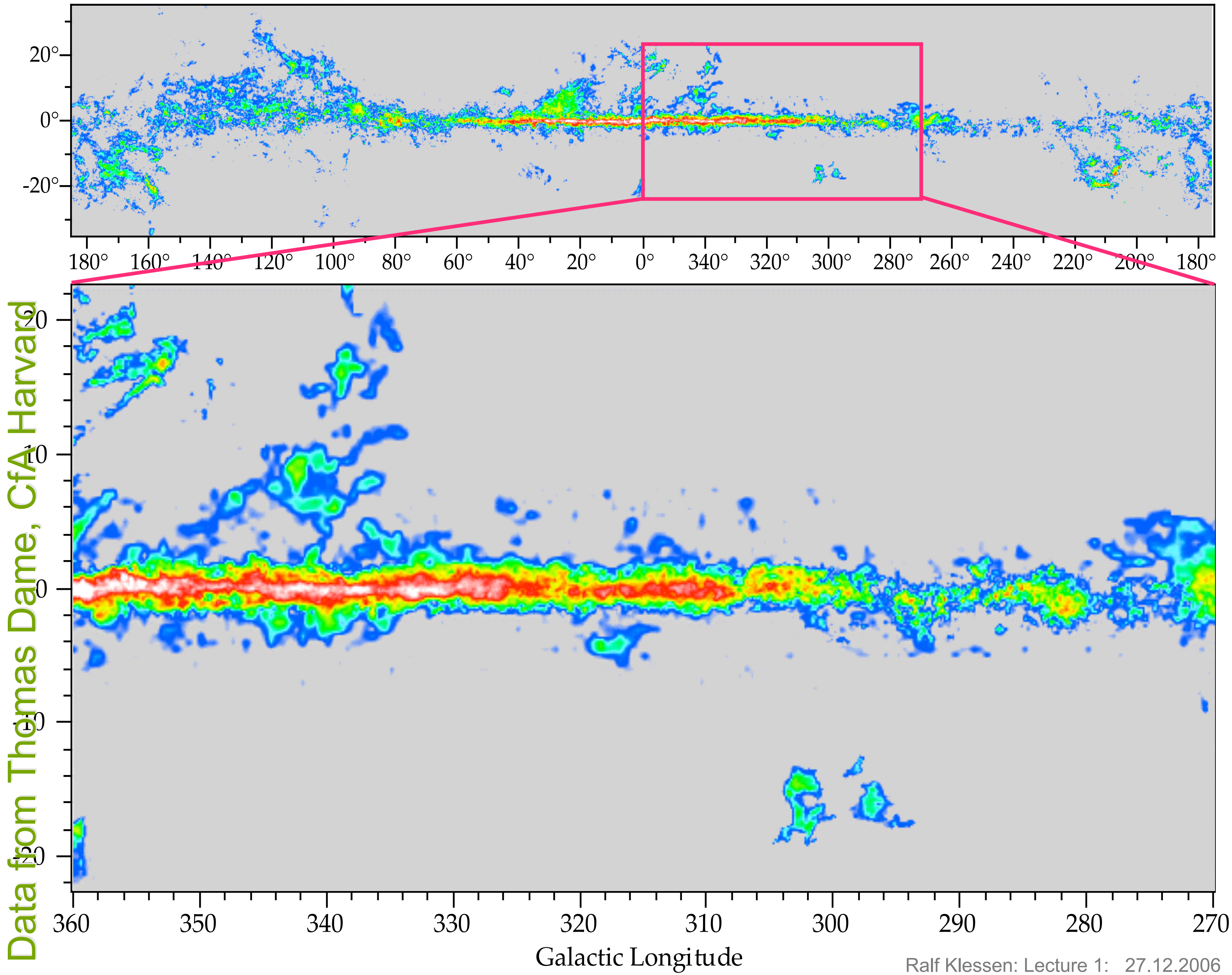

20°
0°
-20°
180°
160°
140°
120°
100°
80°
60°
40°
20°
0°
340°
320°
300°
280°
260°
240°
220°
200°
180°
20
10
0
-10
-20
360
350
340
330
320
310
300
290
280
270
Galactic Longitude
Data from Thomas Dame, CfA Harvard

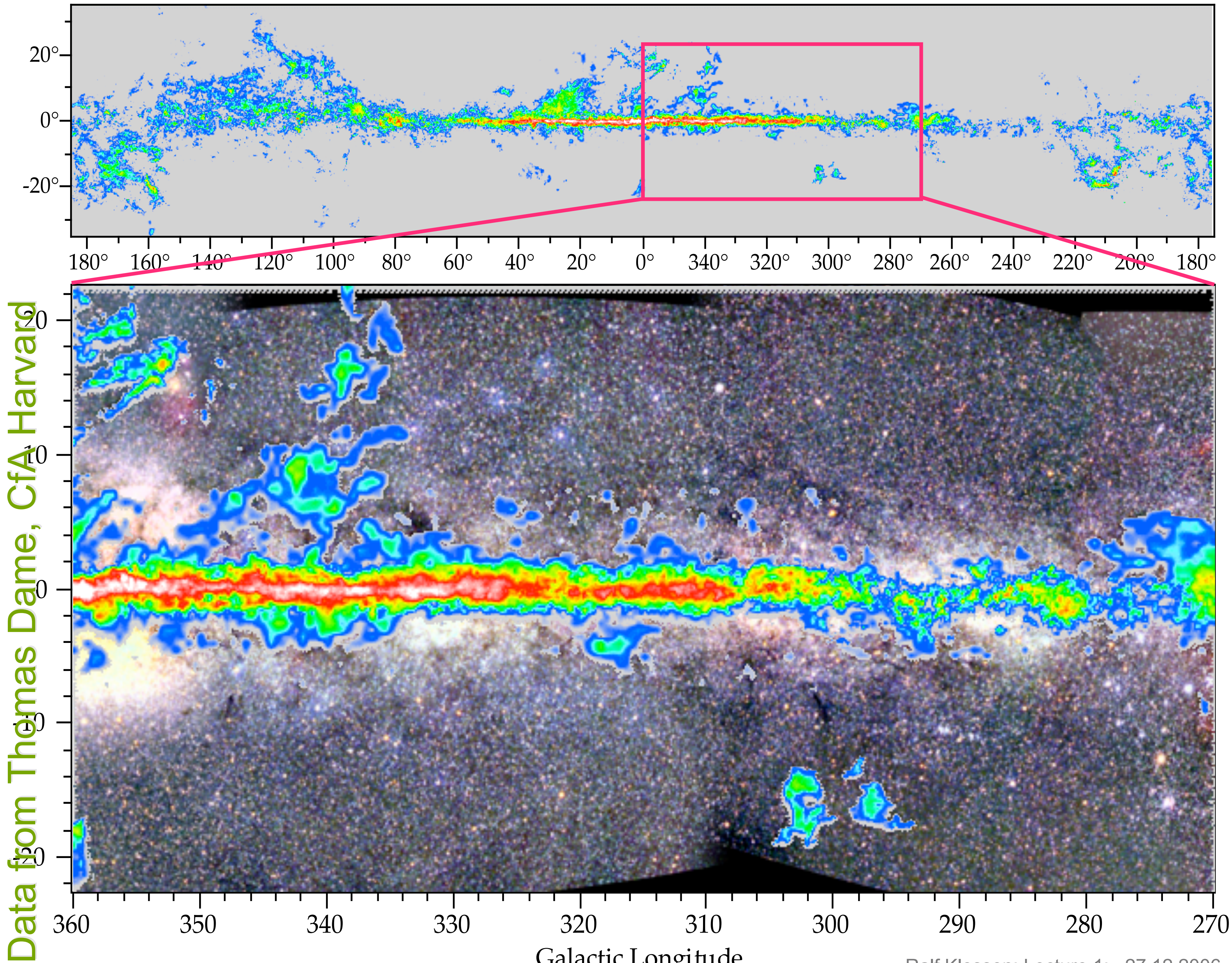

20°
0°
-20°
180°
160°
140°
120°
100°
80°
60°
40°
20°
0°
340°
320°
300°
280°
260°
240°
220°
200°
180°
360
350
340
330
320
310
300
290
280
270
Galactic Longitude
Data from Thomas Dame, CfA Harvard

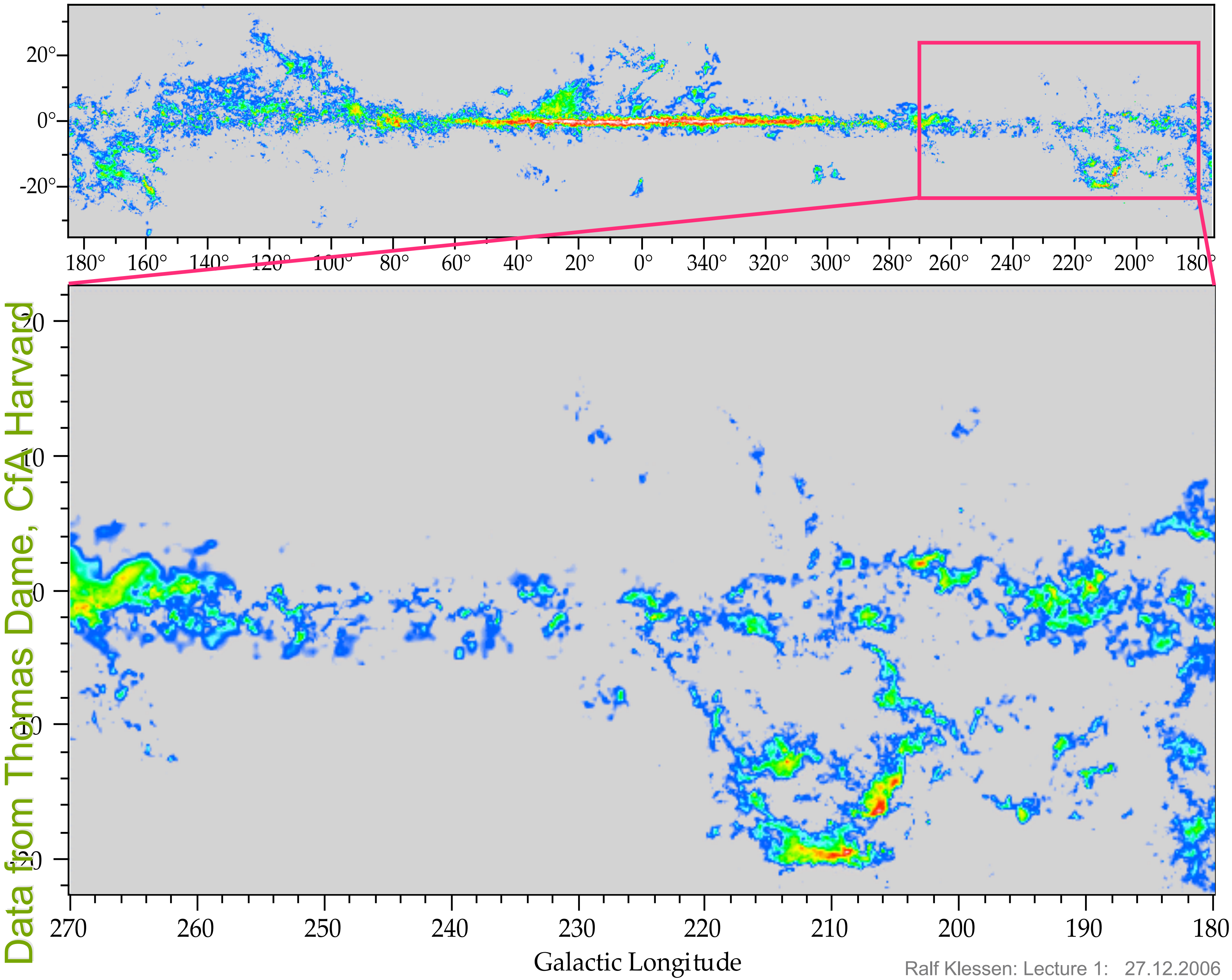

20°
0°
-20°
180°
160°
140°
120°
100°
80°
60°
40°
20°
0°
340°
320°
300°
280°
260°
240°
220°
200°
180°
270
260
250
240
230
220
210
200
190
180
Galactic Longitude
Data from Thomas Dame, CfA Harvard

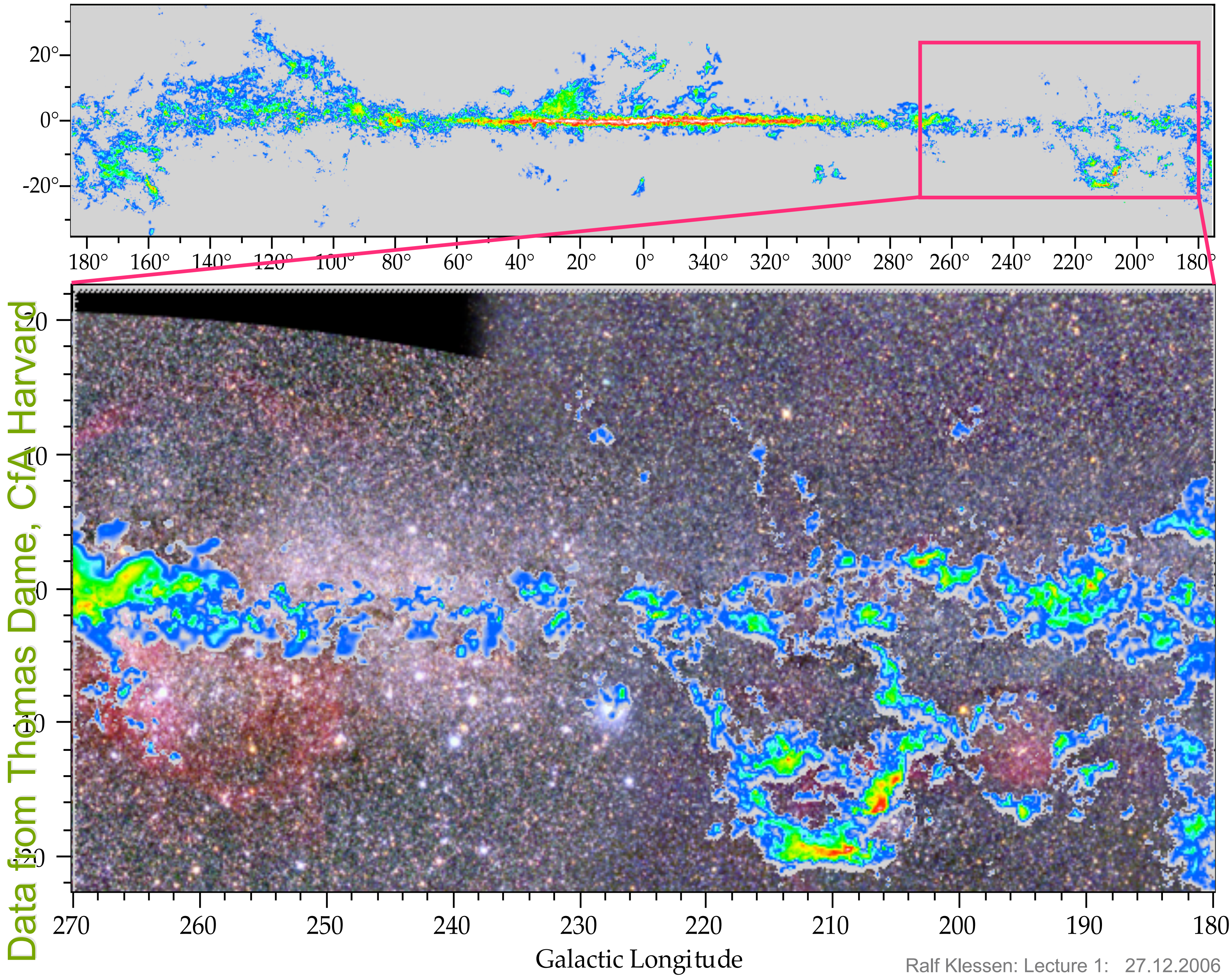

20°
0°
-20°
180°
160°
140°
120°
100°
80°
60°
40°
20°
0°
340°
320°
300°
280°
260°
240°
220°
200°
180°
270
260
250
240
230
220
210
200
190
180
Galactic Longitude
Data from Thomas Dame, CfA Harvard

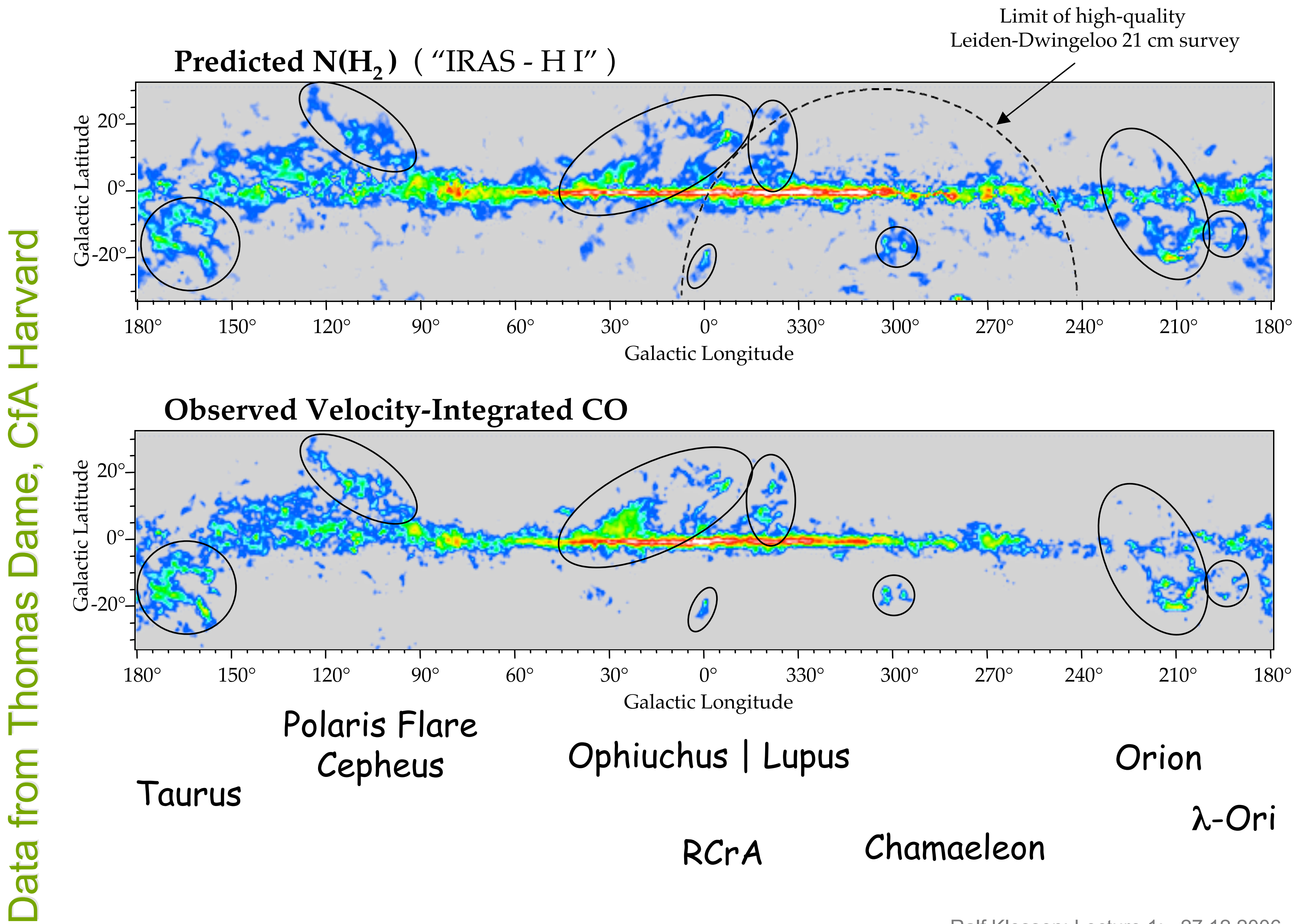
Predicted N(H_2) ("IRAS - H I")
Limit of high-quality
Leiden-Dwingeloo 21 cm survey
Galactic Latitude
20°
0°
-20°
180° 150° 120° 90° 60° 30° 0° 330° 300° 270° 240° 210° 180°
Galactic Longitude
Observed Velocity-Integrated CO
Galactic Latitude
20°
0°
-20°
180° 150° 120° 90° 60° 30° 0° 330° 300° 270° 240° 210° 180°
Galactic Longitude
Polaris Flare
Cepheus
Ophiuchus | Lupus
Orion
Taurus
λ-Ori
RCrA
Chamaeleon
Data from Thomas Dame, CfA Harvard

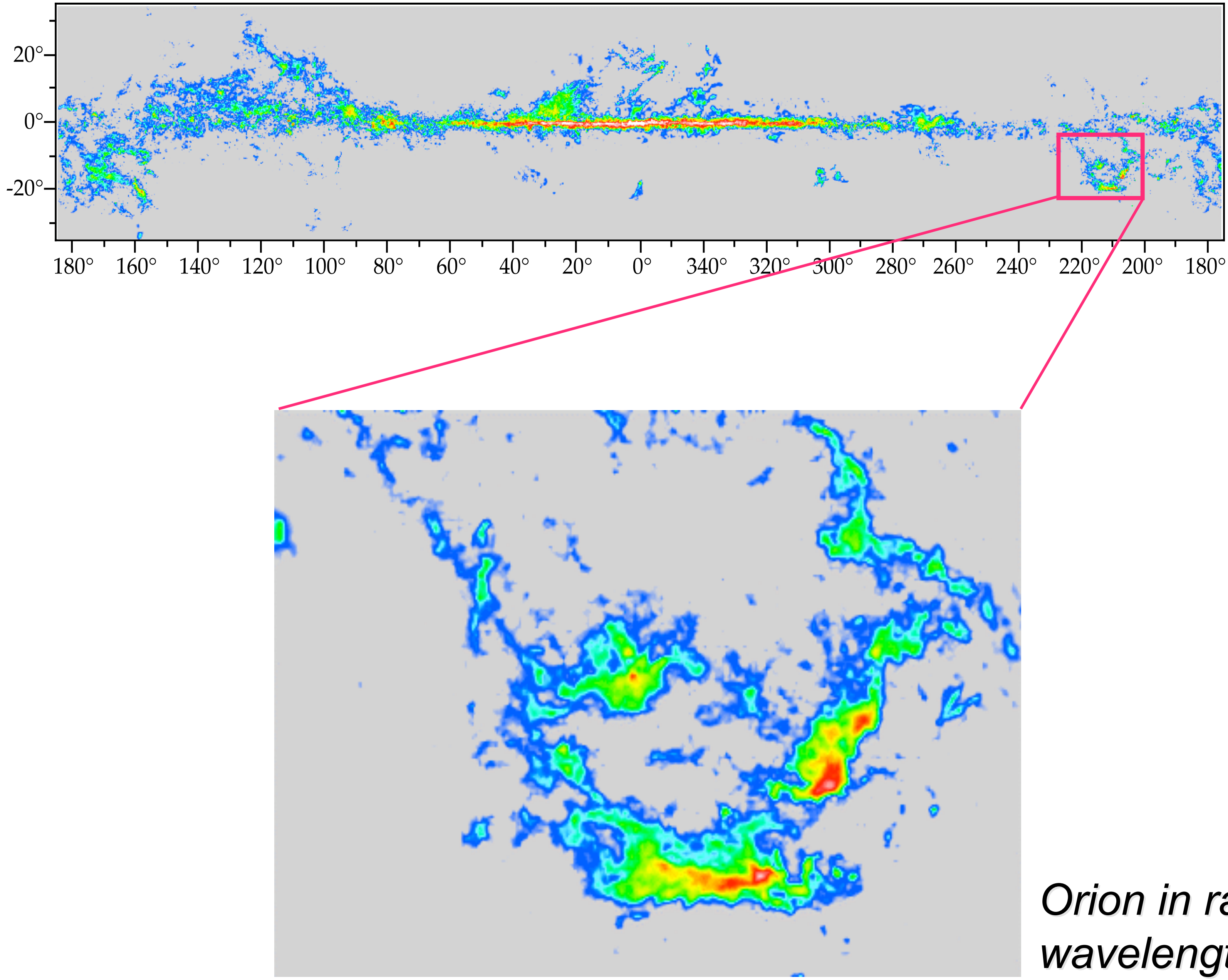

Orion in radio wavelengths

Data from Thomas Dame, CfA Harvard

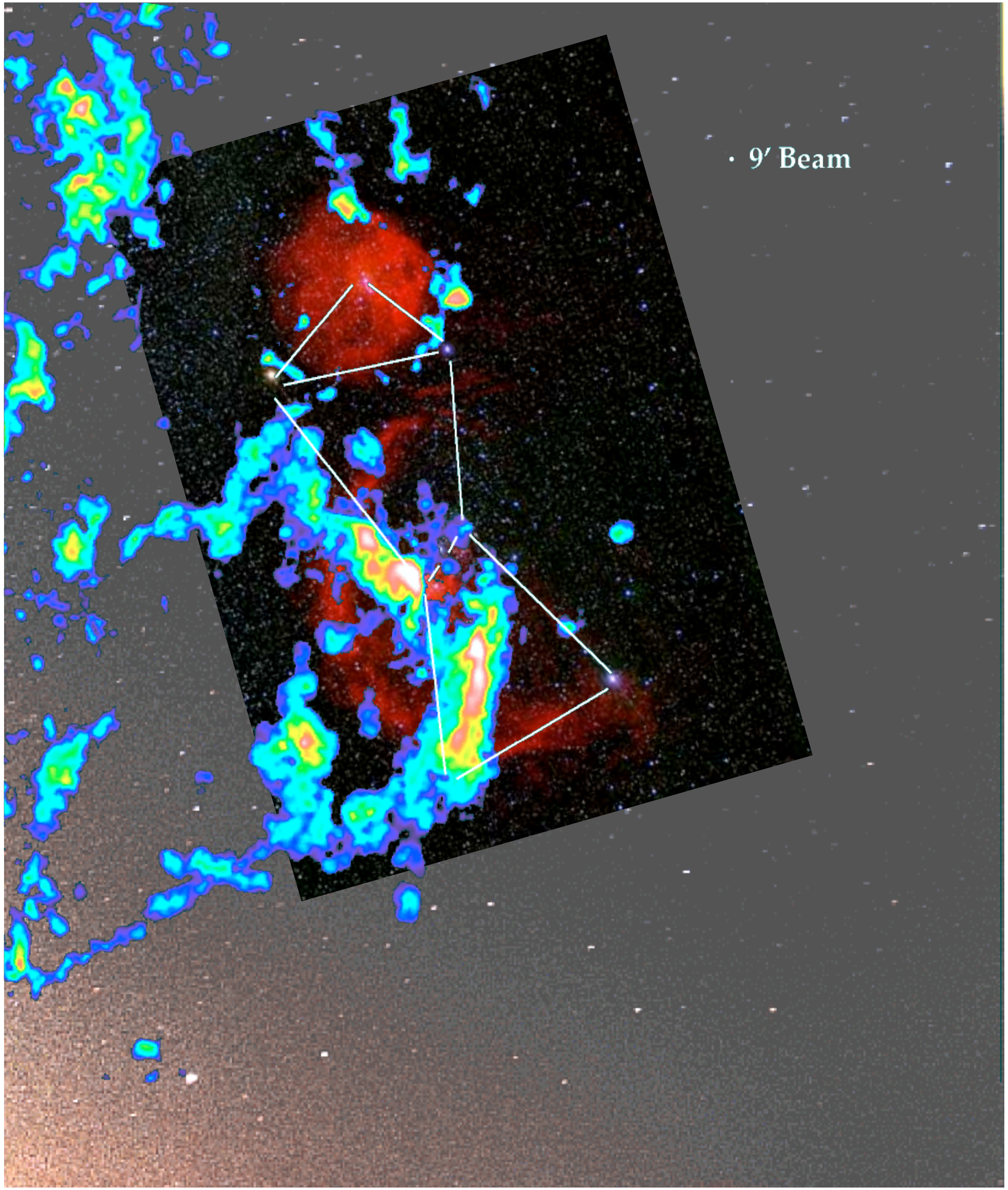

We see

- *stars* (in optical light)
- *atomic hydrogen* (in Hα -- red)
- *molecular hydrogen H_2* (radio -- color coded)

molecular clouds

Properties of Molecular Clouds

- Spatial structure
- Velocity structure
- Thermal structure
- Magnetic field structure
- Larson relations
- The Virial Theorem applied to MC's
- Dynamical evolution

Taurus molecular cloud

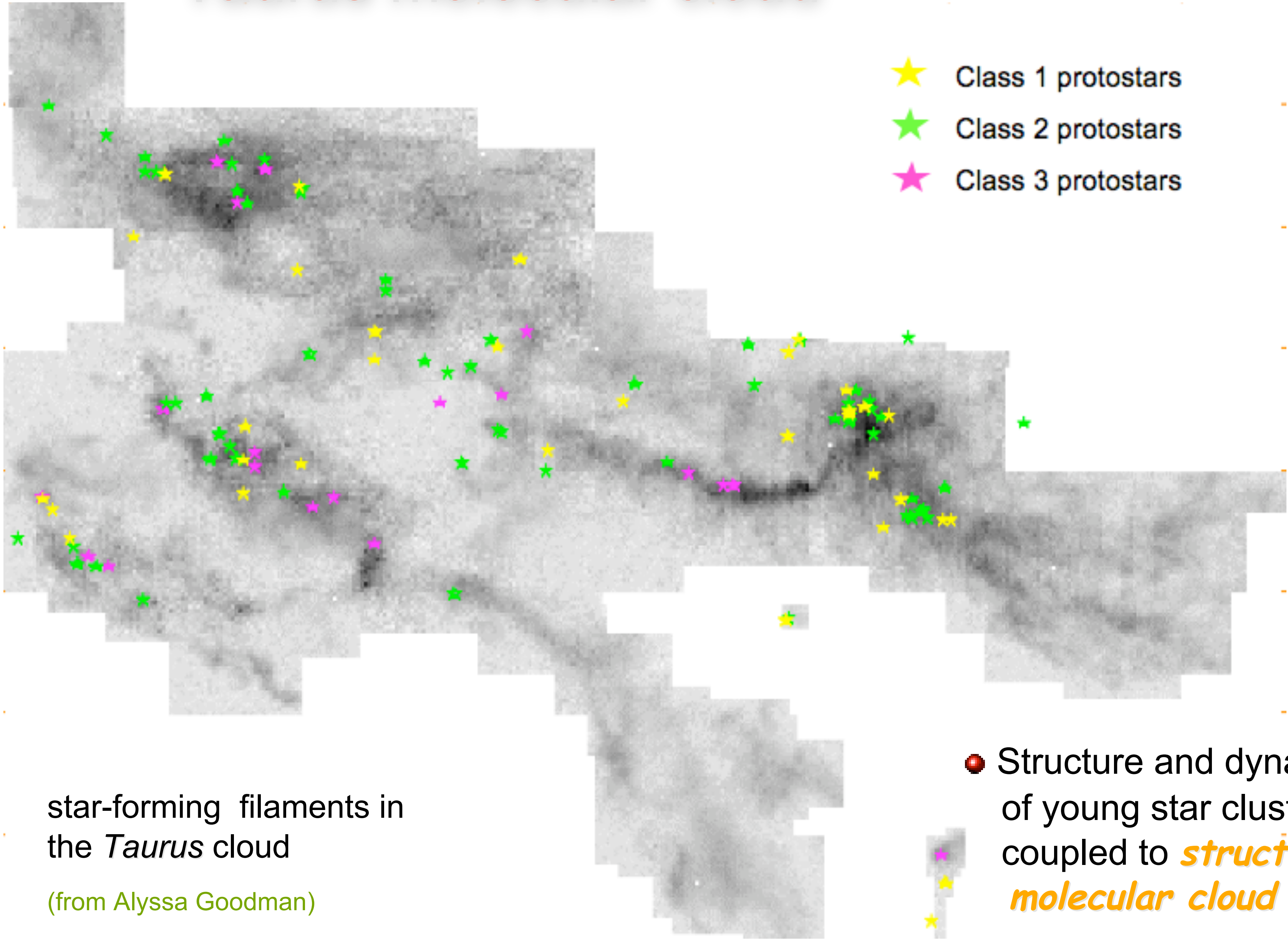

star-forming filaments in the *Taurus* cloud

(from Alyssa Goodman)

- Structure and dynamics of young star clusters is coupled to ***structure of molecular cloud***

Taurus molecular cloud

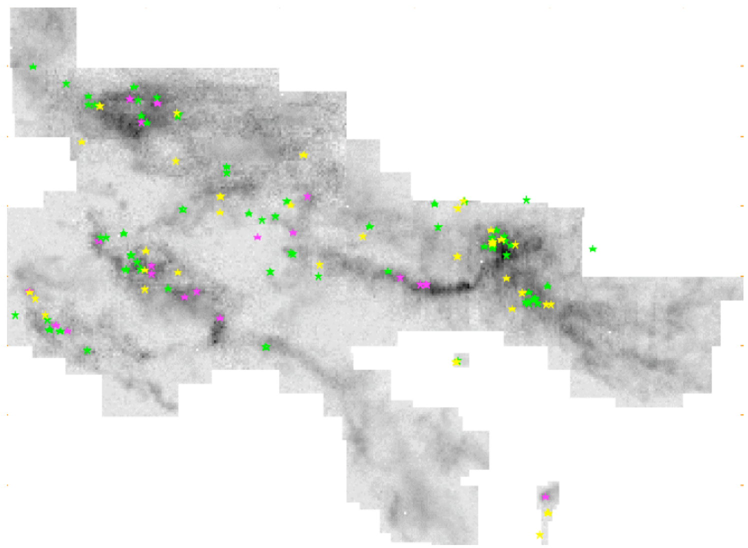

Star-forming filaments in *Taurus* cloud

(from Hartmann 2002)

- Strukture and dynamics of ***molekular cloud*** is determined by ***supersonic turbulence***

- Structure and dynamics of young star clusters is coupled to ***structure of molecular cloud***

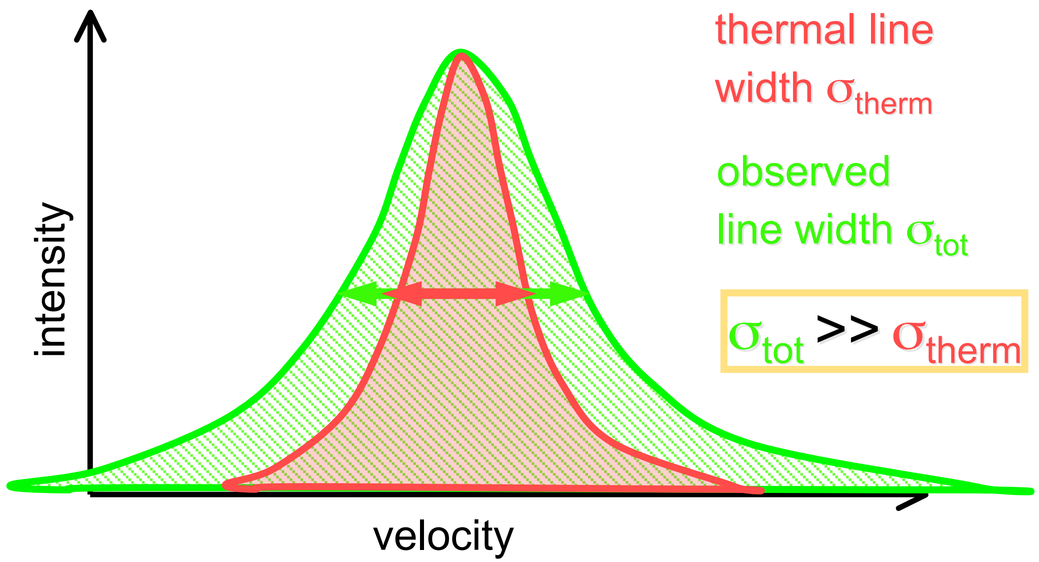

Spatial structure

- extremely complex spatial structure
  - hierarchical / fractal
- low filling factor of dense (star forming) clumps
  - mean densities ~ 100 cm^{-3} BUT in clumps 10^4 - 10^6 cm^{-3}
  - filling factor in volume 5% BUT in mass 50%
- mean density inversely correlated with size: Larson relation
  - $\rho \propto R^{\alpha}$ $\alpha \approx -1$ density size relation
    $\sigma \propto R^{\beta}$ $\beta \approx 1/2$ linewidth size relation
- clump mass spectra follow power law: $dN/dm \propto m^{1.5}$
  - BUT: is that really true (problems: *projection* and *superposition* i.e. PPP vs. PPV)

Chamaeleon 1

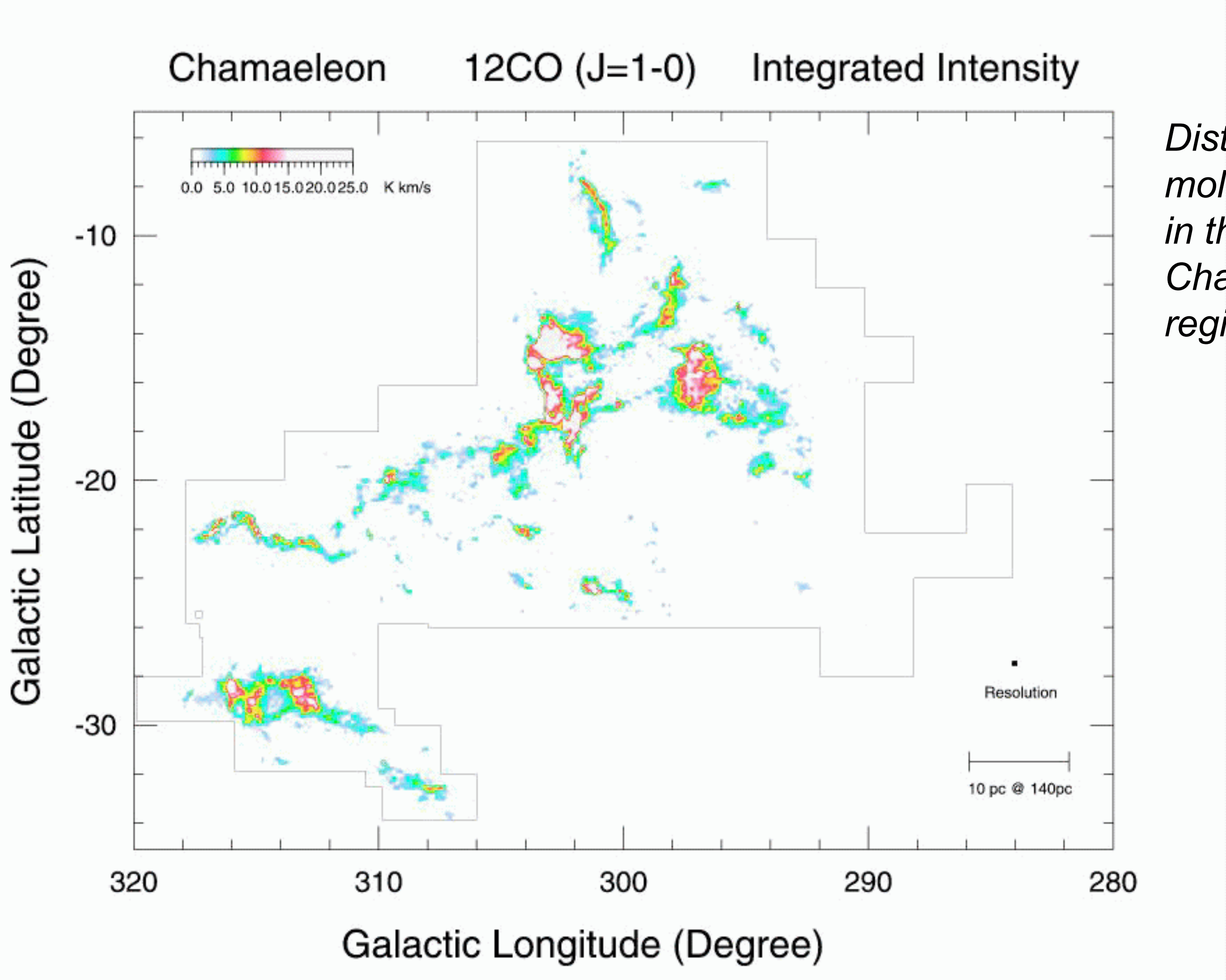

Distribution of molecular gas in the Chamaeleon region

Mizuno et al. (2001)

Chamaeleon 2

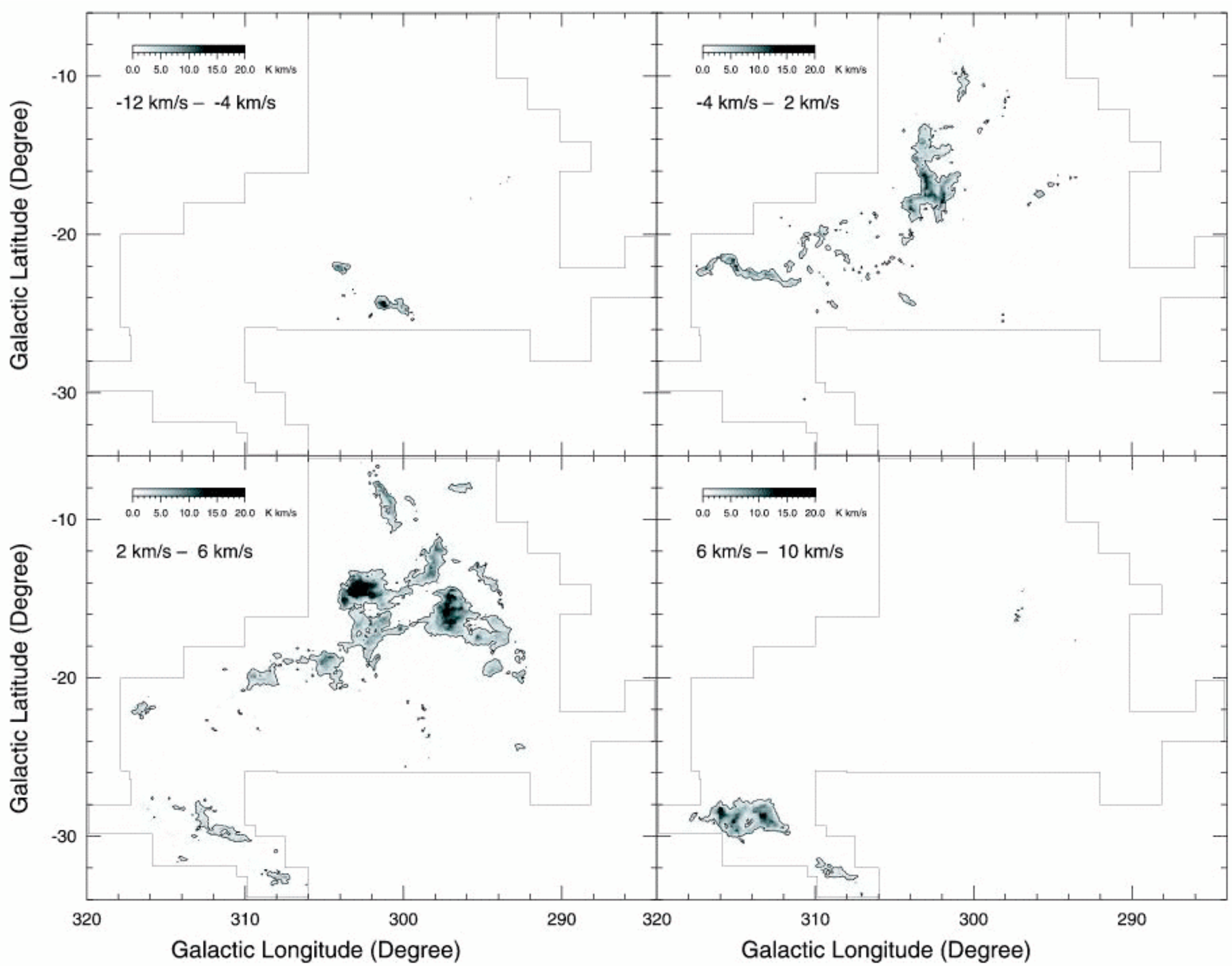

Mizuno et al. (2001)

Distribution of molecular gas in the Chamaeleon region sampled in different velocity bins.

Chamaeleon 3

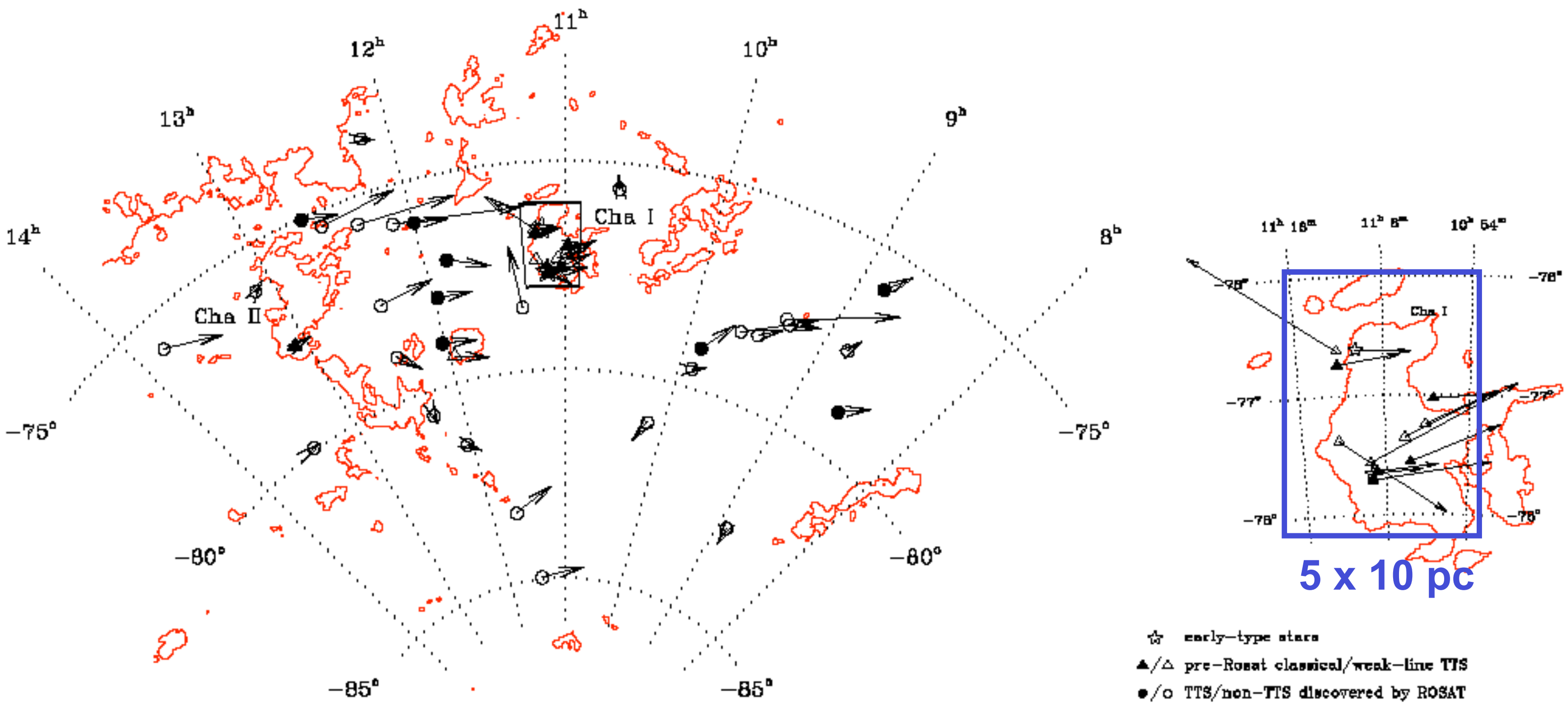

Fig. 1. Positions and proper motions of the stars in Tables 1 and 2. Contours are from the IRAS 100 μm survey. The region around Cha I is shown on an enlarged scale, too. Most of the new ROSAT discovered stars are either located between these two clouds or west of Cha I. 1° corresponds to 50 mas yr^{-1}; the largest arrow in the figure (RXJ 1207.9-7555 between Cha I and Cha II) corresponds to 156 mas yr^{-1}.

Frink et al. (1998)

Distribution of molecular gas and young stars in the Chamaeleon region (only stars with proper motions from Hipparchos)

Taurus

Distribution of molecular gas and young stars in Taurus

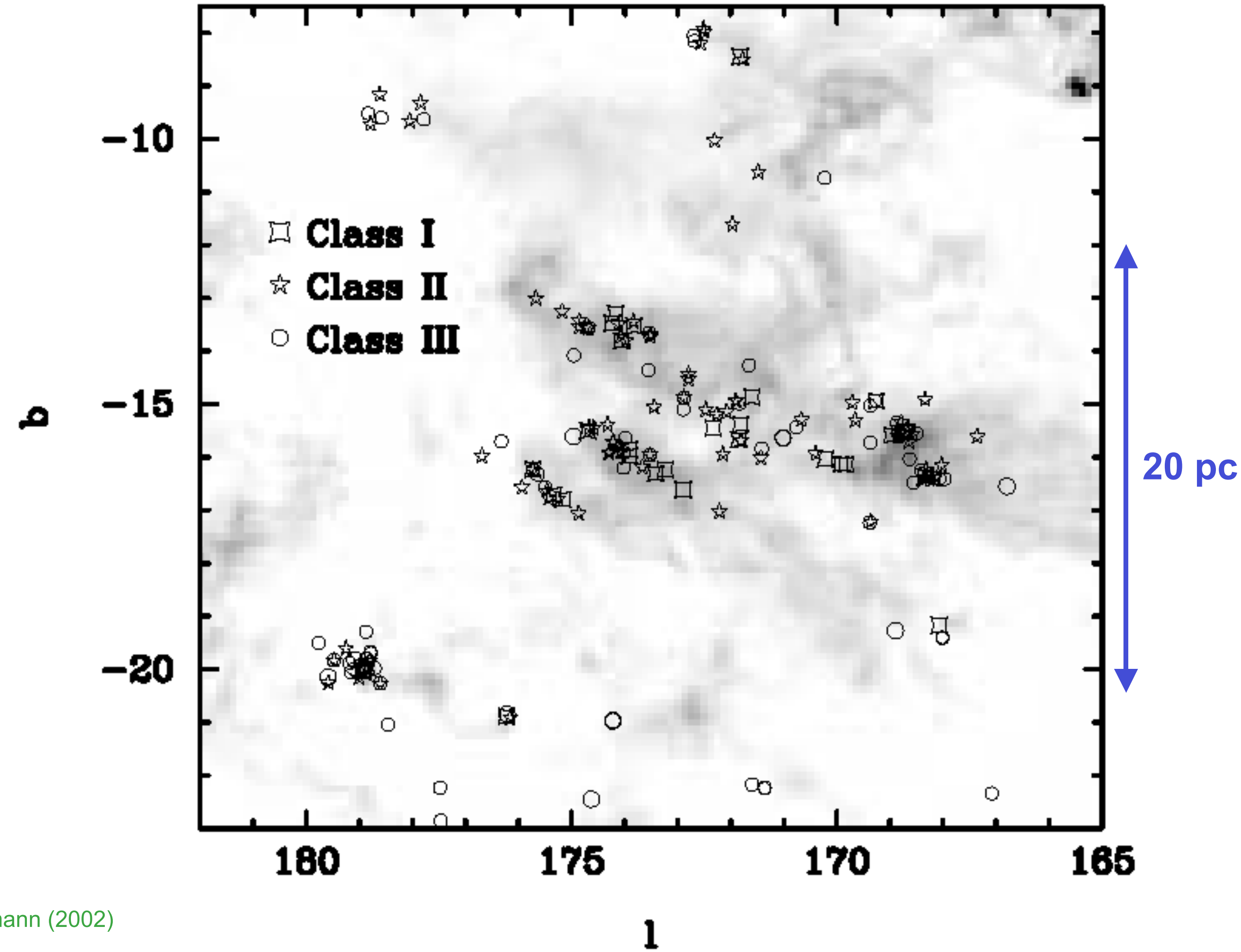

Hartmann (2002)

ρ Ophiuchus

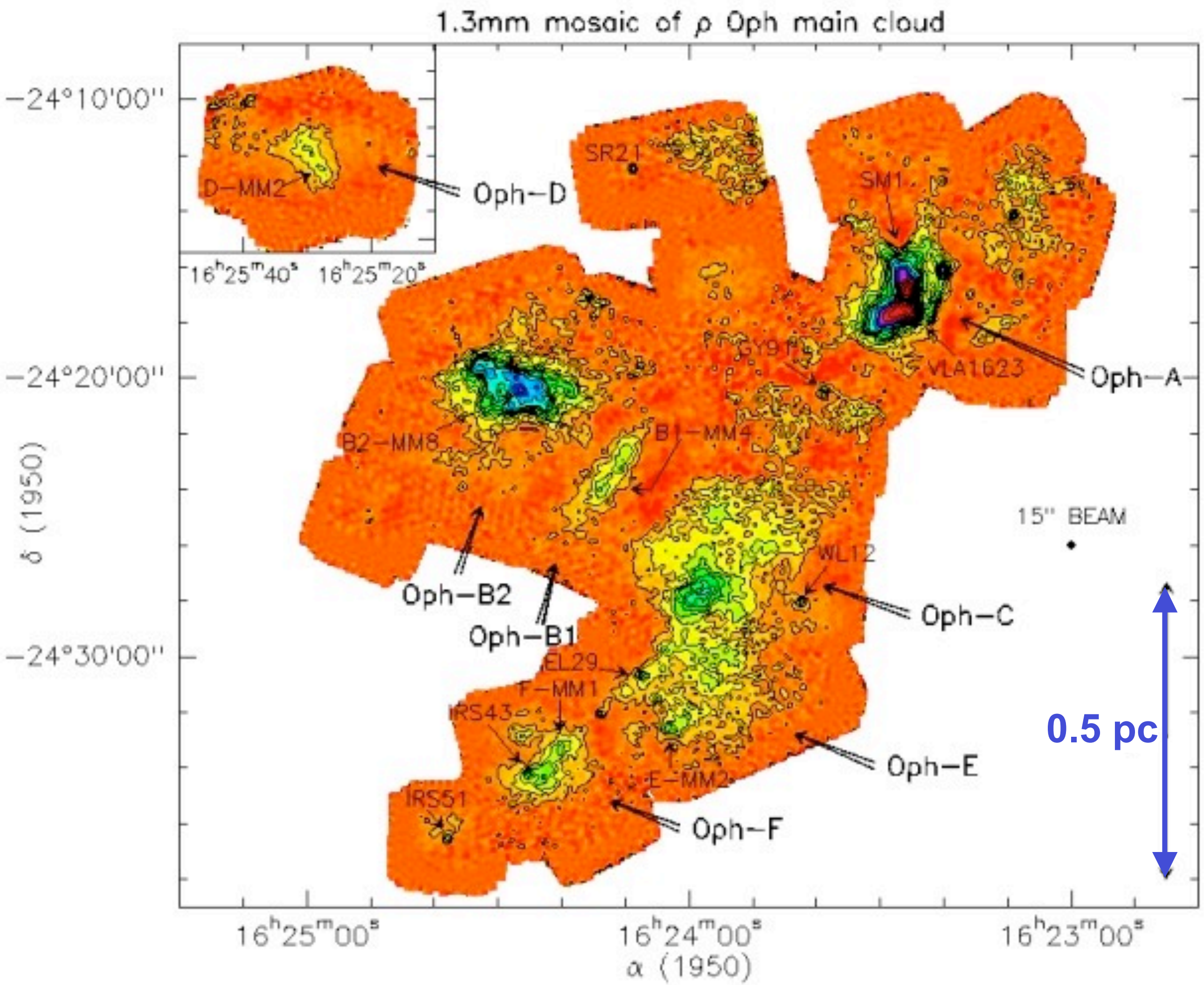

Motte, Andre, & Neri (1998)

Hierarchical density structure

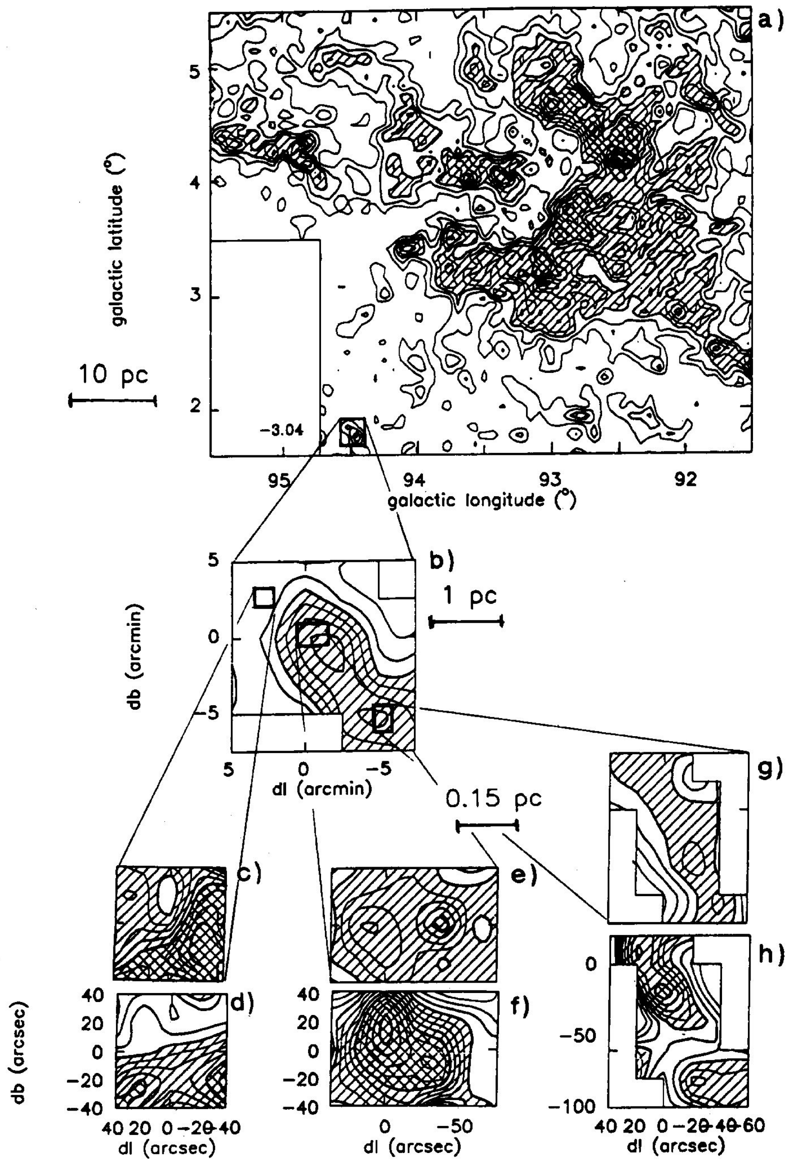

Falgarone et al. (1992, IRAM Key Project)

Molecular clouds exhibit hierarchical density distribution and exhibit complex (possibly fractal) structure down to the smalles scales observable.

What causes this complex structure? (mostly due to interstellar turbulence)

How is it related to the velocity field? (compressible turbulence)

How can it be quantified (measured) in a statistically meaningful sense? (e.g. fractal indices, Δ variance, principle component analysis – PCA, structure functions, etc.
← *NONE* OF THESE MEASURES IS REALLY GOOD!)

Fractal density structure?

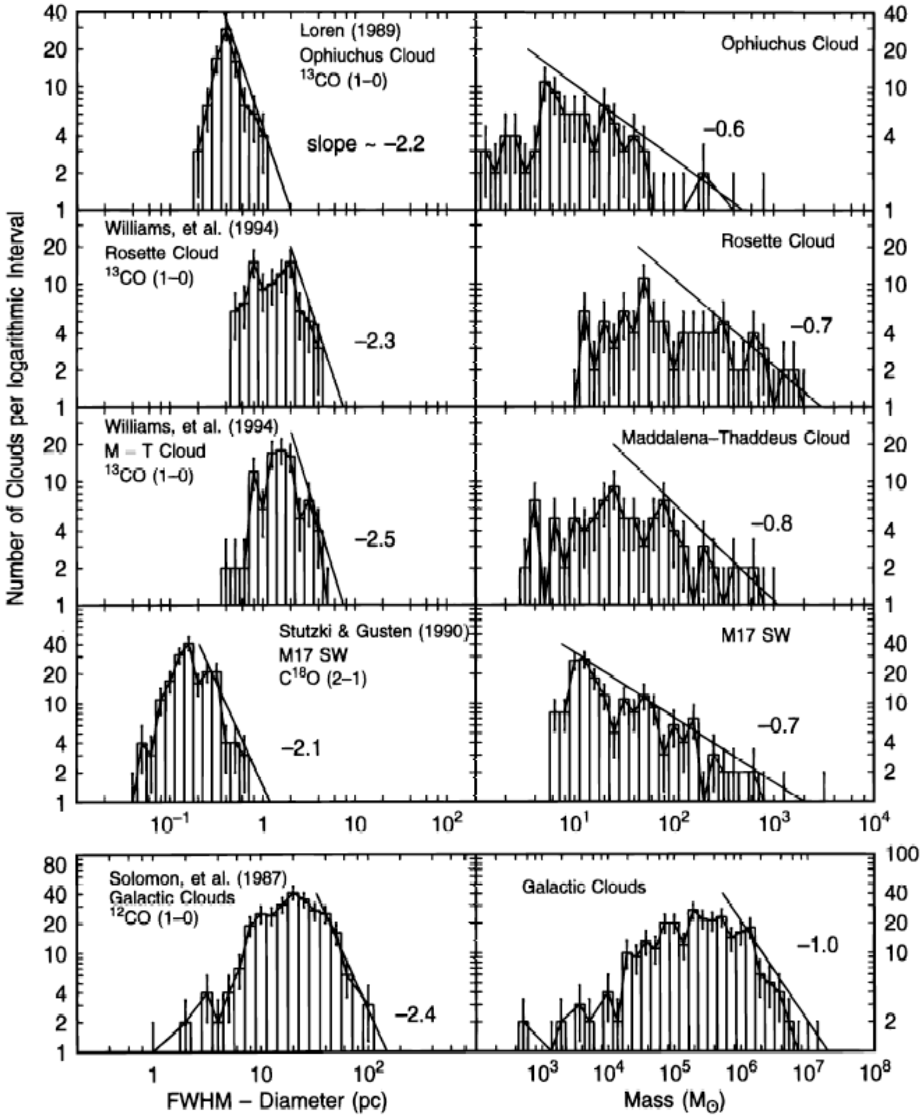

Elmegreen & Falgarone (1997)

Attempts to fit power laws to the observed size distribution (clump-size spectrum) reveal varying (and non-integer) slopes.

Related to Hausdorff definition of fractal index.

However:

- what is really measured?
  (limited dynamic range of tracer molecule)
- 2D projection of real 3D

Clump mass spectra

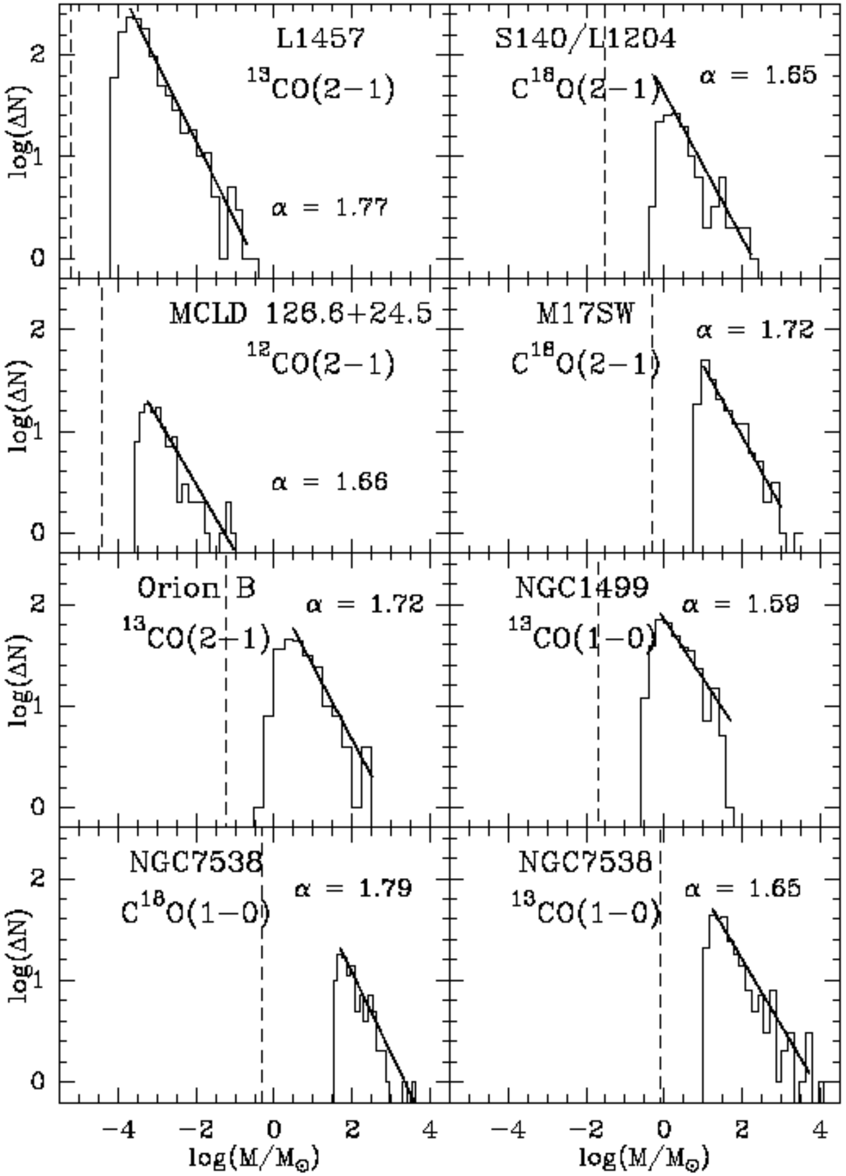

Kramer et al. (1998)

Clump mass spectra exhibit power-law behavior:

$dN/dM \sim M^{-1.5}$

Two main schemes:

- gaussclump (gaussian decomposition)
- clumpfind (identification of connected regions)

BUT: problems with projection render clump mass spectra “meaningless” or at least extremely difficult to interpret physically. (see examples)

Fig. 6. Clump mass spectra of the eight data sets we analyzed. All spectra are fitted by a power law function $dN/dM \propto M^{-\alpha}$. The straight line represents the best linear fit over the range of masses spanned by the line. The resulting indices α lie in the range 1.59 to 1.79. The minimum possible mass M_{min}^{limits}, given by the resolution limits and the rms noise, is denoted by a dashed line for each data set.

Gaussian decomposition

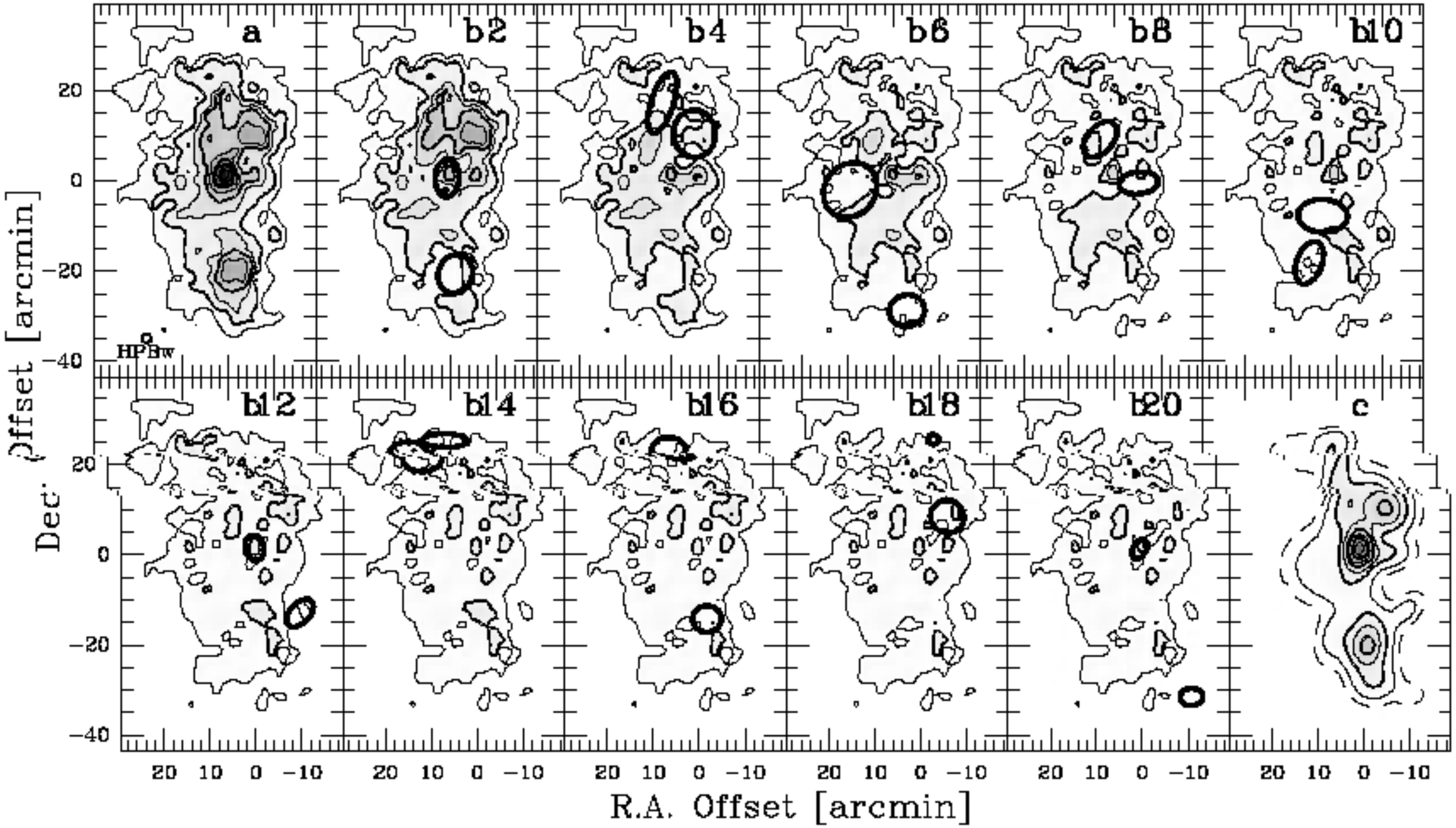

Kramer et al. (1998)

Fig. 1. Orion B South. **a** The original map of integrated $^{13}CO(2\rightarrow1)$ intensities. **b2** to **b20** The maps after subtraction of 2 to 20 clumps by GAUSSCLUMPS (stiffness parameters: $s_0 = 5$, $s_a = s_c = 1$). The spatial (not deconvolved) FWHMs of the last two clumps subtracted are shown. **c** Integrated intensity of the first 20 clumps identified by the algorithm. The range of integration is 0 to 20 $\mathrm{km s^{-1}}$ and contours are at 5.7 (=8σ), 12 by 6 to 60 $\mathrm{K km s^{-1}}$. The dashed contour in **c** is 5% of the maximum. The tiny clump in panel b18 is due to a single channel spike in the corresponding spectrum and is ignored by the follow up analysis of clumps fitted.

Gaussclump by Stutzki et al. (1990)

Search for connected PPV regions

See drawing on black board

Clumpfind by Williams, deGeus, & Blitz (1995)

Problems with clump mass spectra

Ballesteros-Paredes & Mac Low (2002)

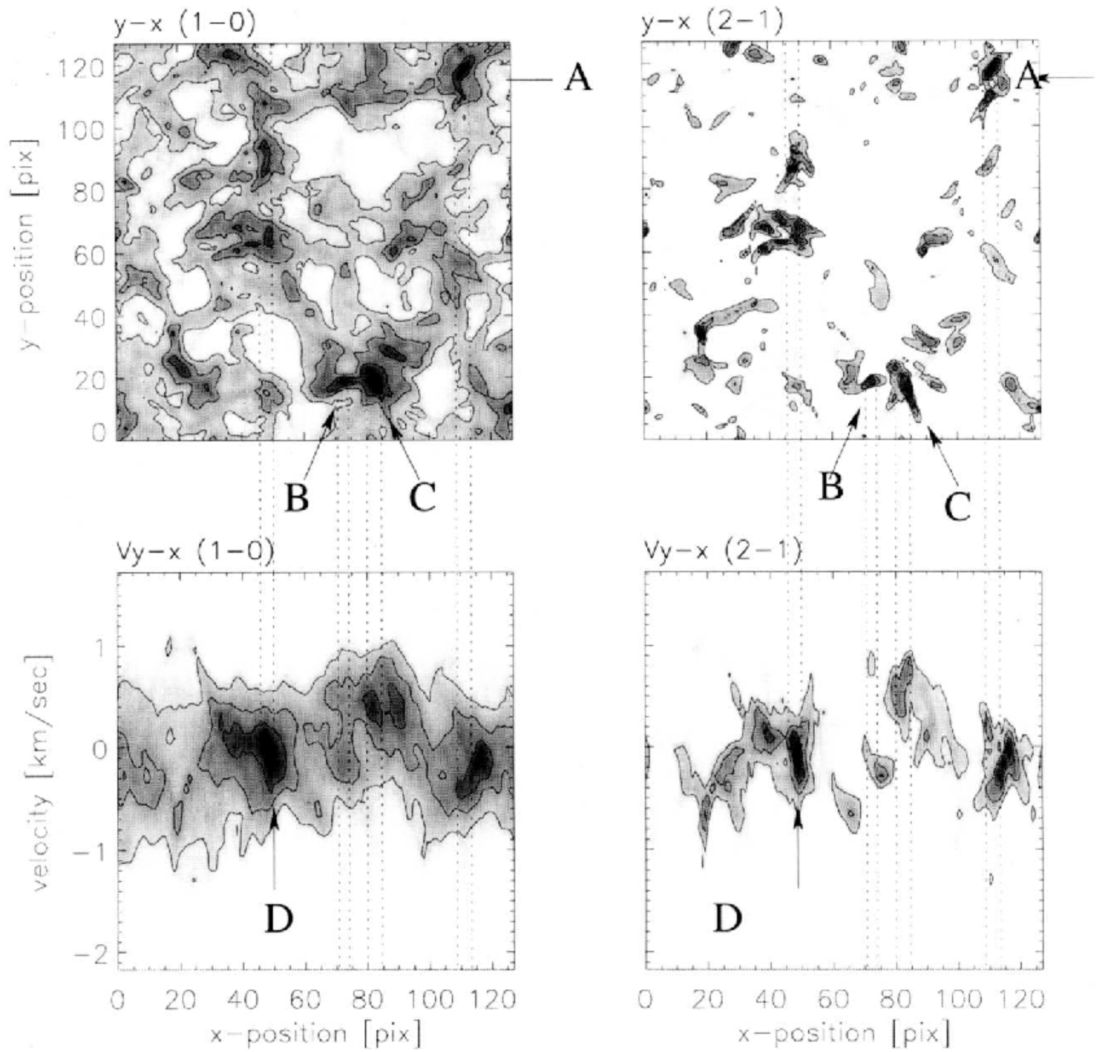

FIG. 6.—Physical and velocity space maps for ^{13}CO (1–0) and (2–1) in run MC41 ($L = 1$, $k = 4$, and $B = 0.1$). Clumps in physical space (A, B, and C, panel) do not necessarily correspond to clumps in the observed velocity space. Observed clumps in velocity space (D, *bottom left panel*) are not nec formed by emission from a single region in physical space.

Projection problem:

deconvolution PPV → PPP

“clumps” identified in PPV may correspond to several real physical gas clumps in PPP

Radiation transfer problem:

only tracer molecules observed (limited dynamic range in density)

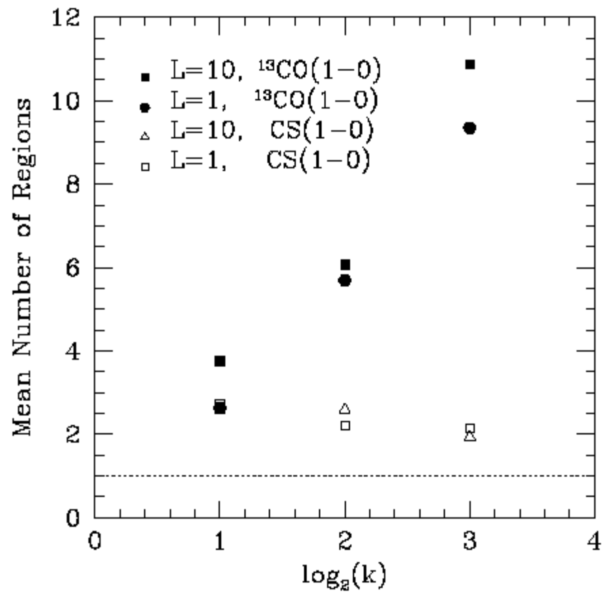

Velocity Structure of MC's

- Supersonic linewidth on all scales (except maybe on the smallest)
- Associated kinetic energy equals (even may exceed) self-gravity
- Supersonic turbulence → velocity determines density
- QUESTION: What causes interstellar turbulence?
- Observed linewidths increase with size of measured region → Larson relation
- Supersonic turbulence is driven on large scales

Linewidth size relation (example)

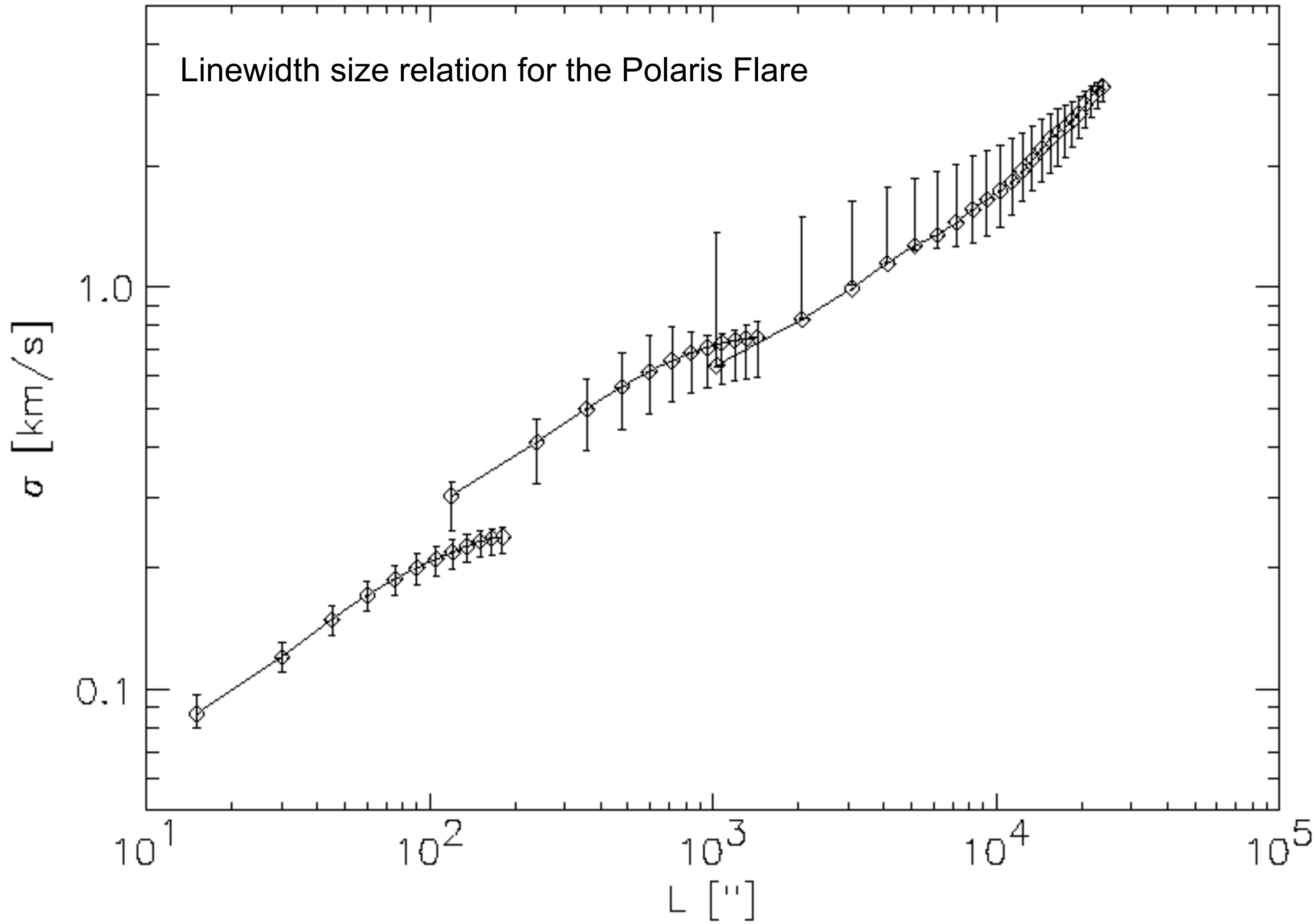

Ossenkopf & Mac Low (2002)

Thermal Structure of MC's

- Approximate energy balance between heating (cosmic rays) and cooling (molecular lines) processes lead to roughly constant temperature of ~ 10K.

Magnetic Fields in MC's

- Magnetic field structure and its importance for our understanding of molecular cloud evolution will be discussed in the next lecture.

Larson Relations

- Larson (1981) found the following relations between linewidth and size and mean density and size:

$\rho \propto R^{\alpha}$	$\alpha \approx -1$	*density size relation*	(1)
$\sigma \propto R^{\beta}$	$\beta \approx 1/2$	*linewidth size relation*	(2)

- In virial equilibrium: $\alpha \approx -1$, $\beta \approx \frac{1}{2}$
- Molecular clouds appear gravitationally bound. (3)
- Values:
  - $\sigma = (0.72 \pm 0.07)$ km/s $(R/pc)^{0.5 \pm 0.05}$ (Solomon et al.)
  - $\sigma = 0.55$ km/s $(R/pc)^{0.51}$ (Caselli & Myers)
  - $\langle N_H \rangle = (1.5 \pm 0.3) \times 10^{22}$ cm^{-2} $(R/pc)^{0.0 \pm 0.1}$ (Solomon et al.)
- Only two of the three statements (1,2,3) are independent.

Larson Relations

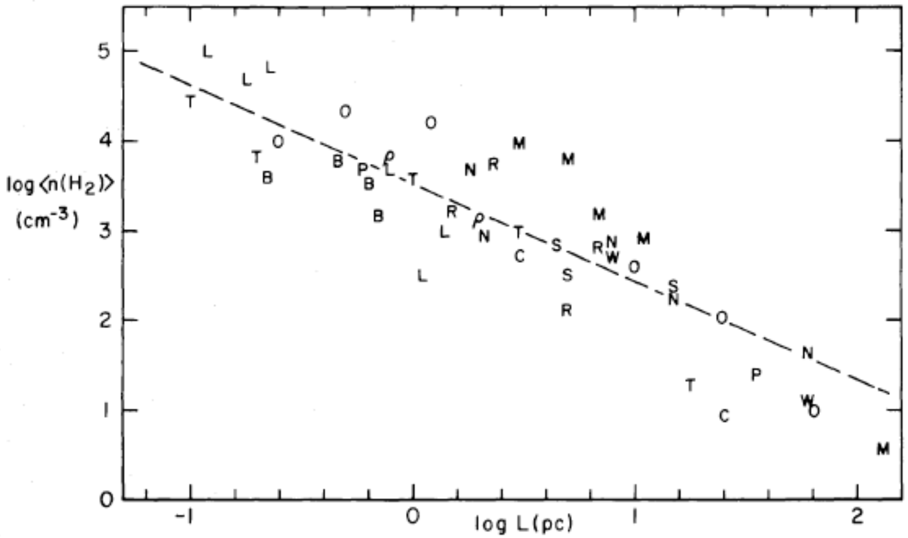

Figure 5. The average density, defined as the density of a sphere of mass M and diameter L, of all the regions shown in Figs 1 and 3 plotted versus region size L. The dashed line represents equation (5), and is derived from equations (1) and (2).

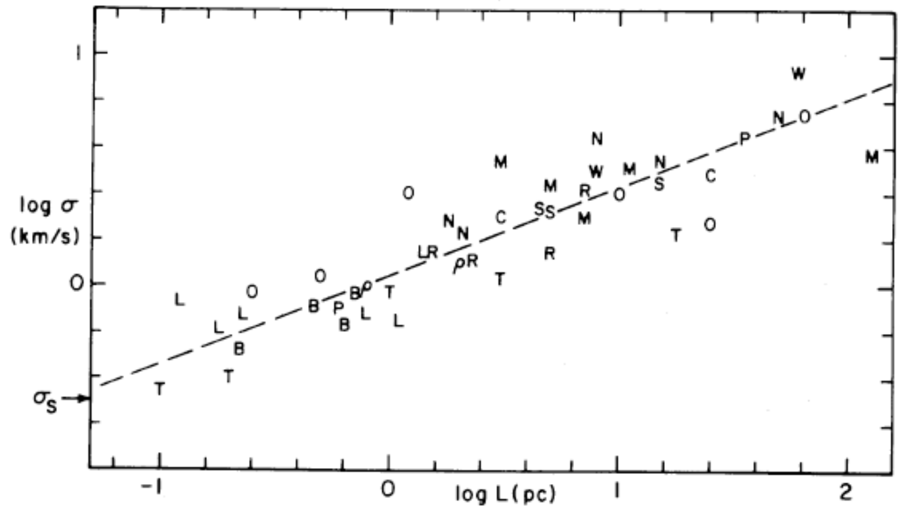

Figure 1. The three-dimensional internal velocity dispersion σ plotted versus the maximum linear dimension L of molecular clouds and condensations, based on data from Table 1; the symbols are identified in Table 1. The dashed line represents equation (1), and σ_S is the thermal velocity dispersion.

Richard Larson (1981, MNRAS, 184, 809)

Larson Relations

- Only *ONE* of the two Larson relation appears real (in the sense that it exists for the real 3D clumps)
- *Density size relation* is likely not to exist in 3D data, but is only observed in projected data due to limited dynamic range of tracer molecules (corresponding to a roughly constant column density)
- Velocity size relation may exist in real 3D data (but may only be marginal).

Larson Relations

Linewidth size relation

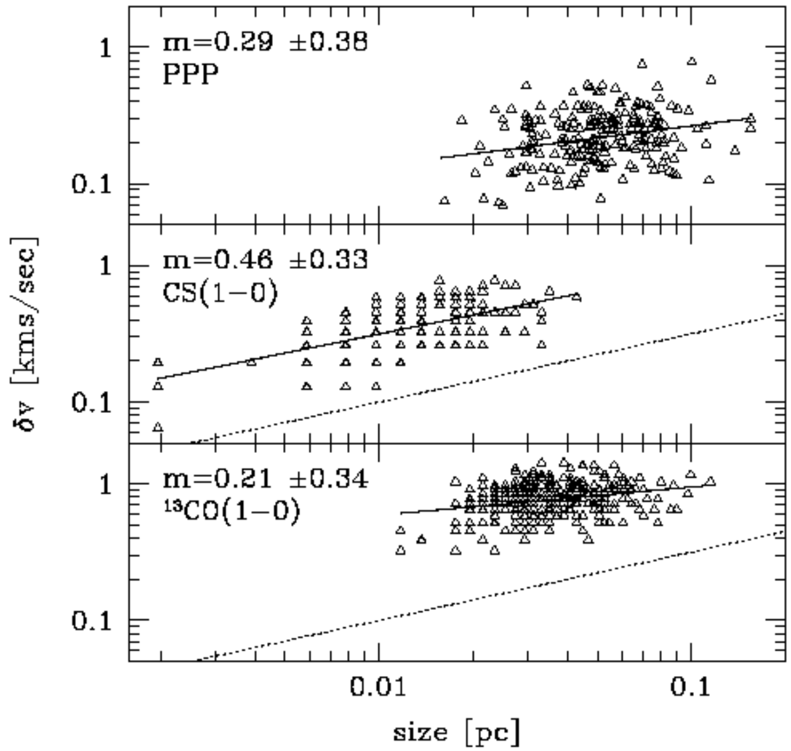

FIG. 10.—Velocity dispersion–size relationships for run HC8-256 in physical space (*top*) and observational space (*middle and bottom*), using CS (1–0) and ^{13}CO (1–0), respectively. The dotted line has a slope of $\frac{1}{2}$, the expected value for a turbulent medium dominated by shocks (see, e.g., Vázquez-Semadeni et al. 2000). The solid line is the least-squares fit to the data points, with a slope m, and its uncertainty shown in each frame.

density size relation

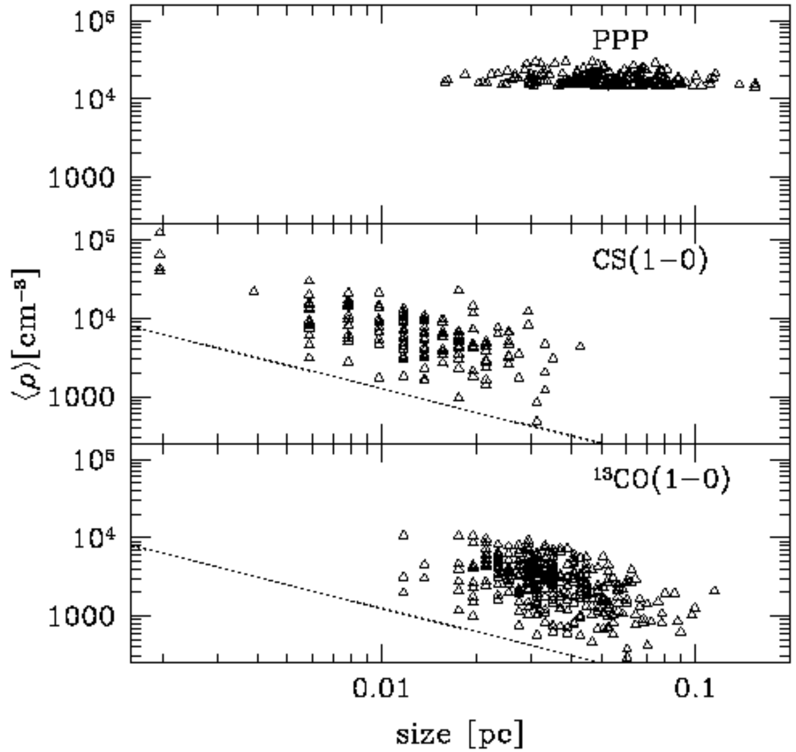

FIG. 9.—Mean density–size relationship for physical clumps in physical (*top*) and simulated observational clumps in observational coordinates (*middle and bottom*). The dotted line has a slope of $\alpha = -1$. In physical space we find no correlation, verifying the results by VBR97, but nevertheless the simulated observations show such a correlation, as found by Larson (1981) and many others. The selection of two different density tracers was chosen to show that the apparent correlation does not depend on the selection of the density threshold.

Ballesteros-Paredes & Mac Low (2002)

Magnetic fields

- big controversy in star formation theory:

  HOW IMPORTANT ARE
  MAGNETIC FIELDS?

- determining field strengths is essential!
  - Zeeman effect
  - polarisation of dust emission
- diffuse ISM: mass-to-flux ratio subcritical
- dense H_2 gas: (slightly) supercritical

DR21(OH)

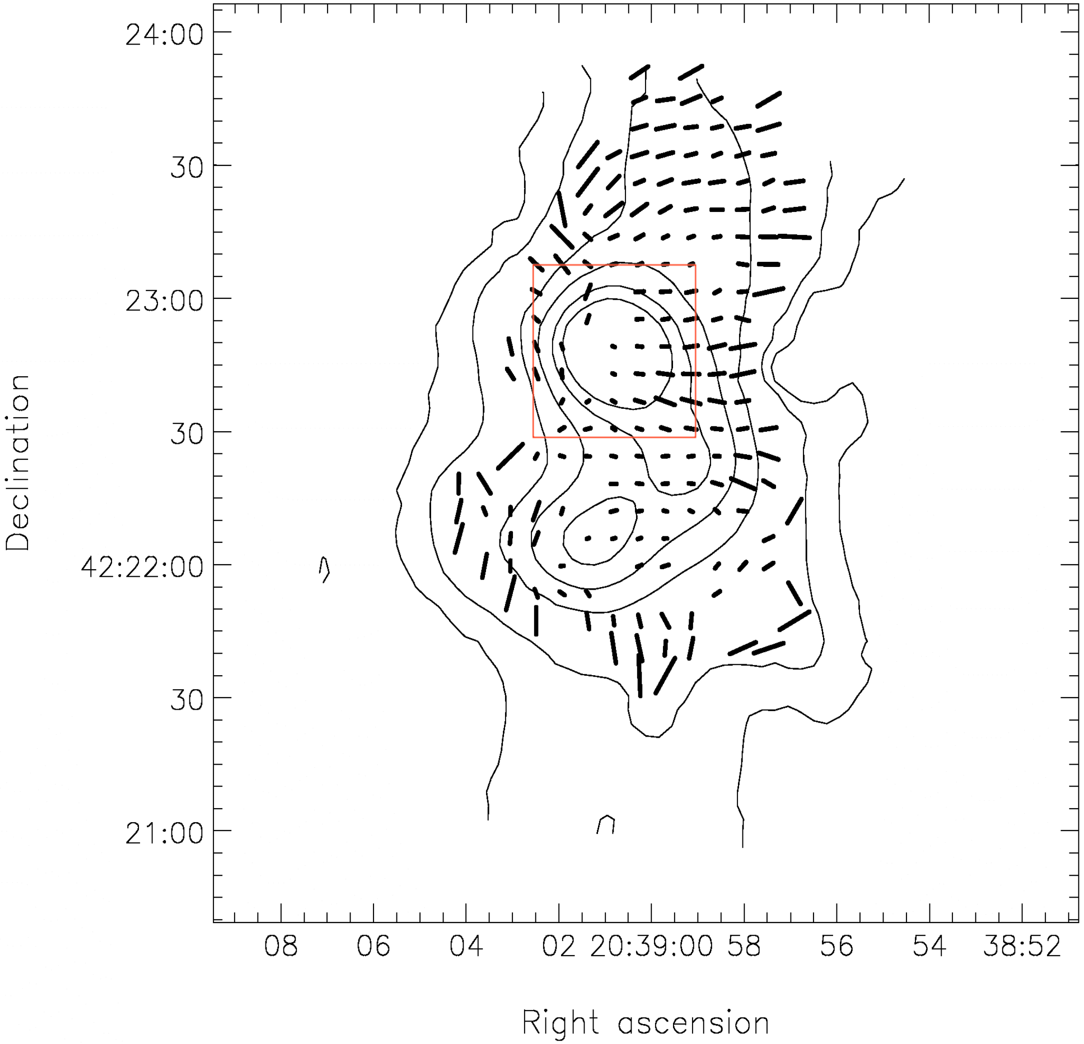

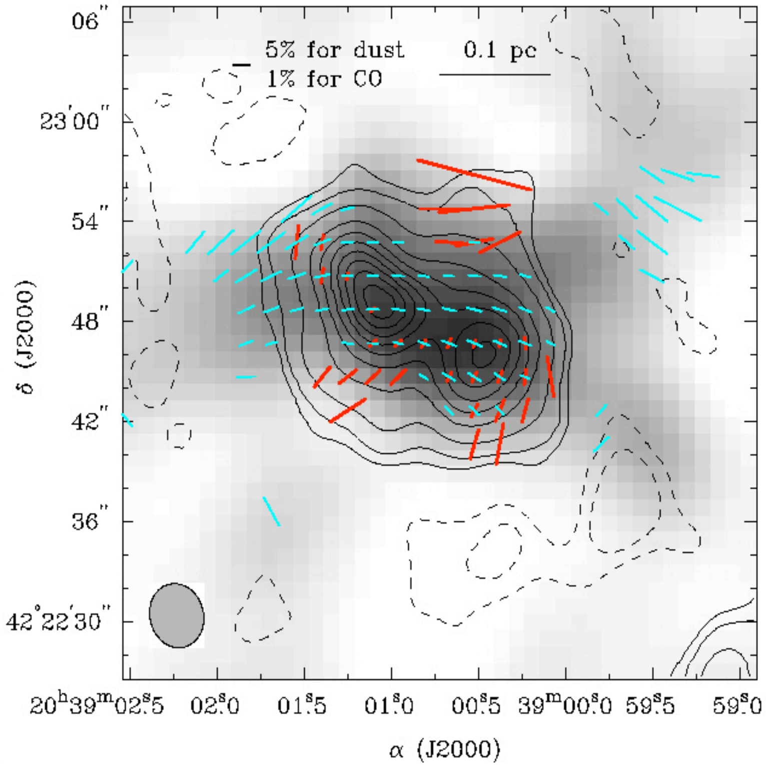

Lai et al. (2003)

Vallee & Fiege (2005)

DR21(OH)

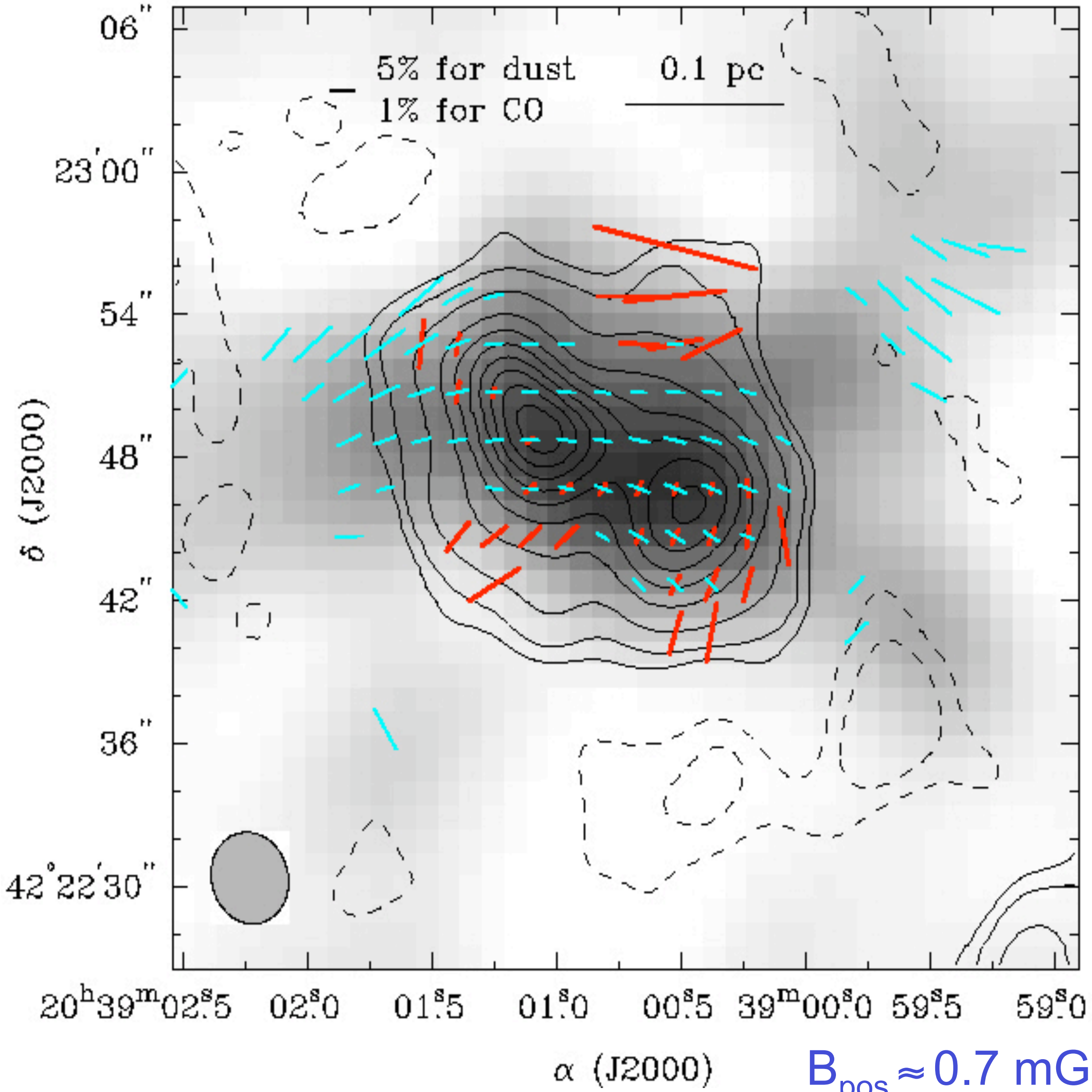

Lai et al. (2003)

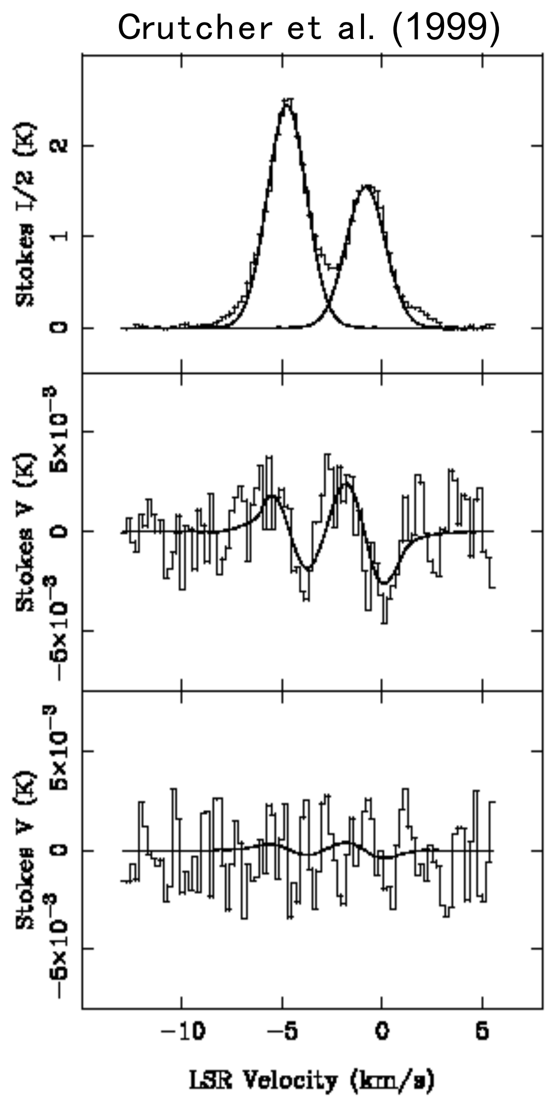

$B_{pos} \approx 0.7$ mG

$B_{los} = 0.4, 0.7$ mG

DR21(OH)

1. CO polarization:
   $n(H_2) \sim 10^2$, $B_{pos} \approx 0.01$ mG

2. Dust polarization & CN Zeeman:
   $n(H_2) \sim 10^6$, $N(H_2) \approx 3 \times 10^{23}$
   $B_{pos} \approx B_{los} \approx 0.7$ mG, $\lambda_c \approx 1.1$

Combining 1 and 2, $\mathbf{B} \propto \rho^{0.45}$

Hydrodynamics

- gases and fluids are *large* ensembles of interacting particles
- $\longrightarrow$ state of system is described by location in $6N$ dimensional phase space $f^{(N)}(\vec{q}_1...\vec{q}_N, \vec{p}_1...\vec{p}_N)d\vec{q}_1...d\vec{q}_N d\vec{p}_1...d\vec{p}_N$
- time evolution governed by 'equation of motion' for $6N$-dim probability distribution function $f^{(N)}$
- $f^{(N)} \rightarrow f^{(n)}$ by integrating over all but n coordinates $\longrightarrow$ BBGKY hierarchy of equations of motion (after Born, Bogoliubov, Green, Kirkwood and Yvon)
- physical observables are typically associated with 1- or 2-body probability density $f^{(1)}$ or $f^{(2)}$
- at lowest level of hierarchy: 1-body distribution function describes the probability of finding a particle at time t in the volume element $d\vec{q}$ at $\vec{q}$ with momenta in the range $d\vec{p}$ at $\vec{p}$.
- **Boltzmann equation** – equation of motion for $f^{(1)}$

$$\boxed{\begin{aligned}\frac{df}{dt} &\equiv \frac{\partial f}{\partial t} + \dot{\vec{q}} \cdot \vec{\nabla}_{\mathrm{q}} f + \dot{\vec{p}} \cdot \vec{\nabla}_{\mathrm{p}} f \\ &= \frac{\partial f}{\partial t} + \vec{v} \cdot \vec{\nabla}_{\mathrm{q}} f + \vec{F} \cdot \vec{\nabla}_{\mathrm{p}} f = f_{\mathbf{c}}\end{aligned}}$$

- **Boltzmann equation**

$$\boxed{\begin{aligned}\frac{df}{dt} &\equiv \frac{\partial f}{\partial t} + \dot{\vec{q}} \cdot \vec{\nabla}_{\mathrm{q}} f + \dot{\vec{p}} \cdot \vec{\nabla}_{\mathrm{p}} f \\ &= \frac{\partial f}{\partial t} + \vec{v} \cdot \vec{\nabla}_{\mathrm{q}} f + \vec{F} \cdot \vec{\nabla}_{\mathrm{p}} f = f_{\mathbf{c}}\end{aligned}}.$$

  → first line: transformation from comoving to spatially fixed coordinate system.

  → second line: velocity $\vec{v} = \dot{\vec{q}}$ and force $\vec{F} = \dot{\vec{p}}$

  → all higher order terms are 'hidden' in the collision term $f_{\mathbf{c}}$

- observable quantities are typically (velocity) moments of the Boltzmann equation, e.g.

  → density:

$$\rho = \int m\, f(\vec{q}, \vec{p}, t) d\vec{p}$$

  → momentum:

$$\rho\vec{v} = \int m\vec{v}\, f(\vec{q}, \vec{p}, t) d\vec{p}$$

  → kinetic energy density:

$$\rho\vec{v}^{\,2} = \int m\vec{v}^{\,2}\, f(\vec{q}, \vec{p}, t) d\vec{p}$$

- in general: the i-th velocity moment $\langle \xi_i \rangle$ (of $\xi_i = m\vec{v}^{\,i}$) is

$$\langle \xi_i \rangle = \frac{1}{n} \int \xi_i \, f(\vec{q}, \vec{p}, t) d\vec{p}$$

with the mean particle number density n defined as

$$n = \int f(\vec{q}, \vec{p}, t) \, d\vec{p}$$

- the equation of motion for $\langle \xi_i \rangle$ is

$$\int \xi_i \left\{ \frac{\partial f}{\partial t} + \vec{v} \cdot \vec{\nabla}_{\mathrm{q}} f + \vec{F} \cdot \vec{\nabla}_{\mathrm{p}} f \right\} d\vec{p} = \int \xi_i \left\{ f_{\mathbf{c}} \right\} \, d\vec{p} \,,$$

which after some complicated rearrangement becomes

$$\boxed{\frac{\partial}{\partial t} n \langle \xi_i \rangle + \vec{\nabla}_{\mathrm{q}} \left(n \langle \xi_i \vec{v} \rangle \right) + n\vec{F} \langle \vec{\nabla}_{\mathrm{p}} \xi_i \rangle = \int \xi_i f_{\mathbf{c}} \, d\vec{p}}$$

(Maxwell-Boltzmann transport equation for $\langle \xi_i \rangle$)

- if the RHS is zero, then ξ_i is a conserved quantity. This is only the case for first three moments, mass $\xi_0 = m$, momentum $\vec{\xi}_1 = m\vec{v}$, and kinetic energy $\xi_2 = m\vec{v}^{\,2}/2$.
- MB equations build a hierarically nested set of equations, as $\langle\xi_i\rangle$ depends on $\langle\xi_{i+1}\rangle$ via $\vec{\nabla}_{\mathrm{q}}\left(n\langle\xi_i\vec{v}\rangle\right)$ and because the collision term cannot be reduced to depend on ξ_i only.
  $\longrightarrow$ need for a closure equation
  $\longrightarrow$ in hydrodynamics this is typically the equation of state.

assumptions

- **continuum limit:**
  - → distribution function f must be a 'smoothly' varying function on the scales of interest ⟶ local average possible
  - → stated differently: the averaging scale (i.e. scale of interest) must be larger than the mean free path of individual particles
  - → stated differently: microscopic behavior of particles can be neglected
  - → concept of fluid element must be meaningful
- **only 'short range forces':**
  - → forces between particles are short range or saturate ⟶ collective effects can be neglected
  - → stated differently: correlation length of particles in the system is finite (and smaller than the scales of interest)

limitations

- shocks (scales of interest become smaller than mean free path)
- phase transitions (correlation length may become infinite)
- description of self-gravitating systems
- description of fully fractal systems

the equations of hydrodynamics

- hydrodynamics ≡ book keeping problem
  One must keep track of the 'change' of a fluid element due to various physical processes acting on it. How do its 'properties' evolve under the influence of compression, heat sources, cooling, etc.?
- Eulerian vs. Lagrangian point of view

Eulerian

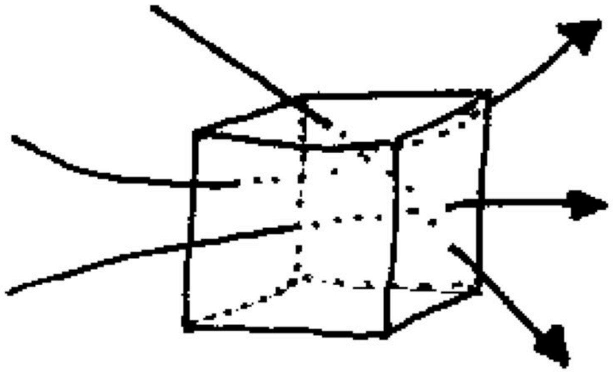

consider spatially fixed volume element

Lagrangian

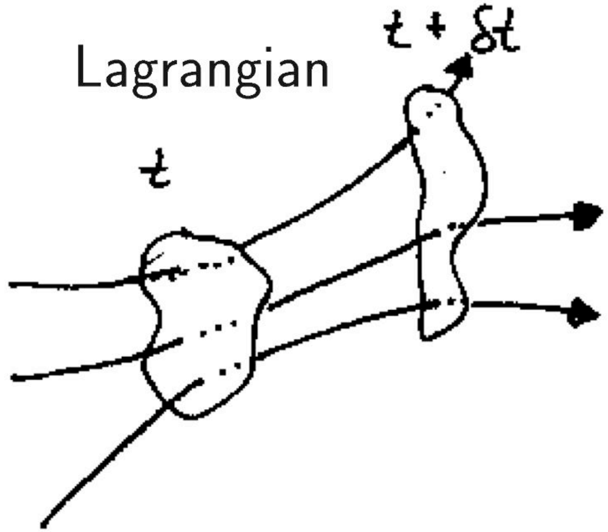

following motion of fluid element

- hydrodynamic equations = set of equations for the five conserved quantities $(\rho, \rho\vec{v}, \rho\vec{v}^{\,2}/2)$ plus closure equation (plus transport equations for 'external' forces if present, e.g. gravity, magnetic field, heat sources, etc.)

- equations of hydrodynamics

$$\frac{d\rho}{dt} = \frac{\partial \rho}{\partial t} + \vec{v} \cdot \vec{\nabla} \rho = -\rho \vec{\nabla} \cdot \vec{v}$$

(continuity equation)

$$\frac{d\vec{v}}{dt} = \frac{\partial \vec{v}}{\partial t} + (\vec{v} \cdot \vec{\nabla})\vec{v} = -\frac{1}{\rho}\vec{\nabla} p - \vec{\nabla}\phi + \eta \vec{\nabla}^2 \vec{v} + \left(\zeta + \frac{\eta}{3}\right)\vec{\nabla}(\vec{\nabla} \cdot \vec{v})$$

(Navier-Stokes equation)

$$\frac{d\epsilon}{dt} = \frac{\partial \epsilon}{\partial t} + \vec{v} \cdot \vec{\nabla} \epsilon = T\frac{ds}{dt} - \frac{p}{\rho}\vec{\nabla} \cdot \vec{v}$$

(energy equation)

$$\vec{\nabla}^2 \phi = 4\pi G \rho$$

(Poisson's equation)

$$p = \mathcal{R} \rho T$$

(equation of state)

$$\vec{F}_B = -\vec{\nabla}\,\frac{\vec{B}^2}{8\pi} + \frac{1}{4\pi}(\vec{B}\cdot\vec{\nabla})\vec{B} \quad \text{(magnetic force)}$$

$$\frac{\partial \vec{B}}{\partial t} = \vec{\nabla} \times (\vec{v} \times \vec{B}) \quad \text{(Lorentz equation)}$$

ρ = density, $\vec{v}$ = velocity, p = pressure, ϕ = gravitational potential, ζ and η viscosity coefficients, $\epsilon = \rho\vec{v}^{\,2}/2$ = kinetic energy density, T = temperature, s = entropy, $\mathcal{R}$ = gas constant, $\vec{B}$ = magnetic field (cgs units)

- mass transport – continuity equation

$$\frac{d\rho}{dt} = \frac{\partial\rho}{\partial t} + \vec{v}\cdot\vec{\nabla}\rho = -\rho\vec{\nabla}\cdot\vec{v}$$

(conservation of mass)

- transport equation for momentum – Navier Stokes equation

$$\frac{d\vec{v}}{dt} = \frac{\partial\vec{v}}{\partial t} + (\vec{v}\cdot\vec{\nabla})\vec{v} = -\frac{1}{\rho}\vec{\nabla}p - \vec{\nabla}\phi + \eta\vec{\nabla}^2\vec{v} + \left(\zeta + \frac{\eta}{3}\right)\vec{\nabla}(\vec{\nabla}\cdot\vec{v})$$

momentum change due to

→ pressure gradients: $(-\rho^{-1}\,\vec{\nabla}p)$

→ (self) gravity: $-\vec{\nabla}\phi$

→ viscous forces (internal friction, contains $\mathrm{div}(\partial v_i/\partial x_j)$ terms): $\eta\vec{\nabla}^2\vec{v} + \left(\zeta + \frac{\eta}{3}\right)\vec{\nabla}(\vec{\nabla}\cdot\vec{v})$

(conservation of momentum, general form of momentum transport: $\partial_t(\rho v_i) = -\partial_j \Pi_{ij}$)

◦ transport equation for internal energy

$$\frac{d\epsilon}{dt} = \frac{\partial \epsilon}{\partial t} + \vec{v} \cdot \vec{\nabla} \epsilon = T \frac{ds}{dt} - \frac{p}{\rho} \vec{\nabla} \cdot \vec{v}$$

$\rightarrow$ follows from the thermodynamic relation $d\epsilon = T\,ds - p\,dV = T\,ds + p/\rho^2 d\rho$ which described changes in ϵ due to entropy changed and to volume changes (compression, expansion)

$\rightarrow$ for adiabatic gas the first term vanishes ($s =$constant)

$\rightarrow$ heating sources, cooling processes can be incorporated in ds

(conservation of energy)

- closure equation – equation of state
  - $\rightarrow$ general form of equation of state $p = p(T, \rho, ...)$
  - $\rightarrow$ ideal gas: $p = \mathcal{R}\rho T$
  - $\rightarrow$ special case – isothermal gas: $p = c_\mathrm{s}^2 T$ (as $\mathcal{R}T = c_\mathrm{s}^2$)

Note:

- in reality, computing the EOS is VERY complex!
- depends on detailed *balance* between *heating* and *cooling*
- these depend on *chemical composition* (which atomic and molecular species, dust)
- and on the ability to radiate away „cooling lines" and black body radiation
  --> problem of *radiation transfer*

virial theorem

Derivation of virial theorem from momentum equation:

- consider pressure gradients, gravity, magnetic fields,
- neglect viscous forces

$$\rightarrow \boxed{\rho \frac{d\vec{v}}{dt} = -\vec{\nabla} p - \rho \vec{\nabla}\phi - \vec{\nabla}\left(\frac{B^2}{8\pi}\right) + \frac{1}{4\pi}(\vec{B}\cdot\vec{\nabla})\vec{B}}$$

pressure term — gravity — magnetic "pressure" — magnetic tension

- in component form:

$$\boxed{\rho \frac{dv_i}{dt} = -\frac{\partial p}{\partial x_i} - \rho \frac{\partial \phi}{\partial x_i} - \frac{\partial}{\partial x_i}\left(\frac{B^2}{8\pi}\right) + \frac{1}{4\pi} B_j \frac{\partial}{\partial x_j} B_i}$$

- multiply by x_i and integrate over volume:
- consider term by term:

① $\int \rho x_i \frac{dv_i}{dt} dV = \int \rho x_i \frac{d^2 x_i}{dt^2} dV$

integrate by parts

$$= \int \rho \frac{d}{dt}\left(x_i \frac{dx_i}{dt}\right) dV - \int \rho \frac{dx_i}{dt}\frac{dx_i}{dt} dV$$

$$= \int \rho \frac{d^2}{dt}\left(\frac{x_i x_i}{2}\right) dV - \int \rho v_i v_i dV$$

$$= \frac{1}{2}\frac{d^2}{dt^2}\int \rho x_i x_i dV - 2 \cdot \int \frac{1}{2}\rho v_i v_i dV$$

$$= \frac{1}{2}\ddot{I} - 2T$$

where $I \equiv \int \rho r^2 dV$ is called moment of inertia

[but not quite, because no axis defined.]

and $T \equiv \frac{1}{2}\int \rho v^2 dV$ is the kinetic energy

[note, does not contain random = thermal motions]

(II) $$-\int x_i \frac{\partial p}{\partial x_i}\, dV = -\int \underbrace{\frac{\partial}{\partial x_i}(x_i p)}_{\mathrm{div}(\vec{x}p) \rightarrow \text{Gauß}} dV + \int p \frac{\partial x_i}{\partial x_i}\, dV$$

$$= -\oint x_i p \cdot dS_i \quad + 3\int p\, dV$$

$$= -\oint p\vec{r}\cdot d\vec{S} \quad + 2U \qquad = -2T_S + 2U$$

where U = thermal energy $= \frac{3}{2}\int p\, dV$

and T_S = surface term of kinetic energy $= \frac{1}{2}\oint p\vec{r}\, d\vec{S}$

(III) $$\int \varrho x_i \frac{\partial \phi}{\partial x_i}\, dV = \int \varrho \vec{r}\cdot\vec{F}_g \cdot dV \qquad \vec{F}_g = -\vec{\nabla}\phi = \text{grav. force}$$

= total potential energy $= \omega$

↳ neglecting magnetic fields for the moment, we get:

$$\boxed{\frac{1}{2}\ddot{I} = 2\cdot(T-T_s) + 2U + W}$$

scalar virial theorem

- virial theorem describes fundamental relation between morphological parameters (I = tensor of inertia, W = tensor of potential energy) and kinematic quantities (tensor of kinetic energy $K = T + U - T_s$)

– in equilibrium: $\ddot{I} = 0$!

$\Rightarrow$ $\boxed{2K + W = 0}$

$K = T + U$, neglecting surface effects T_S

$\Rightarrow$ the system is called <u>virialized.</u>

– total energy: $\boxed{E_{tot} = K + W}$

in virial equilibrium it follows

$$\boxed{E_{tot} = K + W = \frac{W}{2} = -K}$$

virialized systems are always bound with binding energy equal to $-K$.

Jeans condition

Gravitational instability:

$\boxed{\text{Jeans criterion}}$

- often the first approach to determine stability properties is to analyze the linearized set of equations and derive a dispersion relation for the perturbation assumed.

- Linearized equ.'s for isothermal self-gravitating fluid:

$$\boxed{\begin{array}{lll} \dfrac{\partial \rho_1}{\partial t} + \rho_0 \vec{\nabla} \vec{v}_1 = 0 & & \text{continuity} \\ \dfrac{\partial \vec{v}_1}{\partial t} = - \vec{\nabla} c_s^2 \dfrac{\rho_1}{\rho_0} - \vec{\nabla} \phi_1 & & \text{momentum} \\ \vec{\nabla}^2 \phi_1 = 4\pi G \rho_1 & & \text{Poisson} \end{array}}$$

▲ $\vec{\nabla} c_s^2 \dfrac{\rho_1}{\rho_0} = \dfrac{1}{\rho_0} \vec{\nabla} p_1$ with $p_1 = c_s^2 \rho_1$ from EOS.

▲ neglecting viscous effects $(\eta = \xi = 0)$

▲ equilibrium characterized by $\rho_0 = \text{const.}$ and $\vec{v}_0 = 0$

▲ Jeans swindle: Poisson's equ considers only perturbed potential ($\rightarrow$ set $\phi_0 = 0$)

- with $\frac{\partial}{\partial t}$ [continuity] + $\vec{\nabla}$ [momentum] it follows:

$$\boxed{\frac{\partial^2 \rho_1}{\partial t^2} - c_s^2 \vec{\nabla}^2 \rho_1 - 4\pi G \rho_0 \rho_1 = 0}$$

↳ wave equation for $\rho_1(\vec{x}, t)$

- analyze in Fourier space:

$$\boxed{\rho_1(\vec{x}, t) = \int d^3k \, A(\vec{k}) \, e^{i[\vec{k}\vec{x} - \omega(k)t]}}$$

$$\frac{\partial}{\partial t} \mapsto i\omega \cdot$$
$$\vec{\nabla} \mapsto i\vec{k} \cdot$$

- dispersion relation:

$$\boxed{\omega^2 = c_s^2 k^2 - 4\pi G \rho_0}$$

- ▲ if density ρ_0 is small $\longmapsto$ disp. rel. of sound waves $\boxed{\omega^2 = c_s^2 k^2}$
- ▲ or small wavelength $\lambda = \frac{2\pi}{k}$
- ▲ self-gravity acts "strongest" on <u>large scales</u> (small k)
  [gravity is long-range force]
- ▲ λ increases / k decreases / ρ_0 grows: frequency decreases and eventually $\omega^2 < 0$!

  $\hookrightarrow$ time evolution $\propto \exp(\pm \alpha t)$. (if $\alpha^2 = -\omega^2$)

  Exponentially unstable.

- $\longmapsto$ Gravitational collapse for wave numbers

$$\boxed{k^2 < k_J^2 \equiv \frac{4\pi G \rho_0}{c_s^2}}$$

- ▼ k_J : Jeans wavenumber
- ▼ λ_J = Jeans wavelength $= \frac{2\pi}{k_J} = \left(\frac{\pi c_s^2}{G\rho_0}\right)^{1/2}$
- ▼ M_J = Jeans mass $= \frac{4\pi}{3}\rho_0\left(\frac{\lambda_J}{2}\right)^3 = \frac{\pi}{6}\rho_0\left(\frac{\pi c_s^2}{G\rho_0}\right)^{3/2}$

  for a spherical perturbation with $\varnothing = \lambda_J$

$$\boxed{\begin{aligned} M_J &= \frac{\pi^{5/2}}{6}\left(\frac{R}{G}\right)^{3/2} \cdot \rho_0^{-1/2}\, T^{3/2} \qquad c_s^2 = RT \\ &= \frac{\pi^{5/2}}{6}\, G^{-3/2} \cdot \rho_0^{-1/2}\, c_s^3 \end{aligned}}$$

- Energy of sound wave $E_{\text{sound}} > 0$; gravitational Energy < 0

  $\hookrightarrow$ Instability sets in, when net energy is negative, i.e. when λ exceeds λ_J.

Bonnor-Ebert spheres

(4) Isothermal equilibria of (pressure bounded) self-grav. spheres

- force balance $\longrightarrow$ static sln $\longrightarrow$ $\boxed{\vec{\nabla} p = -\rho \vec{\nabla} \Phi}$
- ideal gas: $p = c_s^2 \rho$ with isothermal sound speed $c_s^2 = \frac{R}{\mu} T$
- spherical symmetry: equ. of motion $\frac{c_s^2}{\rho} \frac{d\rho}{dr} = - \frac{d\Phi}{dr}$
- $\longmapsto$ integration $\longrightarrow$ $\boxed{\rho = \rho_0 \exp(-\Phi / c_s^2)}$ hydrostatic equ.
- include Poisson's equ.: $\boxed{\frac{1}{r^2} \frac{d}{dr}\left(r^2 \frac{d\Phi}{dr}\right) = 4\pi G \rho = 4\pi G \rho_0 \exp\left(-\frac{\Phi}{c_s^2}\right)}$ *

  Lane-Emden equation
- regular sln's from $\Phi = 0$ & $\frac{d\Phi}{dr} = 0$ at $r = 0$
- 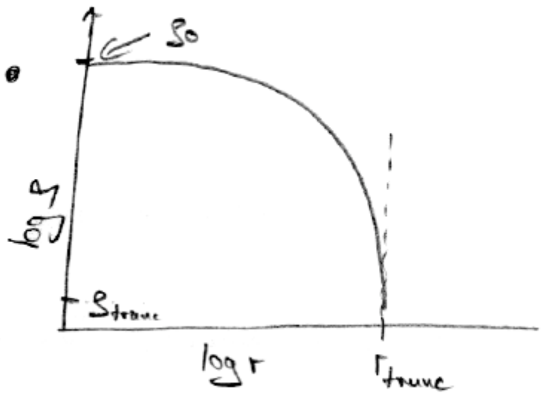

  if $\frac{\rho_0}{\rho_{trunc}} > 14$ only unstable equilibria possible!

- Singular isothermal sphere if $\rho_0/\rho_{trunc} \longrightarrow \infty$
  (or equivalently, if outer edge $r_{trunc} \rightarrow \infty$; or $p_{ext} \rightarrow 0$)

  ↳ SIS: $\boxed{\rho = \frac{c_s^2}{4\pi G r^2} \quad \& \quad \frac{d\phi}{dr} = \frac{2c_s^2}{r}}$

  Shu (1977) assumes SIS & $v=0$; but to reach SIS,
  system evolves throug a sequence of unstable equilibria
  ⟶ collapse sets in much earlier ⟶ SIS with $v=0$
  will never be reached.

- solving *) : define $\xi = \frac{r}{c_s}\sqrt{4\pi G \rho_0}$ $\quad \rho_0$ = core density

  ↳ $\boxed{\frac{d}{d\xi}\left(\xi^2 \frac{d\psi}{d\xi}\right) = \xi^2 e^{-\psi}}$ **) $\quad \psi = \ln \rho/\rho_0$

sln of **) with $\Psi(0)=0$ & $\frac{d\Psi(0)}{d\xi}=0$ are finite at the center $\xi=0$.

↳ further change of variables:

$$y_1 = \xi^2 \frac{d\Psi}{d\xi}$$

$$y_2 = \Psi$$

↳ coupled set of 1. order ODE's:

$$\frac{dy_1}{d\xi} = \frac{y_0}{\xi^2}$$

$$\frac{dy_0}{d\xi} = \xi^2 \exp(-y_1)$$

boundary conditions $y_0(0)=0$ & $y_1(0)=0$.

$\hookrightarrow$ $\exists$ family of solutions characterized by parameter

$$\boxed{\xi_{max} = \frac{r_{trunc}}{c_s}\sqrt{4\pi G \rho_0}}$$

ξ_{max} = value of ξ at outer boundary r_{trunc}

$\xi_{max} > 6{,}5$ unstable equilibria : collaps

$\xi_{max} < 6{,}5$ stable s/u

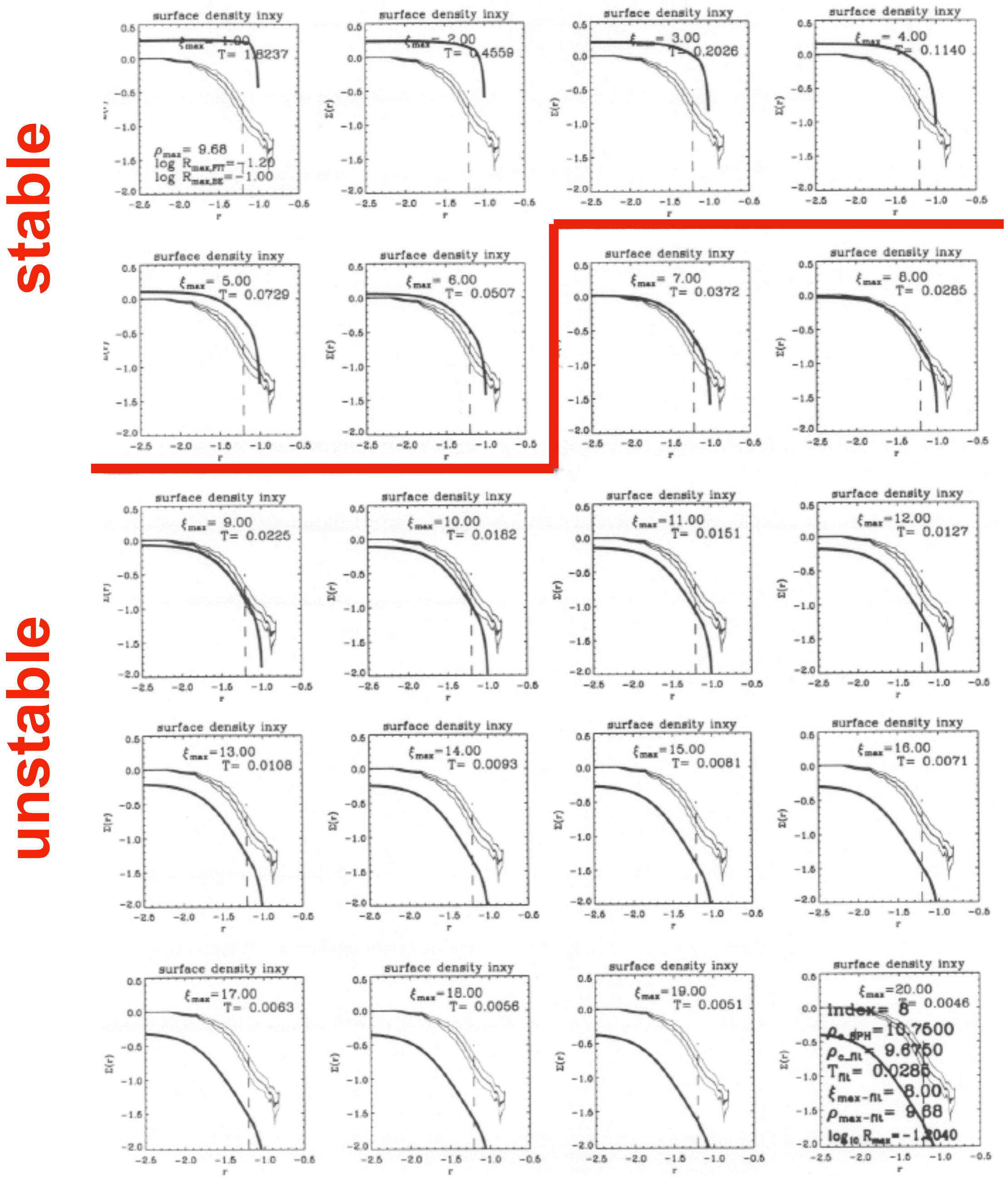
stable
unstable
surface density inxy
ξ_{max}= 1.00 T= 1.8237
ξ_{max}= 2.00 T= 0.4559
ξ_{max}= 3.00 T= 0.2026
ξ_{max}= 4.00 T= 0.1140
ξ_{max}= 5.00 T= 0.0729
ξ_{max}= 6.00 T= 0.0507
ξ_{max}= 7.00 T= 0.0372
ξ_{max}= 8.00 T= 0.0285
ξ_{max}= 9.00 T= 0.0225
ξ_{max}=10.00 T= 0.0182
ξ_{max}=11.00 T= 0.0151
ξ_{max}=12.00 T= 0.0127
ξ_{max}=13.00 T= 0.0108
ξ_{max}=14.00 T= 0.0093
ξ_{max}=15.00 T= 0.0081
ξ_{max}=16.00 T= 0.0071
ξ_{max}=17.00 T= 0.0063
ξ_{max}=18.00 T= 0.0056
ξ_{max}=19.00 T= 0.0051
ξ_{max}=20.00 T= 0.0046
ρ_{max}= 9.68
log $R_{max,FIT}$= -1.20
log $R_{max,BE}$= -1.00
index= 8
ρ_{c_SPH}=10.7500
ρ_{c_fit}= 9.6750
T_{fit}= 0.0286
$\xi_{max-fit}$= 8.00
$\rho_{max-fit}$= 9.68
$\log_{10} R_{max}$=-1.2040
$\Sigma(r)$
r

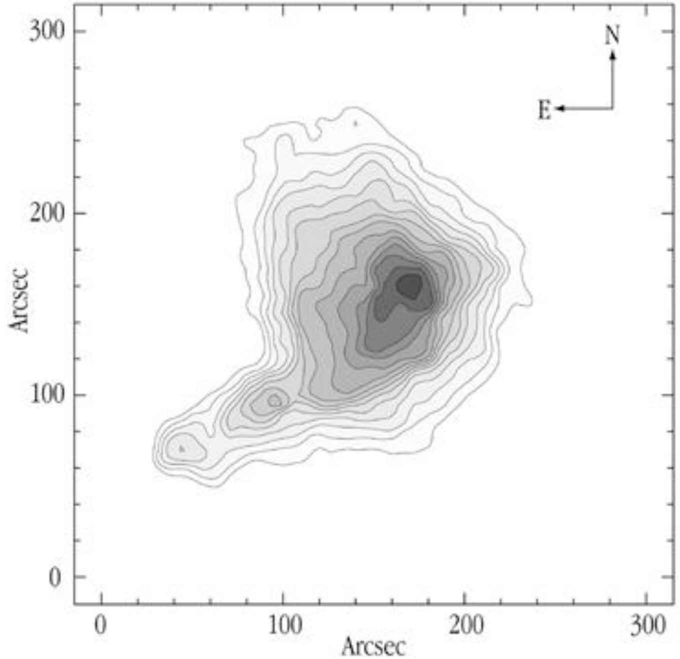

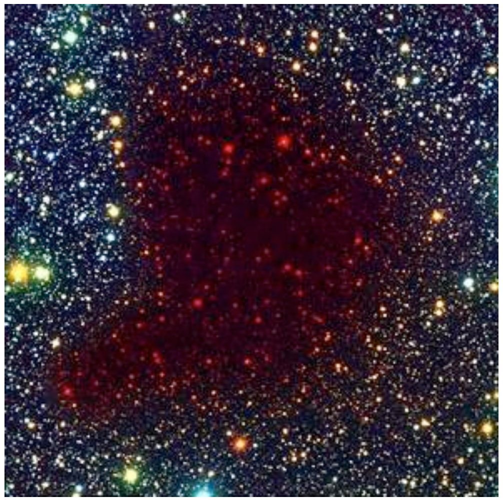

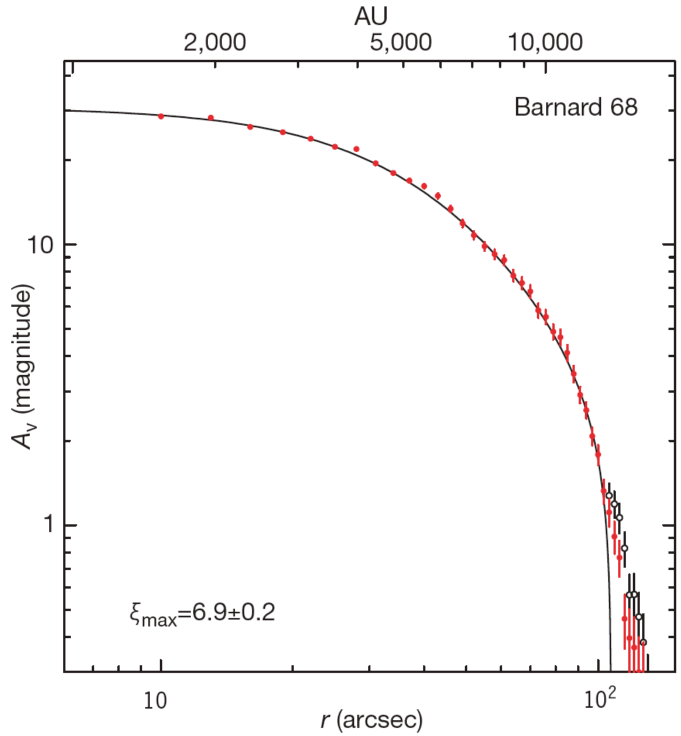

Alves, Lada, Lada (2001)

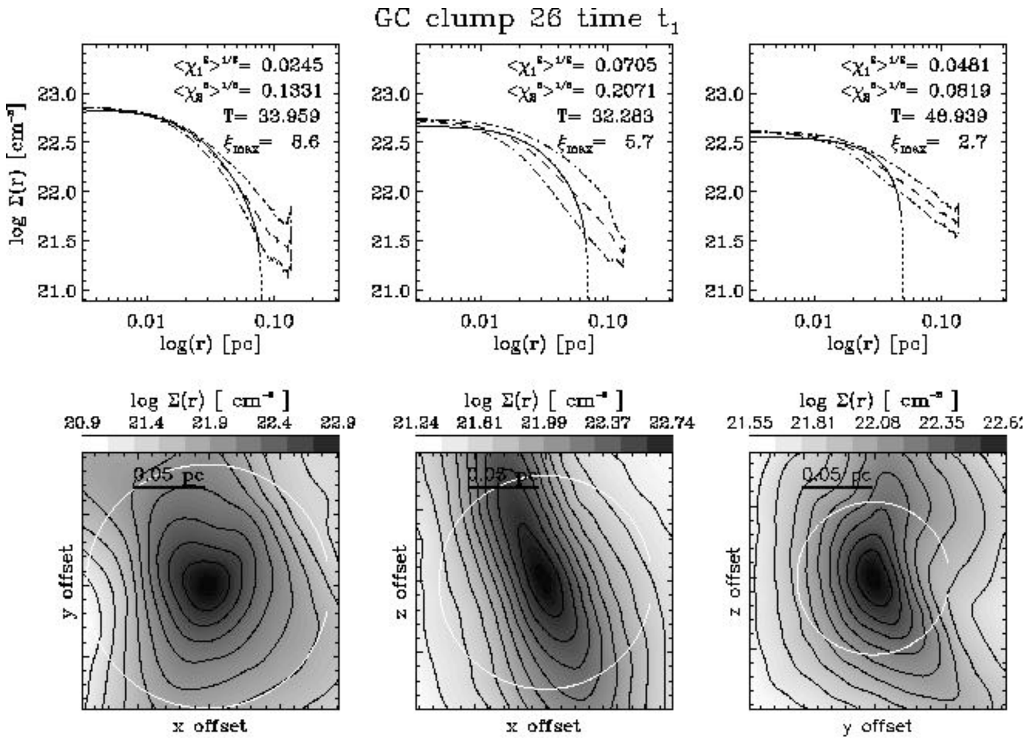
GC clump 26 time t_1
$<\chi_1^2>^{1/2}$= 0.0245
$<\chi_2^2>^{1/2}$= 0.1331
T= 33.959
ξ_{max}= 8.6
$<\chi_1^2>^{1/2}$= 0.0705
$<\chi_2^2>^{1/2}$= 0.2071
T= 32.283
ξ_{max}= 5.7
$<\chi_1^2>^{1/2}$= 0.0481
$<\chi_2^2>^{1/2}$= 0.0819
T= 46.939
ξ_{max}= 2.7
log Σ(r) [cm^{-2}]
log(r) [pc]
log Σ(r) [cm^{-2}]
20.9 21.4 21.9 22.4 22.9
21.24 21.61 21.99 22.37 22.74
21.55 21.81 22.08 22.35 22.6
0.05 pc
y offset
z offset
x offset
y offset

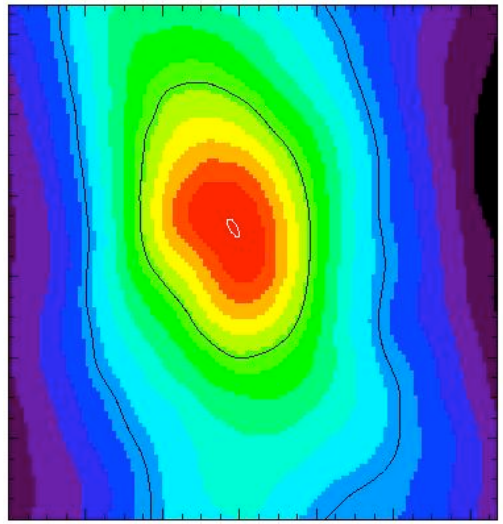

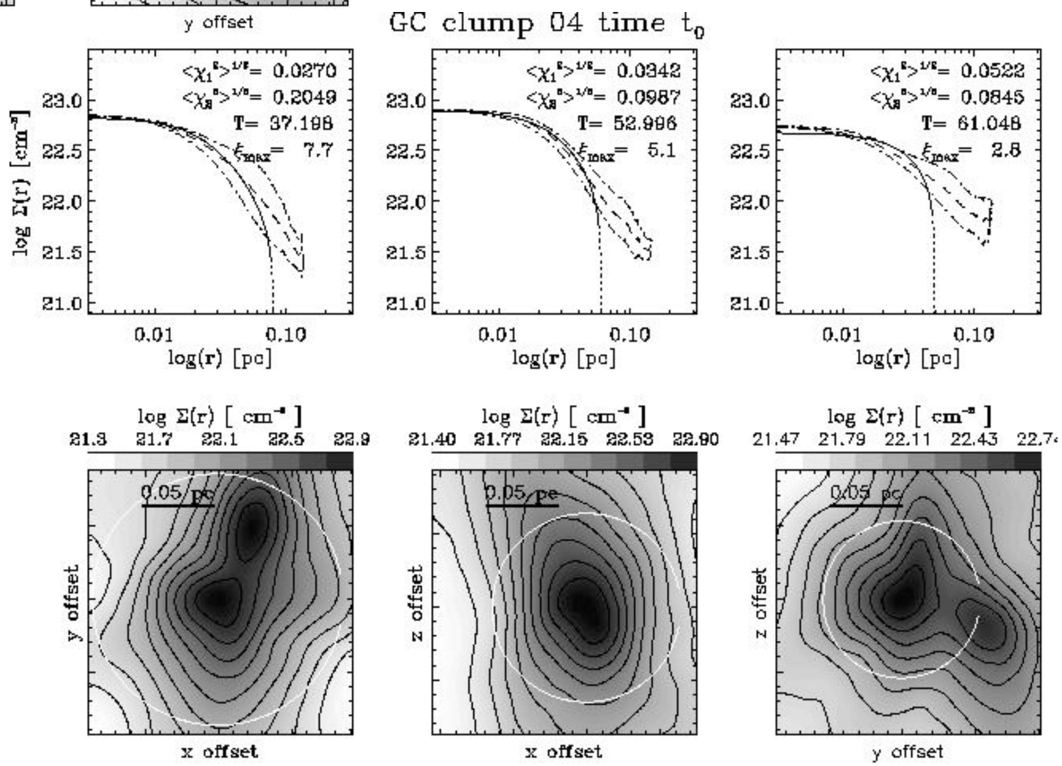
GC clump 04 time t_0
$<\chi_1^2>^{1/2}$= 0.0270
$<\chi_2^2>^{1/2}$= 0.2049
T= 37.198
ξ_{max}= 7.7
$<\chi_1^2>^{1/2}$= 0.0342
$<\chi_2^2>^{1/2}$= 0.0987
T= 52.996
ξ_{max}= 5.1
$<\chi_1^2>^{1/2}$= 0.0522
$<\chi_2^2>^{1/2}$= 0.0845
T= 61.048
ξ_{max}= 2.8
log Σ(r) [cm^{-2}]
log(r) [pc]
log Σ(r) [cm^{-2}]
21.3 21.7 22.1 22.5 22.9
21.40 21.77 22.15 22.53 22.90
21.47 21.79 22.11 22.43 22.7
0.05 pc
y offset
z offset
x offset
y offset

thanks